Descending control of locomotion in the lamprey

Inaugural-Dissertation

zur

Erlangung des Doktorgrades

der Mathematisch-Naturwissenschaftlichen Fakultät

der Universität zu Köln

vorgelegt von

Swantje Grätsch

aus Schleswig

Köln, Mai 2018

Berichterstatter/in:

Prof. Dr. Ansgar Büschges

Prof. Dr. Silvia Daun

Prof. Dr. Réjean Dubuc

Tag der mündlichen Prüfung :

16. Juli 2018

Contents

1. Zusammenfassung

Lokomotion entsteht aus einem dynamischen Zusammenspiel dreierlei Komponenten: Den rhythmischen Bewegungsmustern, die von neuronalen Netzwerken im Rückenmark generiert werden, den absteigenden Einflüssen von supraspinalen Hirnstrukturen und den sensorischen Eingängen aus der Peripherie. Durch dieses Zusammenspiel können periodische Bewegungssequenzen generiert werden, die gestartet, aufrechterhalten und gestoppt werden müssen. Um die Bewegungskontrolle auf zellulärer Ebene untersuchen zu können, wurde in den letzten Jahrzehnten das Neunauge als Modellorganismus etabliert. In diesem basalen Wirbeltier wurden neuronale Netzwerke im Rückenmark identifiziert, zentrale Mustergeneratoren (ZMGs), die rhythmische Aktivität generieren und Muskelaktivität während der Fortbewegung steuern. Diese ZMGs werden von retikulospinalen (RS) Neuronen im Hirnstamm kontrolliert, welche wiederum von lokomotorischen Regionen, wie der mesenzephalen lokomotorischen Region (MLR), aktiviert werden. Die MLR kontrolliert die Initiierung und Aufrechterhaltung von Bewegung und spielt eine entscheidende Rolle bei der zielgerichteten Fortbewegung. Die Aktivität der MLR unterliegt dabei der Kontrolle von Hirnstrukturen im Vorderhirn, wie den Basalganglien. Diese Dissertation beschäftigt sich mit den absteigenden Eingängen, die die MLR aus dem Vorderhirn erreichen, sowie mit den absteigenden Projektionen der MLR zu unterschiedlichen RS Zellpopulationen im Hirnstamm. Hierfür wurden elektrophysiologische, neuroanatomische, bildgebende und Verhaltensversuche im Neunauge durchgeführt.

Klassischerweise werden Projektionen von dopaminergen Neuronen der *substantia nigra pars compacta* (SNc) so beschrieben, dass sie aufsteigend zum Striatum, der Eingangsstation der Basalganglien, führen. In der ersten Studie (Ryczko et al., 2013) konnten dopaminerge Neurone des *posterior tumberculum* (PT, homolog zur SNc in Säugetieren) identifiziert werden, die absteigend auf die MLR projizieren. Versuche in semi-intakten Präparationen ermöglichen eine Korrelation der RS Zellaktivität mit aktiven Schwimmbewegungen. Hierbei wurde beobachtet, dass eine elektrische Stimulation des PT zu Aktivität in RS Zellen und zu aktiven Schwimmbewegungen führt. Im selben experimentellen Aufbau wurde außerdem eine signifikante Erhöhung der Aktivität in RS Zellen und im Schwimmverhalten beobachtet, wenn Dopaminrezeptoren der MLR lokal aktiviert wurden. Auf der anderen Seite führte ein pharmakologisches Blockieren von D1 Rezeptoren in der MLR zu einer Reduzierung der RS Zellaktitivät und des Schwimmverhaltens. Somit konnte in diesem Teil der Arbeit gezeigt werden, dass absteigende dopaminerge Nervenbahnen des PT die MLR direkt innervieren und die Aktivität der MLR sowie des Schwimmverhaltens erhöhen.

Aufgrund von Vorstudien wurde bereits angenommen, dass neben den absteigenden dopaminergen Projektionen auch glutamaterge Neurone des PT die MLR direkt innervieren. Diese glutamatergen Projektionen wurde in der zweiten Studie untersucht (Ryczko et al., 2017). Eine wichtige Beobachtung dieser Studie war, dass die Aktivität der MLR und der Bewegungsgeschwindigkeit durch eine elektrische PT Stimulation graduell kontrolliert werden kann: je höher die Intensität der PT Stimulation, desto schneller wurden Bewegungsabläufe ausgeführt. Die Blockierung von Glutamatrezeptoren in der MLR hatte eine

erhebliche Beeinträchtigung der Initiierung von Bewegungsabläufen zur Folge. Die Blockierung von D1 Dopaminrezeptoren in der MLR setzte die Schwimmgeschwindigkeit zwar signifikant herunter, eine graduelle Kontrolle der Schwimmgeschwindigkeit durch elektrische PT Stimulation war aber nach wie vor möglich. Daraus ergibt sich, dass absteigende glutamaterge PT Neurone für die graduelle Kontrolle der Schwimmgeschwindigkeit verantwortlich sind.

In der dritten Studie (Juvin*, Grätsch* et al., 2016) konnte gezeigt werden, dass RS Zellen nicht uniform auf eine elektrische MLR Stimulation antworten, sondern drei unterschiedliche Aktivitätsmuster aufweisen. Eine Population von RS Zellen wird kurz am Beginn einer MLR Stimulation aktiviert, während eine zweite Zellpopulation Aktionspotentiale während der gesamten MLR Stimulation generiert. Interessanterweise wurde eine dritte Gruppe von RS Zellen identifiziert, die eine Salve von Aktionspotenzialen am Anfang und eine weitere Salve nach dem Ende einer MLR Stimulation produziert. In semi-intakten Präparationen wurde gezeigt, dass diese letzte Salve von Aktionspotentialen stark mit dem Ende der Schwimmepisode korreliert. Des Weitern wurde nachgewiesen, dass eine pharmakologische Aktivierung dieser RS Zellen Schwimmbewegungen beendet, während eine Inaktivierung dieser RS Zellen den Beendigungsprozess der Schwimmepisode stark beeinträchtigt. Da diese RS Zellen funktionell eng mit dem Ende von Bewegungsabläufen verknüpft ist, wurden sie Stopp Zellen genannt.

Es war bisher unklar, wie Stopp Zellen währen einer Bewegung aktiviert werden und sie wiesen keine Membraneigenschaften auf, die ihr charakteristisches Aktivitätsmuster erklären. Daher wurden sie in der vierten Studie (Grätsch et al., in Begutachtung) auf synaptische Eingänge untersucht, die die zweite Salve von Aktionspotenzialen auslösen könnten. In dieser Studie konnte gezeigt werden, dass durch eine Stimulation der MLR während einer Bewegungsepisode, Stopp Zellen rekrutiert werden und somit das Ende des Bewegungsablaufs kontrolliert wird. Elektrophysiologische und anatomische Versuche weisen außerdem darauf hin, dass eine monosynaptische Verbindung zwischen der MLR und Stopp Zellen besteht.

Teile dieser Arbeit wurden bereits in Fachzeitschriften publiziert (Ryczko et al., 2013; Ryczko et al., 2017; Juvin*, Grätsch* et al., 2016) oder sind im Begutachtungsverfahren (Grätsch et al.).

* Ko-Erstautoren

2. Summary

Locomotion underlies a dynamic interplay of a basic motor pattern that is generated by spinal neural networks, descending control originating from supraspinal structures, and sensory feedback from the periphery. Locomotion usually occurs intermittently and thus, it must be initiated, maintained, and eventually stopped. Over the past decades, the lamprey has been used as an experimental model to define the cellular mechanisms controlling locomotion in vertebrates. In this model, spinal central pattern generators (CPGs) have been characterized and shown to generate rhythmic muscle contractions needed for body propulsion. The spinal CPGs are controlled by brainstem reticulospinal (RS) neurons, which are activated by upstream brain structures, such as the mesencephalic locomotor region (MLR). The MLR initiates and controls locomotion in a graded fashion and plays a role in goal-directed locomotion. Its activity is in turn controlled by forebrain structures, such as the basal ganglia. The focus of my thesis was to examine descending projections from forebrain structures to the MLR as well as MLR projections to different RS cell populations in the lamprey lower brainstem. For this, electrophysiological, neuroanatomical, Ca^{2+} - imaging, and behavioral experiments were performed.

In vertebrates, forebrain dopaminergic neurons of the *substantia nigra pars compacta* (SNc) are classically described to send ascending projections to the striatum, the input structure of the basal ganglia. In a first study (Ryczko et al., 2013), we identified in the lamprey a previously unknown descending dopaminergic pathway from the posterior tuberculum (PT; the homologue structure to the mammalian SNc) that directly innervates the MLR. Experiments were performed in semi-intact preparations, in which cellular activity can be correlated to active swimming movements of the intact body. It was demonstrated that electrical PT stimulation elicits RS cell activity as well as motor behavior. Both RS cell activity and locomotor output were significantly increased when dopamine was injected locally into the MLR. On the other hand, local injections of a D1 receptor antagonist in the MLR dramatically decreased RS cell activity and locomotor activity. It was concluded that this descending dopaminergic pathway provides extra excitation to the MLR and consequently increases the locomotor output.

It was thought that this newly identified dopaminergic pathway acts in parallel with a descending glutamatergic pathway from the PT to the MLR. In a second study (Ryczko et al., 2017), the glutamatergic projection was examined in detail. One important finding was that the PT controls MLR activity and consequently the locomotor speed in a graded fashion: increasing stimulation intensity of the PT leads to increasing MLR cell activity and locomotor speed. Local blockade of glutamate receptors in the MLR dramatically diminishes locomotor activity elicited by PT stimulation. Local injections of a D1 receptor antagonist in the MLR also decreases locomotor frequency but surprisingly, the graded control of locomotor speed was still present. It was concluded that the PT controls the locomotor speed in a graded fashion through direct descending glutamatergic projections to the MLR.

In a third study (Juvin*, Grätsch* et al., 2016), it was demonstrated that RS cells do not respond to MLR stimulation uniformly, but with three distinct activity patterns. One RS cell population responds with a

transient burst of activity at the beginning of a MLR stimulation, a second group displays a sustained response throughout the MLR stimulation, and a third group of RS cells was shown to display two transient bursts of activity: a first burst of activity is generated at the beginning and a second burst occurs at the end of a MLR stimulation. These RS cells were recorded in semi-intact preparations, and it was demonstrated that the second burst of activity is strongly correlated to the end of a locomotor bout ('termination burst'). Local application of glutamate on these RS cells was shown to stop ongoing swimming movements, whereas inactivation of glutamate receptors elicits a slower termination. As they contribute to the termination of locomotion, these RS cells are referred to as stop cells.

It was shown that the 'termination burst' does not underlie specific membrane properties of stop cells but rather synaptic inputs to those cells. The aim of a fourth study (Grätsch et al., under review) was to define the origin of these synaptic inputs. An important finding was that ongoing locomotion can be stopped by electrical and pharmacological MLR activation. When the animal is at rest, MLR stimulation elicits locomotion, but it produces very different effects if stimulated during locomotion. It stops swimming if it is stimulated at low intensity and prolongs swimming if stimulated at a higher intensity. Furthermore it was shown that MLR stimulation at low intensity also triggers the 'termination burst' in stop cells. Electrophysiological and anatomical experiments revealed that at least some connections between MLR and stop cells are monosynaptic.

Parts of this work are published in peer-reviewed journals (Ryczko et al., 2013; Ryczko et al., 2017; Juvin*, Grätsch* et al., 2016) or are under review (Grätsch et al.).

* co-first authors

3. List of Abbreviations

AMPA: α-amino-3-hydroxy-5-methyl-4-isoxazolepropionic acid

AP5: (2*R*)-amino-5-phosphonovaleric acid; (2*R*)-amino-5-phosphonopentanoate; NMDA receptor antagonist

ARRN: anterior rhombencephalic reticular nucleus

CNQX: 6-cyano-7-nitroquinoxaline-2,3-dione; AMPA/kianate receptor antagonist

CNS: central nervous system

CPG: central pattern generator

CuN: *cuneiform nucleus*

DLR: diencephalic locomotor region

EPSP: excitatory postsynaptic potential

GABA: gamma-aminobutyric acid

GPe: *globus pallidus externa*

GPi: *globus pallidus interna*

I_{CAN}: Calcium-activated nonselective cation current

LDT: laterodorsal tegmental nucleus

MHR: mid-hindbrain neurons

MLR: mesencephalic locomotor region

MPTP: 1-methyl-4-phenyl-1,2,3,6-tetrahydropyridine

MRN: mesencephalic reticular nucleus

MRRN: middle rhombencephalic reticular nucleus

NMDA: N-methyl-D-aspartate

PD: Parkinson's disease

PPN: *pedunclopontine nucleus*

PRRN: posterior rhombencephalic reticular nucleus

PT: *posterior tuberculum*

RS: reticulospinal

SCH29930: halobenzazepine; D1 receptor antagonist

SNc: *substantia nigra pars compacta*

SNr: *substantia nigra par reticulata*

STN: *subthalamic nucleus*

4. Introduction

Locomotion is a complex motor behavior that plays a crucial role in our daily life. Animals have developed different locomotor strategies to survive in their environment and to explore it: a stick insect coordinates six legs while walking through shrub lands; a hummingbird uses its two wings to perform ultra-fast flight maneuvers; and a humpback whale can travel long distances by swimming through the ocean water. Even though the biomechanics of their movement are very different, the general scheme for locomotor control is very similar in invertebrate and vertebrate species: Central pattern generators (CPGs) produce a basic motor pattern and control sequential muscle contractions, needed for body propulsion. These CPGs are in turn controlled by descending inputs from the central nervous system (CNS) and modulated by sensory feedback from the periphery (for review see Rossignol et al., 2006; Dubuc et al., 2008; Büschges et al, 2011; Grillner and Robertson, 2017). In vertebrates, the locomotor CPGs are located in the spinal cord and they receive synaptic inputs from reticulospinal (RS) neurons in the hindbrain (see Figure 1). These RS cells are command cells for locomotion and are controlled by upstream locomotor regions such as the mesencephalic and the diencephalic locomotor region (MLR and DLR, respectively). The MLR controls the initiation of locomotion and is controlled by forebrain structures, including the basal ganglia. Additionally, the motor cortex is involved in fine adjustment of the locomotor output.

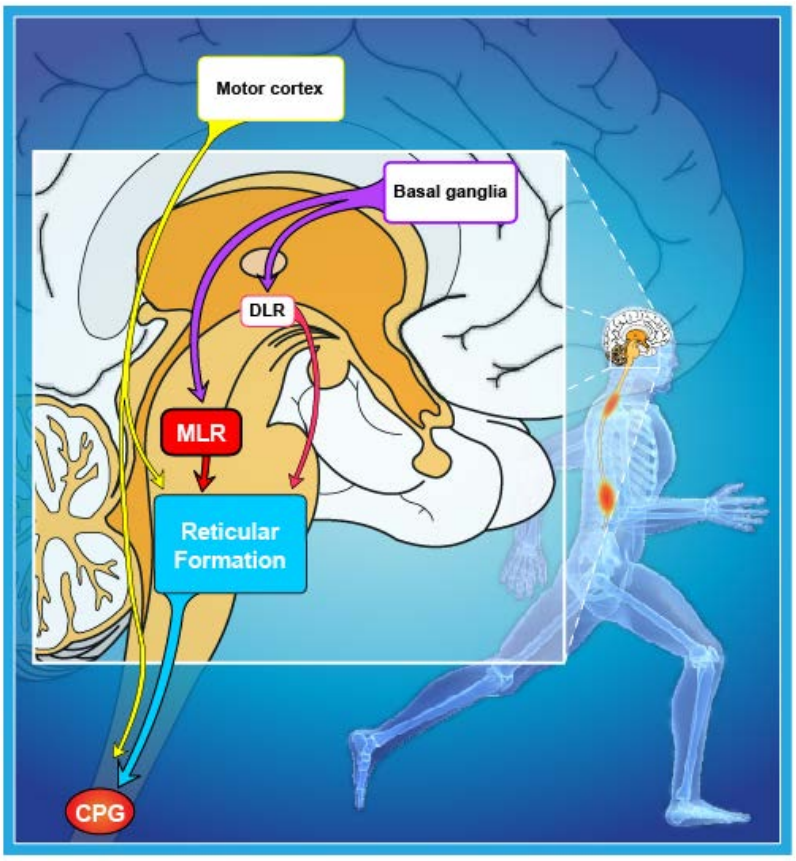

Figure 1. Neural control of locomotion in vertebrates.
Schematic representation of a human brain (sagittal view) with the approximate locations and connections of selected supraspinal brain structures that are relevant for locomotor control in vertebrates. (CPG, central pattern generator; DLR, Diencephalic locomotor region, MLR, Mesencephalic locomotor region; modified from Le Ray et al., 2011).

4.1. Locomotor control in vertebrates

Early motor control studies

The general concept of neural control of locomotion was developed based on discoveries made in cat studies that were performed in the 1960s and 1970s. Grillner and Zangger (1979) demonstrated after a complete low thoracic spinal transection in acute mesencephalic cats that neural networks in the spinal cord generate rhythmic activity and control sequential activation of muscle groups during body movements. Interestingly, it could be demonstrated that these neural networks have the capacity to generate an unchanged rhythmic activity in isolated conditions, namely after deafferentation of dorsal roots. For that reason, these spinal networks were referred to as 'central pattern generators' (Griller and Zangger, 1975). As described above, the spinal CPGs are controlled by supraspinal structures such as the MLR that activates spinal networks via RS cells in the hindbrain. The MLR itself was discovered in the late 1960 by the muscovite research group of Orlovskii. They discovered in decerebrated cats that locomotion can be elicited by electrically stimulating a brain region located at the junction of the mid- and hindbrain (Shik et al., 1966). In this study it was demonstrated that the locomotor output can be controlled in a graded fashion by stimulating this region electrically: stimulation at low intensities initiated walking in cats and increasing stimulation intensities systematically changed the locomotion pattern to trotting and then galloping gait. Since this brainstem region appeared to be dedicated to controlling locomotion, it was then named 'mesencephalic locomotor region'. It was later confirmed that the MLR initiates locomotion not by directly projecting to the spinal cord, but by activating RS cells which in turn relay the locomotor command to spinal locomotor networks (Garcia-Rill and Skinner, 1987 a, b; Orlovskii, 1970; Steeves and Jordan, 1984). Garcia-Rill and Skinner (1987 b) demonstrated in cats that RS neurons in the medioventral medulla receive inputs from the MLR and project directly to the spinal cord. Additionally, they showed that electrical as well as pharmacological activation of this area initiates locomotor activity (Garcia-Rill and Skinner, 1987a). In conclusion, these important studies laid the foundation of today's knowledge about the neural mechanisms involved in motor control.

Further development

Following studies were later performed in different model organisms and striking similarities were observed in the neural organization of the locomotor networks throughout vertebrate species. For example, locomotor CPGs were identified in the spinal cord of many different vertebrates and shown to generate a basic locomotor pattern (*e.g. Xenopus* tadpole: Kahn and Roberts, 1982; rat: Kudo and Yamada, 1987; goldfish: Fetcho and Svoboda, 1993; zebrafish: McDearmid and Drapeau, 2006; for review, see Grillner et al., 2003; Ryczko et al., 2010).

RS cells were also shown to constitute the interface between the locomotor centers and spinal networks and provide mainly excitatory input to spinal interneurons and motor neurons (*e.g.* Peterson et al., 1979; Perrins et al., 2002; Bouvier et al., 2015; Capelli et al., 2017). Interestingly, multiple studies in different vertebrate models revealed that different groups of RS cells control various motor functions, such as locomotor initiation (Garcia-Rill and Skinner, 1987a; Kimura et al, 2013; Capelli et al., 2017), maintenance (Bretzner and Brownstone, 2013), termination (Bouvier et al., 2015; Perrins et al., 2002; Capelli et al, 2017), and steering (Thiele et al., 2014).

Importantly, the MLR has been shown to be highly conserved and has been identified in all vertebrate species tested (*e.g.* rats: Skinner and Garcia-Rill, 1984; mice: Lee et al., 2014; salamanders: Cabelguen et al., 2003; ducks and geese: Sholomenko et al., 1991; lamprey: Sirota et al, 2000, for review, see Jordan, 1998; Dubuc et al., 2008). It is classically described to be located at the border between the midbrain and hindbrain and electrical, pharmacological, or optogenetic stimulation initiates stable locomotor bouts (Shik et al., 1966; Garcia-Rill et al., 1985; Lee et al., 2014; Roseberry et al, 2016; Caggiano et al., 2018; Josset et al, 2018). The key characteristic of the MLR to control the locomotor speed in a graded fashion was also shown to be present in other species (Sirota et al., 2000; Cabelguen et al., 2003; Lee et al., 2014; for review, see Le Ray et al, 2011; Ryczko and Dubuc, 2013). The mammalian MLR comprises cholinergic, glutamatergic, and GABAergic neurons that are localized in different nuclei, the pedunculopontine nucleus (PPN) and the cuneiform nucleus (CuN) (Skinner and Garcia-Rill, 1984; Martinez-Gonzalez et al., 2011; Roseberry et al., 2016; for review, see Ryczko and Dubuc, 2013). It has not yet been resolved whether different sub-nuclei of the MLR control different motor functions, but this matter has been extensively studied. Sinnamon (1993) proposed that different MLR regions control different motor functions such as appetitive behavior that is used to approach a consummatory stimulus, escape behavior in response to threat, and exploratory behavior. Recent optogenetic studies support this hypothesis (Roseberry et al., 2016; Caggiano et al., 2018; Josset et al., 2018). Examination of the functional role of different cell types in the MLR demonstrated that glutamatergic MLR cells drive locomotor activity, whereas cholinergic cells contribute to speed control. GABAergic cells inhibit glutamatergic MLR neurons, which leads to locomotor arrest (Roseberry et al., 2016). Caggiano and colleagues (2018) revealed that glutamatergic neurons in both PPN and CuN contribute to slow exploratory movements but only activation of glutamatergic CuN neurons can elicit high-speed escape-like behavior. Similar observations were made by Josset and colleagues (2018), who demonstrated that optogenetic stimulations of glutamatergic CuN neurons trigger fast locomotion, as it is seen in escape behavior. Furthermore, it was shown that both glutamatergic as well as cholinergic neurons in the PPN contribute and modulate slow walking movements, as observed in exploratory behavior (Josset et al., 2018).

The mammalian MLR in turn is controlled by forebrain structures, such as the basal ganglia, which are involved in the selection of actions and motor programs (for review, see Kreitzer and Malenka, 2008; Grillner and Robertson, 2016). At rest, GABAergic neurons from the *substantia nigra pars reticulata* (SNr) and the *globus pallidus interna* (GPi), the output structures of the basal ganglia, keep the MLR under tonic inhibition

(Saitoh et al., 2003; Roseberry et al., 2016; for review, see Takakusaki et al., 2008). In order to generate and suppress goal-directed locomotion, the basal ganglia recruit their direct and indirect pathway respectively (Kravitz et al., 2010; Roseberry et al., 2016). The direct pathway is composed of GABAergic neurons that project from the striatum, the input structure of the basal ganglia, directly to the SNr and GPi. Activation of this direct pathway inhibits the GABAergic neurons of the SNr and GPi and thus disinhibits the MLR, which then leads to the initiation of locomotion. Striatal neurons of the indirect pathway, on the other hand, project to the *globus pallidus externa* (GPe), which in turn projects to the *subthalamic nucleus* (STN). The STN activates the GPi and the SNr, which then leads to suppression of motor activity (Kravitz et al., 2010; for review, see Grillner and Robertson, 2016; Roseberry and Kreitzer, 2017).

In the past decades, motor control studies have given a broad insight into the neural control of locomotor behavior. Cross-linking concepts that were found in invertebrates, basal vertebrates, and more recently-evolved vertebrates is one reason for this progress (for review, see Mullins et al., 2011). Furthermore, technological advances allowed the establishment of new techniques, such as Ca^{2+} imaging or optogenetic tools. The latter provide many advantages, since the functional role of neurons with specific genetic markers can be examined (e.g. Kimura et al., 2013; Lee, 2014; Thiele et al., 2014; Bouvier et al., 2015; Capelli et al., 2017; Caggiano et al., 2018; Josset et al., 2018). However, the mammalian nervous system is very complex and single cell recordings remain challenging, notably during ongoing locomotion. Therefore, studies in organisms with simpler nervous systems, like the lamprey, remain of great importance in order to reveal details about neural connectivity and properties involved in locomotor control.

4.2. The control of locomotion in lampreys

Studies performed in mammalian models could not yet bring detailed insights into the cellular organization and connectivity within the locomotor network. In the 1980s, Grillner and colleagues started to investigate the cellular organization of the spinal locomotor CPG in a basal vertebrate, the lamprey. The lamprey was chosen as an experimental model for several reasons. It is a basal vertebrate that diverged from the vertebrate phylum some 560 million years ago (Kumar and Hedges, 1998) and the anatomical organization of the lamprey and mammalian CNS is strikingly similar (for review, see Nieuwenhuys et al., 1998; Robertson et al., 2014 Grillner and Robertson, 2017). Another advantage was the simplicity of the undulary, limbless movements. Lampreys swim in the horizontal plane and movements underlie reciprocal muscle contractions of the left and right side of the body. For the most common forward propulsion, those contractions propagate along the body axis like a mechanical wave that propagates from the rostral to the caudal body segments, with an intersegmental phase lag of approximately 1% (Wallén and Williams, 1984). In very rare cases, the lamprey performs backward swimming, characterized by undulary movements that start in caudal segments and propagate rostrally with a phase lag of approximately -1% (Matsushima and Grillner, 1992; Islam et al.,

2006). Compared to the mammalian CNS, there are considerably fewer neurons present in the lamprey CNS and many are larger and thus more accessible for intracellular recording. Another advantage is that he lamprey brain can survive *in vitro* for a few days, which makes it very valuable for anatomical and physiological experiments. Moreover, a semi-intact preparation was developed in lampreys to study neural activity during active behavior (Sirota et al, 2000). Here, the brain is exposed and accessible to recording electrodes while the intact body is still attached and may perform active swimming movements, cellular activity in the intact brain can thus be correlated to the behavioral output. Over the past decades, these features allowed the development and the combination of multiple *in vitro* and *in vivo* techniques that are now used to examine neural networks from the single cell to the behavioral level (*e.g.* Derjean et al., 2010; Brocard et al., 2010; Ryczko et al., 2013; Juvin et al., 2016).

The locomotor CPGs in the lamprey spinal cord

As mentioned above, Grillner and his group began to characterize the cellular organization of the locomotor CPGs in the lamprey spinal cord. Buchanan and Grillner (1987) discovered that excitatory glutamatergic premotor neurons build networks that intrinsically generate burst activity and excite ipsilateral motor neurons (Buchanan and Grillner, 1987). Rhythmic bursting activity can be generated by these networks even in isolated spinal cord preparations in which supraspinal and sensory inputs are removed. Pharmacological application of glutamate agonists to the spinal cord or electrical stimulation of supraspinal brain areas as well as RS cell axons induce stable bursting pattern in spinal ventral roots. This motor output is referred to as 'fictive locomotion' (Cohen and Wallén, 1980; Wallén and Williams, 1984). The rhythmogenetic networks were shown to be located in individual spinal cord segments and are interconnected through ipsilateral (intersegmental) and contralateral (intrasegmental) projections, originating from excitatory and inhibitory interneurons that allow rostro-caudal and left-right coordination of body segments (for review, see Grillner, 2003). For the propagation of the mechanical wave from rostral to caudal, intersegmental coordination of ipsilateral rhythmogenetic networks is needed. Excitatory interneurons of each segment project collateral axons to rostral and caudal segments (Dale, 1986). This interconnection allows the generation of rostro-caudal body undulations, but can also induce caudo-rostral body movements during backward swimming. Decisive for the direction of propagation of burst activity is the excitatory gradient of rostral and caudal spinal cord segments: if rostral segments are more excited than caudal segments, the wave of bursting activity propagates from rostral to caudal and *vice versa* (Matsushima and Griller, 1992). Glycinergic commissural interneurons coordinate alternating activity of rhythmogenetic networks located on the left and right side of one segment. These neurons are activated by the excitatory interneurons of the rhythmogenetic networks and inhibit contralateral CPG interneurons as well as contralateral motor neurons (Buchanan, 1982). Application of strychnine, a glycinergic antagonist, on the isolated spinal cord does not prevent rhythmic bursting activity in the spinal cord, but it results in a change from alternating bursting activity to simultaneous bilateral activity of motor neurons within one segment (Cohen and Harris-Warrick, 1984). These results indicate that contralateral

inhibition is not essential to generate bursting activity in the hemi-segments but it is essential for coordinated left-right alternation of bursting activity in one segment.

The RS neurons in the lamprey

The majority of the discoveries described above were made in the isolated spinal cord preparation and pharmacological or electrical stimulations were used to induce 'fictive locomotion'. In the intact animal however, the CPGs are activated by supraspinal inputs from the RS cells (Rovainen, 1974b; Buchanan et al., 1987a; Ohta and Grillner, 1989; Swain et al., 1993). RS cells are command cells for locomotion that receive and integrate sensory inputs from the olfactory, visual, vestibular, or mechanical systems (Derjean et al., 2010; Zompa and Dubuc, 1996; Deliagina et al., 1993; Deliagina et al., 1992a; b; Deliagina and Orlovskii, 2002; McClellan and Grillner, 1984; Dubuc et al., 1993a; b; for review, see Daghfous et al., 2016). Furthermore, they receive central feedback from the spinal CPGs (Einum and Buchanan, 2005; Antri et al., 2009; Buchanan, 2011). In the lamprey, there are approximately 2500 RS cells, which are located in the brainstem and organized in four distinct nuclei: the mesencephalic reticular nucleus (MRN), the anterior rhombencephalic reticular nucleus (ARRN), the middle rhombencephalic reticular nucleus (MRRN), and the posterior rhombencephalic reticular nucleus (PRRN) (Bussières, 1994; Shaw et al., 2010). The reticular nuclei of the lamprey were described to be homologous to those of other vertebrates: the ARRN and MRRN are thought to be homologous to the mammalian nuclei pontis oralis and caudalis (Rovainen, 1967; Cruce and Newman, 1984). The ARRN and MRRN contain identifiable pairs of RS cells, the Müller and the Mauthner cells, which have been extensively studied in the past because of the large size of their cell bodies (Rovainen 1967a; Rovainen et al., 1973; for review, see Rovainen, 1978; Buchanan, 2001). The axons of Müller cells project ipsilaterally in the middle axon tracts along the spinal cord, where they make en passage synapses with spinal motor neurons and interneurons (Rovainen, 1976a; for review, see Buchanan, 2001). The axons of the Mauthner cells project contralaterally. The PRRN is thought to be homologous to mammalian nucleus gigantocellularis (Cruce and Newman, 1984). RS cells in the PRRN are not identifiable but their axons where shown to project in the lateral tracts of the spinal cord (Shaw et al., 2010). The RS cells in the lamprey have been shown to be functionally and neurochemically heterogenous. The majority of MRRN and PRRN cells are glutamatergic (Buchanan et al., 1987b; Ohta and Grillner, 1989), but next to these excitatory cells, a few glycinergic RS cells were identified that project to the spinal cord and synapse to spinal interneurons and motor neurons (Wannier et al., 1995). Studies performed in different labs over the past years revealed that RS cells control different locomotor functions, such as steering (Fagerstaedt et al., 2001; Kozlov et al., 2002), locomotor speed (Brocard and Dubuc, 2003), postural control (Deliagina and Orlovsky, 2002; Zelenin et al., 2007), and forward and backward swimming (Zelenin, 2011). It is noteworthy, that most of these studies examined the activity of the Müller and Mauthner cells in the MRRN, because they were relatively easy to target for intracellular recording. The use of Ca^{2+}-imaging allowed us to also examine activity of different populations of RS cells, which will be presented in a following section (Juvin et al., 2016).

The mesencephalic locomotor region of the lamprey

Other than inputs from the sensory system and the spinal cord, RS cells receive descending inputs from upstream motor centers, such as the mesencephalic locomotor region and the diencephalic locomotor region (MLR and DLR respectively; El Manira et al., 1997; Sirota et al., 2000; Brocard et al., 2010). The MLR of lampreys comprises cholinergic and glutamatergic neurons that are localized in the PPN and laterodorsal tegmental nucleus (LDT). These neurons project bilaterally and symmetrically to RS cells in the brainstem via monosynaptic connections (Le Ray et al., 2003; Brocard et al., 2010). Whether the two neurotransmitter systems in the MLR contribute to different locomotor functions, as it has recently been shown in mice (Roseberry et al., 2016), has not been confirmed in lampreys. Yet, local applications of acetylcholine or nicotine elicit dose-dependent responses in RS cells and can initiate or accelerate locomotion in semi-intact preparations (Le Ray et al., 2003). Interestingly, blocking nicotinic receptors in the brainstem increased the threshold of MLR stimulation but did not prevent the initiation of locomotion as such, which indicates the cooperative nature of the two neurotransmitter systems that are present in the MLR (Le Ray et al., 2003). Apart from the initiation of locomotion, the graded control of locomotor intensity is another characteristic of the MLR (Sirota et al., 2000). This mechanism works similarly to a rheostat: the stronger the MLR is activated, either electrically or pharmacologically, the higher is the activation of RS cells and consequently, the locomotor output (Sirota et al., 2000). Direct recruitment of different RS cell populations in the MRRN and PRRN (for slow and fast locomotor activity, respectively) underlies this fine control of the intensity of the locomotor output (Brocard and Dubuc, 2003). Additionally, a parallel pathway has been shown to boost locomotor activity (Smetana et al., 2010). Here, the MLR activates a group of muscarinoceptive hindbrain neurons, which in turn project to the RS cells in the MRRN (Smetana et al., 2010). These muscarinoceptive neurons provide extra excitation to RS cells in order to amplify the locomotor output. Interestingly, the MLR not only controls the locomotor output but also participates in other vital functions, by adjusting the activity in neural networks responsible for respiration or gating sensory inputs that reach RS cells (Gariépy et al., 2012; Le Ray et al., 2010; for review, see Le Ray et al., 2011; Missaghi et al., 2016).

The basal ganglia of the lamprey

Like in mammalian species, the lamprey MLR is under the control of forebrain structures, such as the basal ganglia. In vertebrates, the basal ganglia are responsible for the selection of appropriate motor programs. Interestingly, it was shown that the main structures that were identified in the mammalian basal ganglia are also present in the lamprey nervous system (Stephenson- Jones et al., 2011; 2012; for review, see Grillner and Robertson, 2017). GABAergic projections originating from the basal ganglia innervate the MLR and keep them under tonic inhibition (Ménard et al., 2007; Stephenson-Jones et al., 2011; 2012; Pombal et al., 1997; for review, see Robertson et al., 2014). Physiological experiments demonstrated that a blockade of GABAergic receptors in the MLR induced well-coordinated swimming movements in a semi-intact preparation, whereas

activation of GABAergic receptors suppressed ongoing locomotion (Ménard et al., 2007). Meanwhile, the input structure of the basal ganglia, the striatum, receives input from the thalamus and from the pallium, the homologue structure of the mammalian cortex (Ericsson et al., 2013; Ocaña et al., 2015). Additionally, the striatum receives dopaminergic inputs from the posterior tuberculum (PT), the homologue of the mammalian *substantia nigra pars compacta* (SNc) and the ventral tegmental area (Pombal et al., 1997; Ryczko et al., 2013; Peréz-Frenández et al., 2014). As mentioned above for the mammalian basal ganglia, the afferent projections of the striatum form two distinct pathways: the direct pathway and the indirect pathway (Stephenson- Jones et al., 2011; 2012). GABAergic striatal neurons that express substance P constitute the direct pathway and project to the pallidal output structures of the basal ganglia (Stephenson-Jones et al., 2011). Like in the direct pathway in mammals, activation of this pathway in lampreys should suppress the GABAergic neurons of the basal ganglia output region and disinhibit the motor control regions which would in turn lead to locomotor activity. Striatal neurons that form the indirect pathway of the lamprey express enkephalin and project to the output region of the basal ganglia via the GPe and the STN (Ericsson et al., 2013; Stephenson- Jones et al., 2012). The circuitry is strikingly similar to the indirect pathway of mammals so it could be expected that activation of this pathway leads to disinhibition of the basal ganglia output region, which in turn would set the motor regions under tonic inhibition and suppress locomotor activity. Together these findings demonstrate that the building blocks and the connectivity within the basal ganglia were present in the first stages of vertebrate evolution (Stephenson-Jones et al., 2011; 2012; Ryczko et al., 2013) and it is tempting to suggest that this neural substrate for action selection has been used by all vertebrate species since then, with gradual modifications and complexification (for review, see Grillner and Robertson, 2017).

4.3. Aims and objectives

The locomotor network of the lamprey has been examined extensively in the past and many details are known about the descending control of locomotion. However, important details remain elusive such as detailed information regarding the descending input from the forebrain to the MLR and the output of the MLR to different RS cell populations. These topics are at the base of the specific aims of my thesis.

Classically, dopaminergic cells in the SNc were described to send ascending projections to the striatum, the input regions of the basal ganglia (for review, see Ryczko and Dubuc, 2017). But in mammals, some studies suggested the presence of a descending projection, possibly dopaminergic, from the SNc to the MLR (Rolland et al., 2009; Beckstedt et al., 1979). Similarly in the lamprey, anatomical studies demonstrated that dopaminergic neurons of the PT not only send ascending projections to the striatum but also descending projections (Pombal et al., 1997). In a first study (Ryczko et al., 2013), we examined this dopaminergic projection of the PT in more detail and identified a previously unknown descending dopaminergic pathway from the PT to the MLR. Anatomical and physiological experiments were performed and confirmed the

functional relevance of this descending dopaminergic pathway in locomotor control. Dopaminergic inputs from the PT increase MLR activity and consequently the locomotor output via a D1 receptor-dependent mechanism.

Based on studies that were performed previously in the lamprey, it was thought that the PT not only sends dopaminergic projections to the MLR, but that an additional descending pathway provides a parallel excitatory input. For example, it has been shown that electrical stimulation of the PT provides a strong excitatory input to the MLR and that it can initiate locomotion (Derjean et al., 2010; Gariépy et al., 2012; Ryczko et al., 2013). Intracellularly recorded MLR neurons respond to PT stimulation with fast excitatory postsynaptic potentials and a blockade of D1 receptors in the MLR reduces but does not prevent locomotion (Gariépy et al., 2012; Ryczko et al., 2013). Additionally, anatomical studies identified glutamatergic neurons in the PT and physiological studies revealed that activation of glutamatergic receptors in the MLR induces stable locomotor bouts (Sirota et al., 2000; Ménard et al., 2007; Villar-Cervino et al., 2011). Therefore, it seemed very likely that glutamate is present in this parallel pathway. The goal of a second study (Ryczko et al., 2017), was to examine this pathway from the PT to the MLR in more detail. Using anatomical, Ca^{2+} imaging, and electrophysiological techniques, the presence of a descending glutamatergic pathway from the PT to the MLR was confirmed. Moreover, it was shown to be responsible for the graded control of locomotor speed.

It had long been demonstrated that electrical stimulation of the MLR directly activates RS cells in the hindbrain. In the lamprey, RS cells of larger size were preferably examined in the past and the aim of a third study (Juvin*, Grätsch* et al., 2016) was to investigate RS cell responses to MLR stimulation in different populations of RS cells. We found that MLR stimulation elicits three distinct patterns of activity in different RS cell populations. One group of RS cells is transiently active at the beginning of the MLR stimulation and a second group responds with a sustained activity throughout the whole MLR stimulation. A third group of RS cells displayed two transient bursts of activity: one at the beginning and one at the end of the MLR stimulation. Experiments in semi-intact preparations demonstrated that the second burst of activity is correlated to the end of a swimming bout. We thus hypothesised that this RS cell population plays a role in ending locomotor activity. These cells became of great interest because little was known at the time about the neural mechanisms controlling the termination of locomotion (for review, see Klemm, 2001; Mullins et al., 2011). Only recent studies brought insights into the brain regions and neurotransmitter systems that could be involved in stopping locomotion (for review, see Roseberry and Kreitzer, 2017). In our study (Juvin*, Grätsch* et al., 2016), we showed that the pharmacological activation of the RS cells displaying a second burst of activity at the end of a swimming bout halted ongoing swimming. Their inactivation on the other hand slowed the termination of locomotion down. We concluded that these cells played a crucial part in the termination process of locomotion and named them ‘stop cells’.

It was not resolved how the stop cells are activated during ongoing locomotor movements, but synaptic inputs rather than membrane properties were suggested to play a significant role (Juvin*, Grätsch* et al., 2016). As the MLR provides major input to RS cells (Orlovskii, 1970; Steeves and Jordan, 1984; Le Ray et al., 2003; Brocard and Dubuc, 2003; Brocard et al., 2010; Ryczko et al, 2016) it was considered to be a promising candidate for providing such a synaptic input to stop cells. In cats, it has been proposed that projections from the PPN to neurons in the *nucleus reticularis points oralis* that in turn activate RS neurons in the medullary reticular formation are responsible for suppression of muscle tone (for review, see Takakusaki, 2008). But details about this pathway have not yet been described. The aim of the fourth study was therefore to find the source that activates stop cells during ongoing locomotion. Using physiological and anatomical techniques, we could confirm that the MLR is able to activate RS stop cells during ongoing locomotion and can thus stop ongoing locomotion (Grätsch et al., under review).

Altogether, my thesis investigated the descending control of locomotion in the lamprey and revealed details about the direct control of the MLR by forebrain structures as well as descending outputs of the MLR to different RS cell populations in the hindbrain. Furthermore, a neural substrate underlying the neural control of termination of locomotion was identified.

* co-first authors

5. Published studies

5.1. Forebrain dopamine neurons project down to a brainstem region controlling locomotion

Ryczko, D., Grätsch, S., Auclair, F., Dubé, C., Bergeron, S., Alpert, M.H., Cone, J.J., Roitman, M.F., Alford, S., and Dubuc, R.

Published 2013 in *Proceedings of the National Academy of Sciences*, 110(34):E3235-42.

Author contributions

Designed research:
Dimitri Ryczko, François Auclair, and Réjean Dubuc.

Performed research:
Dimitri Ryczko, Swantje Grätsch, François Auclair, Catherine Dubé, Saskia Bergeron, Michael H. Alpert, Jackson J. Cone, Mitchell F. Roitman, Simon Alford, and Réjean Dubuc.

Analyzed data:
Dimitri Ryczko, Swantje Grätsch, François Auclair, Catherine Dubé, Saskia Bergeron, Michael H. Alpert, Jackson J. Cone, Mitchell F. Roitman, Simon Alford, and Réjean Dubuc.

Wrote the paper:
Dimitri Ryczko, François Auclair, and Réjean Dubuc.

Forebrain dopamine neurons project down to a brainstem region controlling locomotion

Dimitri Ryczko[a], Swantje Grätsch[a], François Auclair[a], Catherine Dubé[a], Saskia Bergeron[b], Michael H. Alpert[c], Jackson J. Cone[c], Mitchell F. Roitman[c], Simon Alford[c], and Réjean Dubuc[a,b,1]

[a]Groupe de Recherche sur le Système Nerveux Central, Département de Physiologie, Université de Montréal, Montréal, QC, Canada H3C 3J7; [b]Groupe de Recherche en Activité Physique Adaptée, Département de Kinanthropologie, Université du Québec à Montréal, Montréal, QC, Canada H3C 3P8; and [c]Laboratory of Integrative Neuroscience, University of Illinois at Chicago, Chicago, IL 60607

Edited by Sten Grillner, Karolinska Institutet, Stockholm, Sweden, and approved June 28, 2013 (received for review January 18, 2013)

The contribution of dopamine (DA) to locomotor control is traditionally attributed to ascending dopaminergic projections from the substantia nigra pars compacta and the ventral tegmental area to the basal ganglia, which in turn project down to the mesencephalic locomotor region (MLR), a brainstem region controlling locomotion in vertebrates. However, a dopaminergic innervation of the pedunculopontine nucleus, considered part of the MLR, was recently identified in the monkey. The origin and role of this dopaminergic input are unknown. We addressed these questions in a basal vertebrate, the lamprey. Here we report a functional descending dopaminergic pathway from the posterior tuberculum (PT; homologous to the substantia nigra pars compacta and/or ventral tegmental area of mammals) to the MLR. By using triple labeling, we found that dopaminergic cells from the PT not only project an ascending pathway to the striatum, but send a descending projection to the MLR. In an isolated brain preparation, PT stimulation elicited excitatory synaptic inputs into patch-clamped MLR cells, accompanied by activity in reticulospinal cells. By using voltammetry coupled with electrophysiological recordings, we demonstrate that PT stimulation evoked DA release in the MLR, together with the activation of reticulospinal cells. In a semi-intact preparation, stimulation of the PT elicited reticulospinal activity together with locomotor movements. Microinjections of a D1 antagonist in the MLR decreased the locomotor output elicited by PT stimulation, whereas injection of DA had an opposite effect. It appears that this descending dopaminergic pathway has a modulatory role on MLR cells that are known to receive glutamatergic projections and promotes locomotor output.

motor system | Parkinson disease

Dopamine (DA) neurons of the substantia nigra pars compacta (SNc) and ventral tegmental area (VTA) modulate motor behaviors, including locomotion, through ascending projections to the basal ganglia, the output of which projects to the mesencephalic locomotor region (MLR) (1–3), a brainstem region known to control locomotion in all vertebrate species tested to date (reviewed in ref. 4). DA is known to control the excitability of striatal cells, and a dysfunction of the ascending DA pathway to the striatum is considered to be the main cause for the motor deficits in Parkinson disease (1). However, there have been hints of descending DA projections that would be in position to directly modulate the MLR and hence locomotor activity. In monkeys, DA terminals of unknown origin were observed in the pedunculopontine nucleus (PPN) (5), considered part of the MLR (reviewed in ref. 4). In addition, there is an axonal projection from the SNc to the PPN in rats, but the transmitter system is unknown (6).

We examined the DA system in a basal vertebrate, the lamprey, and found a previously unknown descending DA pathway from the posterior tuberculum (PT) to the MLR, which comprises the PPN and the laterodorsal tegmental nucleus (LDT) in lampreys (ref. 7; reviewed in ref. 4). In lampreys, the PT is considered homologous to the SNc and/or VTA of mammals because of its DA projection to the striatum (3). Further, we determined a role for this DA pathway in the control of locomotion.

Results

Descending DA Projections from the PT to the MLR. Immunofluorescence against tyrosine hydroxylase (TH) or against DA was used to visualize PT neurons containing DA. The distribution of TH and DA immunoreactive cell bodies and fibers were very similar in the PT and the MLR (Fig. S1 *A–F*). Fibers and varicosities positive for TH ($n = 8$ animals) or DA ($n = 3$ animals) were present throughout the LDT and the PPN (Fig. 1 *B* and *C* and Fig. S1 *A–C*), both considered parts of the MLR (ref. 7; reviewed in ref. 4). TH-positive terminals were found in close proximity to cholinergic MLR cell bodies and dendrites (Fig. 1 *A–D*) and in the vicinity of MLR cells traced from the middle rhombencephalic reticular nucleus (MRRN; $n = 5$ animals; Fig. 1 *E–G*). The location of tracer injection sites in the MRRN was verified by histologic examination (Fig. S2 *A* and *B*). As the MLR cholinergic projection to the reticular formation can initiate locomotion (7, 8), the juxtaposition of TH-positive terminals suggests that they are in position to directly modulate locomotor output.

We looked for the origin of this DA projection by using tracer injections in the MLR coupled with TH immunofluorescence. The MLR was considered to overlap largely with the cholinergic neuronal population of the isthmic region, with the conspicuous Müller cell I1 lying at the caudal limit as a landmark (detailed description provided in ref. 9). The PT refers to a region of the caudal diencephalon located ventral to the pretectum. The PT contains a prominent population of dopaminergic neurons, some of them projecting to the striatum, that are intensely labeled by

Significance

We found in lampreys that dopaminergic cells from the posterior tuberculum (homologue of the mammalian substantia nigra pars compacta and/or ventral tegmental area) not only send ascending projections to the striatum, but also have a direct descending projection to a brainstem region controlling locomotion—the mesencephalic locomotor region—where it releases dopamine (DA). DA increased locomotor output through a D1 receptor-dependent mechanism. The presence of this descending dopaminergic projection may have considerable implication for our understanding of the role of DA in motor control under physiological and pathological (i.e. Parkinson disease) conditions.

Author contributions: D.R., F.A., and R.D. designed research; D.R., S.G., F.A., C.D., S.B., M.H.A., J.J.C., M.F.R., S.A., and R.D. performed research; D.R., S.G., F.A., C.D., S.B., M.H.A., J.J.C., M.F.R., S.A., and R.D. analyzed data; and D.R., F.A., and R.D. wrote the paper.

The authors declare no conflict of interest.

This article is a PNAS Direct Submission.

[1]To whom correspondence should be addressed. E-mail: rejean.dubuc@gmail.com.

This article contains supporting information online at www.pnas.org/lookup/suppl/doi:10.1073/pnas.1301125110/-/DCSupplemental.

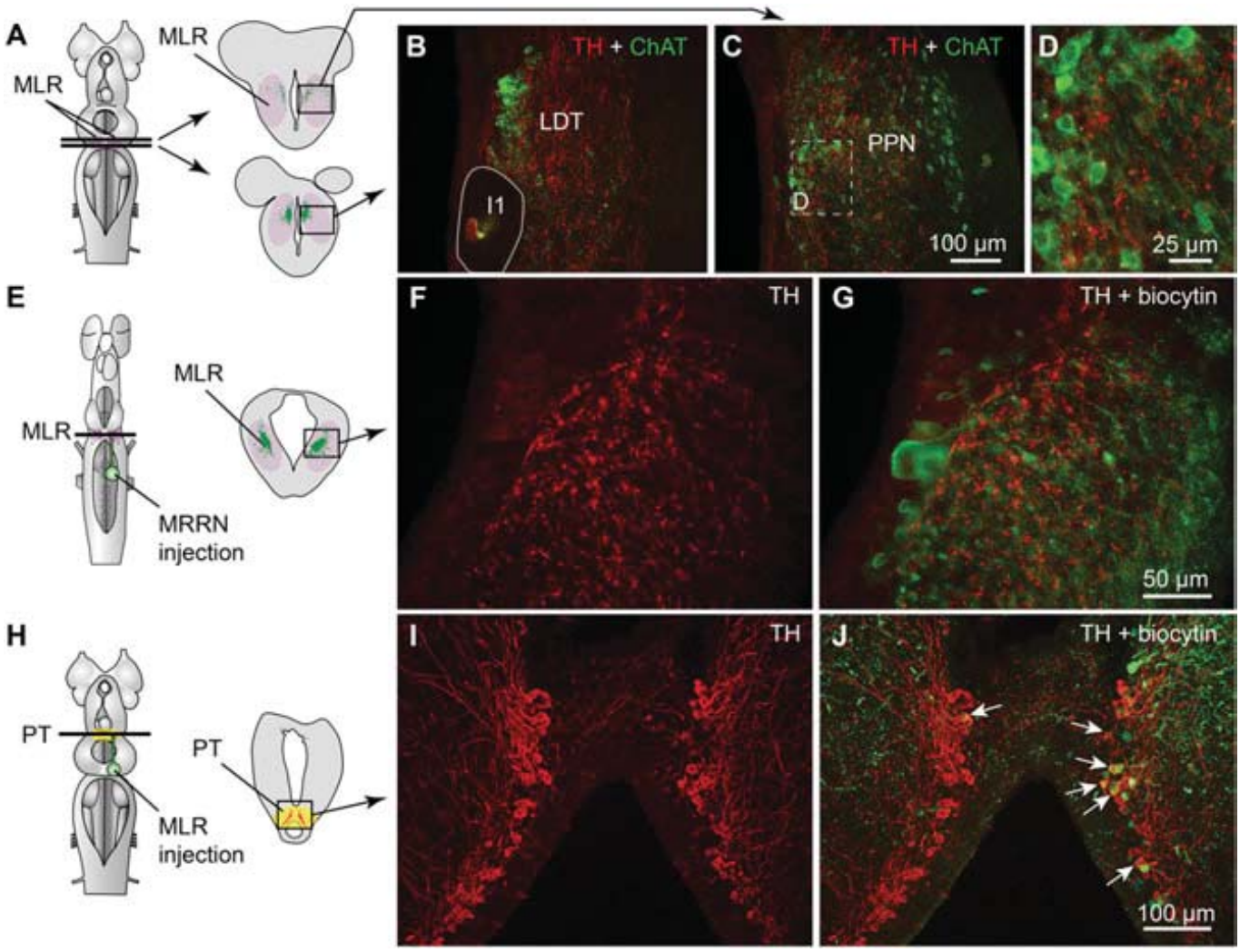

Fig. 1. Dopaminergic (DA) neurons of the PT send descending projections to the MLR. (*A–D*) TH (red)-containing fibers and varicosities in proximity with MLR cells positive for ChAT (green) in the LDT and the PPN in adult lampreys. The giant I1 reticulospinal cell is outlined in *B*. (*D*) Magnification of the dashed rectangle in *C*. (*E–G*) Fibers and varicosities immunoreactive to TH (red) surrounded the laterally oriented dendrites of MLR cells retrogradely labeled from an injection of the tracer biocytin (green) in the reticulospinal population of the MRRN in larval lampreys. (*H–J*) A unilateral injection of the tracer biocytin in the MLR (*H*, *Right*, green) followed by immunofluorescence against TH (*I*, red) revealed double-labeled cells in the PT (white arrows, *J*). The innervation of the MLR by TH-positive fibers was very similar in larval and adult lampreys.

TH immunofluorescence (3). The rostrocaudal extent of the population in spawning phase animals is around 500 µm, spreading approximately 100 to 300 µm from the midline (Fig. 1 *H–J*). The PT contained 189 ± 21 TH-positive cells (n = 12 animals). Many TH-positive cells of the PT were retrogradely labeled from MLR tracer injections (24 ± 3 cells, i.e., 15.4 ± 2.4%), largely on the ipsilateral side (2 ± 1 cells labeled contralaterally, i.e., 1.6 ± 0.6%; n = 6 animals; Fig. 1 *H–J*). Again, these results were confirmed by DA immunofluorescence (n = 3 preparations; Fig. S1 *G–I*). It is noteworthy that retrogradely labeled neurons were found only among the intensely labeled TH-positive population of the PT (outlined in Fig. S1 *E* and *F*), both in the dorsomedial portion that contains larger neurons and in the lateroventral portion that contains smaller neurons. No labeled cells were found in the periventricular TH (and DA) neuron population of the mammillary area, or in any other TH-positive cell population of the brain and spinal cord. By using triple labeling, we found that DA cells in the PT projecting to the striatum were intermingled with those projecting to the MLR (n = 4 preparations; Fig. 2). In all cases, occasional TH-positive neurons of the PT (n = 1–2 cells) were found to project to the MLR and the striatum (Fig. 2*E*). Overall in the PT, TH-positive neurons with descending projections to the MLR (n = 16–52 cells) were, on average, 11 ± 2 times more numerous than those with ascending projections to the striatum (n = 1–5 cells; n = 4 animals).

Activation of the Locomotor System by Stimulation of the PT. Physiological experiments were carried out to examine the role of this descending DA projection in motor control. For this purpose, a semi-intact preparation was used in which the activity of reticulospinal cells is recorded intracellularly while the body freely swims in the chamber. Trains of stimuli applied to the PT (10-s train, 4–5 Hz, 4–30 µA, 2-ms pulses) elicited reticulospinal cell discharges and swimming (n = 13 preparations; Fig. 3 *A–E*). The location of the stimulation sites was confirmed by histologic examination (Fig. 3*D*). Chemical stimulation of the PT with local microinjections of 3.0 to 8.0 pmol of D-glutamate (5 mM, 17–43 pulses of 20 ms, 0.6–1.6 nL per microinjection) into the site used for electrical stimulation, was confirmed to elicit locomotion and reticulospinal discharges in one preparation. This is consistent with previous observations that electrical or chemical stimulation

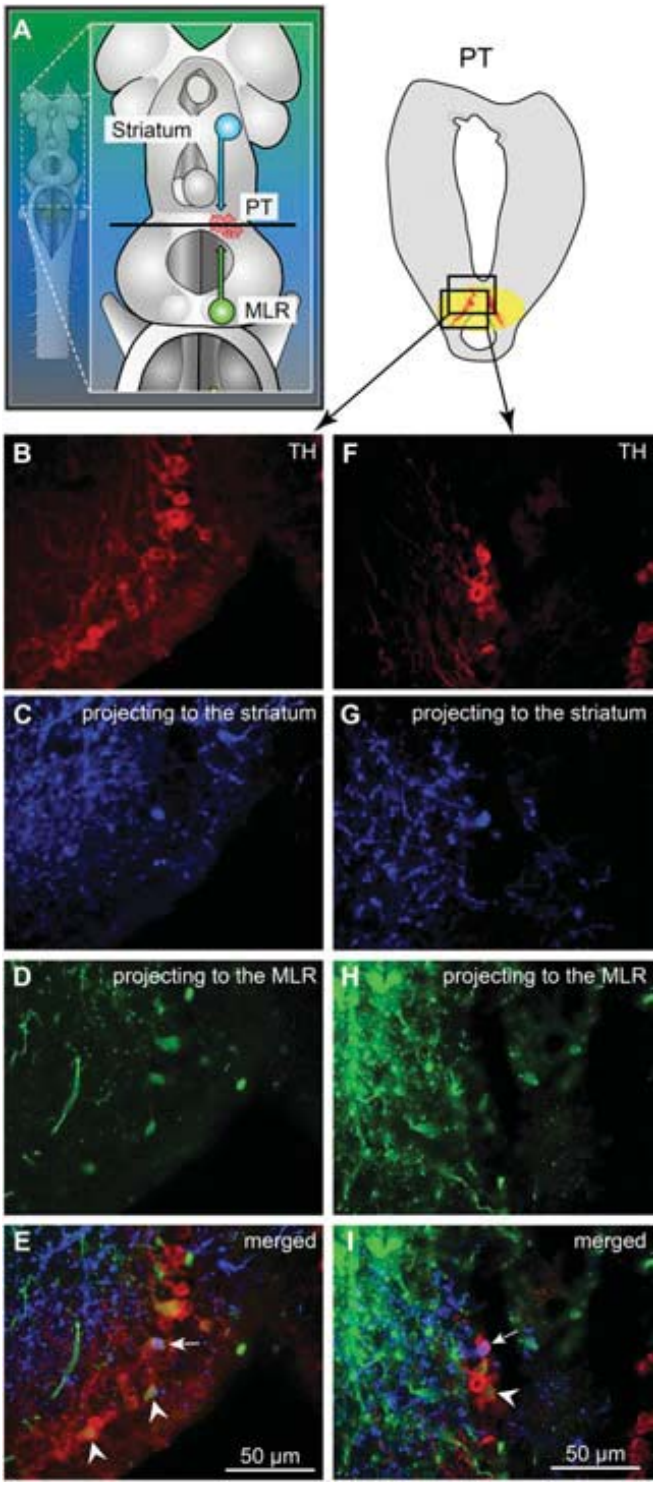

Fig. 2. TH-positive cells projecting to the striatum or to the MLR are intermingled in the PT as shown in triple-labeling experiments. (*A*) Dorsal view of a lamprey brain showing the injection sites of the tracers in the MLR (green) and in the striatum (blue). (*B–E* and *F–I*) Photomicrographs of two examples of transverse sections in the PT at the level indicated on the diagram in *A*. (*Top Right*) Diagram illustrates a cross-section at the level of the PT with the approximate location of the photomicrographic frames shown in *B–I*. DA cells of the PT were labeled with immunofluorescence against TH (red, *A, B,* and *F*). Some cells of the PT were retrogradely labeled by a unilateral injection of one tracer in the striatum (blue, *A, C,* and *G*). Some cells of the PT were retrogradely labeled by another tracer injection, this time in the MLR (green, *A, D,* and *H*). (*E*) The photomicrographs from *B–D* were merged to show the three markers. White arrowheads indicate some examples of TH-positive cells of the PT that project to the MLR, whereas the white arrow points to a TH-positive cell projecting to the MLR and the striatum. (*I*) The photomicrographs from *F–H* were merged. The white arrowhead indicates a PT cell projecting to the MLR and containing TH. The white arrow points to a cell that projects to the striatum and contains TH.

with D-glutamate of this region initiates locomotion (10, 11). By using targeted whole-cell patch clamp recordings in an isolated brain preparation (*Materials and Methods*), we found that trains of stimuli (10-s train, 4–5 Hz, 10–35 μA, 2-ms pulses) to the PT (Fig. S2 *G* and *H*) directly activate MLR cells projecting to reticulospinal neurons ($n = 6$ cells from six preparations; Fig. 3 *F–I*). When comparing simultaneous recordings from an MLR cell and reticulospinal cells (extracellular), we found a very similar activation following trains of stimuli to the PT (Fig. 3*H*). Single stimuli to the PT evoked short-latency, large excitatory postsynaptic currents in whole-cell patch recorded MLR cells (Fig. 3*I*). Glutamatergic receptors are involved in these responses, as previously demonstrated (10), and the DA input from PT to the MLR could modulate this glutamatergic excitatory connection. The rest of our study was aimed at examining this possibility.

Stimulation of the PT Evokes DA Release in the MLR. Fast-scanning cyclic voltammetry (12) was used to measure changes in DA concentration in the MLR while stimulating the PT (Fig. 4). The location of the recording site was confirmed to be within the MLR (Fig. S2 *J* and *K*). A reticulospinal neuron was recorded intracellularly to monitor locomotor network activation. Trains of stimuli (10-s train, 5 Hz, 14–25 μA, 2-ms pulses) in the PT (Fig. S2 *G* and *I*) elicited a large increase in DA concentration in the MLR ($n = 6$ preparations; Fig. 4 *A–C*). We found a strong positive correlation between the increase in DA concentration in the MLR elicited by PT stimulation and the increase in the number of spikes per unit time in reticulospinal cells recorded during the same trials ($R = 0.91$; $P < 0.001$; $n = 30$ stimulations in six preparations; Fig. 4 *D* and *E*). DA release in the MLR was also evoked together with reticulospinal spiking activity when chemically activating the PT with local microinjections of 60.5 pmol of D-glutamate (5 mM, 10 pulses of 100 ms, 12.1 nL per microinjection; $n = 20$ stimulations in four preparations; Fig. S3). These data demonstrate that PT activation results in DA release in the MLR and suggest that DA release may contribute to locomotor output.

Blockade of the DA Inputs to the MLR Decreases Locomotor Output. We then tested whether DA had an effect on the locomotor output elicited by PT stimulation (10-s train, 5 Hz, 12–30 μA, 2-ms pulses). Bath-applying DA (10 μM) onto the brain induced a 25% decrease in the PT stimulation intensity threshold required to elicit locomotion in two of three semi-intact preparations [reduction from 16 to 12 μA in both cases (Fig. S4 *A–C*); 20 μA in the remaining preparation in which no effect was observed]. For PT stimulation intensities above locomotor threshold (16–30 μA), bath-applied DA increased locomotor bout duration (+86.8 ± 18.4%; $P < 0.001$ vs. control), the number of locomotor cycles (+102.6 ± 23.8%; $P < 0.001$), and locomotor frequency (+25.8 ± 9.1%; $P < 0.01$; pooled data from three preparations, 18 bouts, and six intensities per preparation; Fig. S4 *D–F*). These effects were reduced after DA washout ($P < 0.05$ or $P < 0.001$ vs. DA). Bath-applied DA also increased the number of reticulospinal spikes (+72.4 ± 17.9%; $P < 0.001$ vs. control) and the duration of spiking activity (+58.4 ± 14.7%; $P < 0.001$ vs. control). These increases were also reversed after approximately 1 h of DA washout ($P < 0.01$ vs. DA in both cases).

Next, we determined that DA has a direct excitatory effect on the MLR. Microinjections of 1.0 to 7.0 pmol of DA (5 mM, $n =$ 5–38 pulses of 20 ms, 0.2–1.4 nL per microinjection) in the MLR

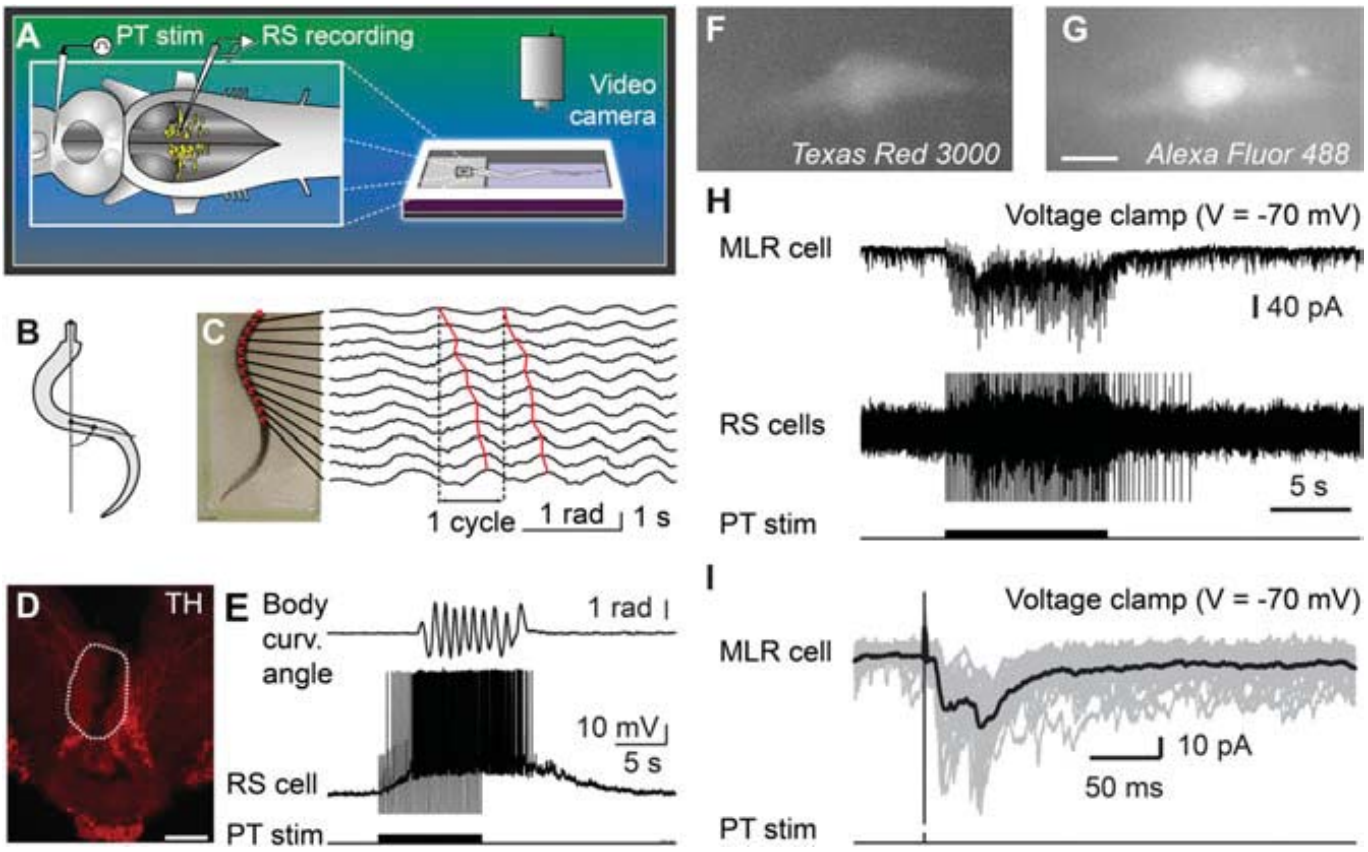

Fig. 3. Stimulation of the PT activates brainstem locomotor circuits. (*A–E*) In a semi-intact preparation, the PT was stimulated and the reticulospinal (RS) cells were recorded together with locomotor movements. (*B* and *C*) Body curvature oscillations during locomotion. (*C*) PT stimulation (10-s train, 5 Hz, 11 μA, 2-ms pulses) elicited swimming as illustrated by the rostrocaudal mechanical wave. (*D*) The PT stimulation site was confirmed histologically by an electrolytic lesion (enclosed by white dashed line) that colocalized with TH-immunoreactive neurons (red). (Scale bar: 200 μm.) (*E*) PT stimulation elicited reticulospinal activity together with swimming. Stimulation artifacts were clipped. (*F–I*) Whole-cell patch-clamp recordings of MLR neurons retrogradely labeled from an injection of dextran amines conjugated to Texas red (MW, 3,000 Da) in the MRRN. (*F* and *G*) MLR neuron labeled by the Texas red–dextran amine injection in the MRRN and by the fluorescent marker added to the patch pipette solution (Alexa Fluor 488 hydrazide). (Scale bar: 10 μm.) (*H*) Trains of stimuli (10-s train, 5 Hz, 7 μA, 2-ms pulses) activated the whole-cell patch-clamped MLR neuron concomitantly with reticulospinal neurons, which were used to monitor locomotor activation. Action potentials were recorded extracellularly from reticulospinal neurons of the MRRN, and stimulation artifacts were clipped. (*I*) Single pulse PT stimulation (0.1 Hz, 7 μA, 2-ms pulses) elicited short-latency excitatory postsynaptic currents in MLR neurons. (*H* and *I*) Data from two different animals.

(as confirmed by histologic examination; Fig. S2 *J* and *L*) increased the locomotor output elicited by trains of electrical stimulation (10-s train, 5 Hz, 4–7 μA, 2-ms pulses) in the PT (Fig. 3*D*) in a semi-intact preparation (n = 25 injections in five preparations; Fig. 5 *A–C*). DA microinjections prolonged the locomotor bout duration (+56.7 ± 14.3%; $P < 0.001$) and increased the number of locomotor cycles (+50.8 ± 12.3%; $P < 0.001$). These effects were reversed after DA washout ($P < 0.05$ vs. injection in both cases; Fig. 5*C*). DA injections in the MLR also increased the duration of reticulospinal cell spiking activity (+33.6 ± 11.8%; $P < 0.01$). This effect was reversed after approximately 1 h of washout ($P < 0.01$; Fig. 5*C*). The effects on locomotor threshold were not measured in these experiments. The excitatory effect of DA microinjections in the MLR was lower than that of bath-applied DA, probably because of the single site of action of DA during local microinjections. For instance, local DA microinjections in the MLR did not significantly modify the locomotor frequency that remained at 95.2 ± 3.0% of control ($P > 0.05$), or the number of reticulospinal spikes that remained at 119.5 ± 11.1% of control ($P > 0.05$).

D1 receptor activation is known to have excitatory effects on striatal cells in mammals (reviewed in ref. 13). Those receptors are also present in lampreys (14, 15). Targeted blocking of D1 receptors in the MLR (Fig. S2 *J* and *L*) dramatically decreased the locomotor output elicited by stimulation of the PT (10-s train, 5 Hz, 7–11 μA, 2-ms pulses; Fig. 3*D*). Local microinjection of 0.1 to 0.8 pmol of the D1 antagonist SCH 23390 (500 μM, 6–43 pulses of 20 ms, 0.2–1.6 nL per microinjection) in the MLR (n = 25 injections in five preparations; Fig. 5 *D–F*) decreased the duration of locomotor bouts (−48.4 ± 10.6%; $P < 0.001$ vs. control), locomotor frequency (−32.2 ± 6.3%; $P < 0.001$), and the number of locomotor cycles (−60.0 ± 9.9%; $P < 0.001$). These decreases in locomotor output were reversed after washout (for all parameters, $P < 0.001$ vs. injection; Fig. 5*F*). Blocking D1 receptors in the MLR also decreased the duration of spiking activity in reticulospinal neurons (−43.8 ± 9.4%; $P < 0.001$ vs. control), their discharge frequency (−30.8 ± 9.9%; $P < 0.01$), and their number of spikes (−41.6 ± 11.9%; $P < 0.001$). Recovery was obtained after approximately 1 h of washout ($P < 0.05$ or $P < 0.01$ vs. injection; Fig. 5*F*).

Discussion

Newly Identified Descending DA Pathway. In this study, we provide evidence for a descending DA projection from the PT to the MLR that modulates motor output. This descending DA pathway supports DA release, which increases locomotor output, and D1 receptors are involved in this excitatory effect. It appears that this descending DA pathway amplifies the previously known excitatory glutamatergic inputs to MLR cells (10). Such a descending DA projection is also very likely to be present in

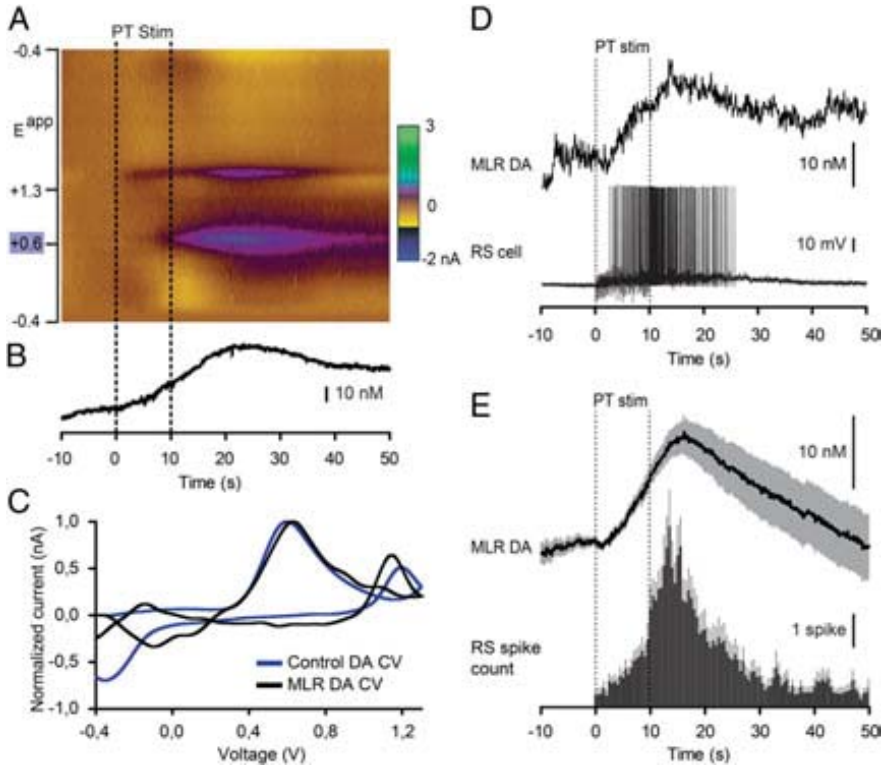

Fig. 4. Stimulation of the PT evokes DA release in the MLR together with reticulospinal (RS) activity. (*A*) DA release evoked by PT stimulation (PT Stim, 10-s train, 5 Hz, 15 μA, 2-ms pulses) in an isolated brain preparation (stimulation period = 0–10 s). The color plot depicts current changes (in color) across the applied voltages (E^{app}; i.e., ordinate) over time (i.e., abscissa). DA is identified by its oxidation peak (~0.6 V) that appears during PT stimulation. (*B*) Changes in DA concentration in the MLR extracted from *A*. (*C*) Plots of normalized current vs. voltage. The DA electrochemical signal (cyclic voltammogram; CV) recorded from the MLR in *A* (black) is similar ($R = 0.82$, $P < 0.001$) to that measured from a 1-μM control DA solution (blue) bath-applied following the experiment, thus confirming DA detection. (*D*) The DA release in the MLR elicited by PT stimulation was positively correlated with the number of spikes evoked in reticulospinal cells. (*E*) Changes in DA concentration plotted vs. the number of reticulospinal spikes per unit time (bin represents 500 ms) in the same trials ($n = 30$ stimulations from six preparations). Mean ± SEM are illustrated.

mammals, although not yet described. For instance, there is a projection from the SNc to the PPN in rats (6), and DA terminals are present in the PPN in monkeys (5). We now confirm in lampreys that DA neurons in the PT project to the striatum as previously described (3). This supports the idea that the lamprey PT is homologous to the SNc and/or VTA of other vertebrates, including other fishes (16, 17), amphibians (18), birds and mammals (reviewed in ref. 19), and humans (20). Moreover, a recent series of studies demonstrated in detail that the basic organization of the basal ganglia, which are target structures of the PT, have physiological and anatomical features that are very similar to those of birds and mammals (refs. 2, 15, 21–25; reviewed in ref. 26). These interesting studies demonstrated that forebrain structures are highly conserved in vertebrates. Therefore, ascending and descending projections of DA cells of the SNc and/or VTA are very likely to have been conserved in vertebrates.

Functional Significance. The presence of a direct DA pathway from SNc/VTA to the MLR may have significant implications for our understanding of the role of DA in motor control under normal and pathological conditions. For instance, DA inputs to the MLR could be involved in the increased exploratory behavior elicited by a novel stimulus, to which a large part of DA neurons are known to respond (reviewed in ref. 27). This pathway could also play a role in the well-documented locomotor effects of the DA drugs of abuse (e.g., hyperlocomotor effects of psychostimulants). In patients with Parkinson disease, DA neurons from the SNc/VTA undergo degeneration, which affects their ascending inputs to the basal ganglia. The descending DA projection we now describe should also be affected and play a role in the locomotor deficits. Interestingly, a depletion of DA terminals was recently shown in the PPN of monkeys treated with 1-methyl-4-phenyl-1,2,3,6-tetrahydropyridine (MPTP) (5), a molecule that has been used extensively in mammals to mimic the motor deficits observed in Parkinson disease. Interestingly, forebrain DA depletion in lampreys injected with MPTP is also associated with severe locomotor deficits, characterized by a decrease in the initiation and maintenance of locomotor activity (28). The locomotor deficits in these pathological conditions may involve, at least in part, the loss of the excitatory DA input to the MLR we describe here. Taken together, these observations suggest that the descending DA projection we report here is conserved across vertebrates and is compromised by the death of DA cells in the SNc/VTA. As such, our results thus provide insights into the role of DA cells of the SNc/VTA in locomotor control.

Materials and Methods

All procedures conformed to the guidelines of the Canadian Council on Animal Care and Association for Assessment and Accreditation of Laboratory Animal Care, and were approved by the animal care and use committee of the Université de Montréal, the Université du Québec à Montréal, and the University of Illinois at Chicago. Care was taken to minimize the number of animals used and their suffering.

Animals. Experiments were performed on 33 larval, 5 newly transformed, and 17 spawning-phase sea lampreys (*Petromyzon marinus*). Larval and newly transformed animals were collected in the wild from the Morpion stream (Québec, Canada) or the Pike River (Québec, Canada), or purchased from ACME Lamprey. Spawning-phase lampreys were captured during their spring run in the Great Chazy river (New York) and given to us by the US Fish and Wildlife Service of Vermont. The animals were kept in aerated water at 5 °C.

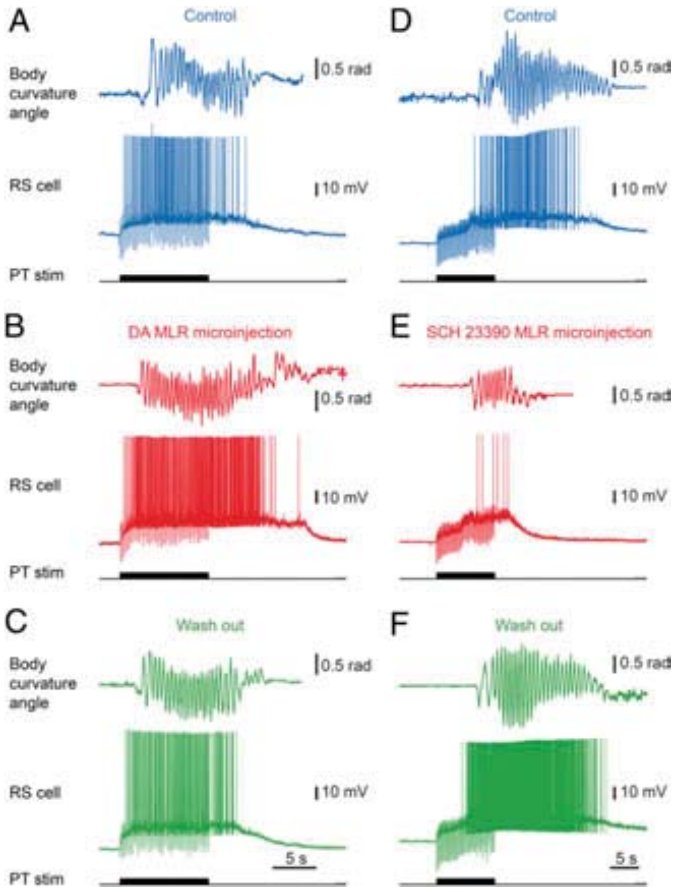

Fig. 5. The descending dopaminergic (DA) projection from the PT to the MLR controls locomotion. DA or the D1 antagonist SCH 23390 was microinjected in the MLR with a Picospritzer in a semi-intact preparation. (*A–C*) Microinjection of DA (5 mM; *Materials and Methods*) in the MLR increased the locomotor and reticulospinal (RS) activities elicited by PT stimulation (10-s train, 5 Hz, 6 μA, 2-ms pulses). (*D–F*) Microinjection of the D1 antagonist SCH 23390 (500 μM; *Materials and Methods*) in the MLR decreased the locomotor output elicited by PT stimulation (10-s train, 5 Hz, 11 μA, 2-ms pulses). In both cases, the locomotor response and the corresponding reticulospinal activity are illustrated. Blue indicates control condition, red indicates microinjection of DA compounds in the MLR, and green indicates washout.

Surgical Procedures. The animals were anesthetized with tricaine methanesulfonate (MS 222; 100 mg/L) and then transferred in a cold oxygenated Ringer solution (8–10 °C, 100% O_2) of the following composition (in millimolar): 130 NaCl, 2.1 KCl, 2.6 $CaCl_2$, 1.8 $MgCl_2$, 4 Hepes, 4 dextrose, and 1 $NaHCO_3$ (pH 7.4). For anatomical experiments, the whole brain was then isolated in vitro and injected with anatomical tracers as described later. A total of 5 larval and 17 spawning-phase animals were used for the anatomical experiments.

Anatomical Tracing. Biocytin was used for retrograde tracing experiments. In the case of double labeling, biocytin and Texas red–dextran amines were used. For both tracers, the injection site was first lesioned with a pulled glass micropipette. Crystals of the tracers were immediately placed inside the lesioned site to dissolve for 10 min, and then the whole brain was rinsed thoroughly for 5 min, including the injection site. The tracer injection sites were chosen on the basis of previous anatomical and physiological studies [MRRN and MLR (refs. 7–10; reviewed in ref. 4) and striatum (2, 3, 23)] and verified by histologic examination (Fig. S2). The preparations were then transferred into a dark refrigerated chamber and continuously perfused with new, oxygenated Ringer solution overnight for retrograde transport of the tracer to occur. The following day, the preparations were transferred into a fixative solution chosen according to the immunofluorescence procedure to follow (as detailed later).

Immunofluorescence. Experimental procedures for immunofluorescence against TH, choline acetyltransferase (ChAT), or DA were undertaken immediately after anatomical tracing. Fixation of the tissue was the first step. For TH and ChAT, the neural tissue was immersed in 4% (wt/vol) paraformaldehyde in PBS solution (0.1 M, pH 7.4, 0.9% NaCl) for 24 h and then transferred to a phosphate-buffered 20% (wt/vol) sucrose solution. For DA, the neural tissue was first immersed for 5 min in 0.1 M cacodylate buffer, pH 6.2, containing 0.9% sodium metabisulfite (MBS), followed by 55 min in 0.1 M cacodylate buffer, pH 7.5, containing 0.9% MBS. The tissue was then rinsed thoroughly with 0.05 M Tris buffer containing 0.9% MBS (TBMBS) and transferred overnight to another vial containing the same solution with 20% (wt/vol) sucrose. The brain tissue was sectioned transversely at 25-μm thickness with a cryostat, and the sections were collected on ColorFrost Plus microscope slides (Fisher Scientific) and air-dried overnight on a warming plate. If biocytin had been injected as a tracer, the sections were first rinsed three times, 10 min each, before being incubated for 30 min in PBS solution (or TBMBS for DA) containing a 1:200 dilution of streptavidin–Alexa Fluor 594, 488, or 350 (Invitrogen), depending on the color needs. The sections were then rinsed again three times for 10 min each with PBS solution (or TBMBS).

For ChAT immunofluorescence, the sections were then preincubated in a PBS solution containing 0.3% Triton X-100 and 5% (vol/vol) normal horse serum for 60 min. The sections were then incubated in the same preincubation solution containing a goat anti-ChAT antibody (diluted 1:80; AB144P; Millipore) overnight at 4 °C. The following day, the sections were rinsed three times for 10 min each in PBS solution and incubated in the preincubation solution containing a donkey anti-goat Alexa Fluor 488 antibody (diluted 1:200; A11055; Invitrogen) for 60 min. The sections were then rinsed three times for 10 min each with PBS solution and once with deionized water, and left to dry on a warming plate for 5 min. The slides were then mounted with Vectashield with or without DAPI (H1000 or H1200; Vector).

For TH immunofluorescence, normal goat serum was used instead of normal horse serum, and the antibodies used were a rabbit anti-TH (diluted 1:400; AB152; Millipore) and a donkey anti-rabbit Alexa Fluor 594 (diluted 1:400; A21207; Invitrogen) or a goat anti-rabbit Alexa Fluor 488 (1:400; A11008; Invitrogen). All other steps were as described for ChAT immunofluorescence. TH immunofluorescence was used to visualize DA neurons. This choice was based on other studies in lampreys (3, 29, 30).

For DA immunofluorescence, PBS solution was replaced with TBMBS, Triton X-100 was increased to 0.5%, and 5% (vol/vol) normal goat serum was used as for TH. The antibodies used were a mouse anti-DA (diluted 1:400; MAB5300; Millipore) and a goat anti-mouse DyLight 594 (diluted 1:200; 115-515-146; Jackson ImmunoResearch). All other steps were as described for ChAT immunofluorescence.

Specificity of the fluorescent secondary antibodies was verified by omitting the primary antibody from the procedures described earlier. In every case, no labeling was obtained under these conditions. The AB144P antibody has been used on lampreys for many years by different research teams, and its selectivity against ChAT is well demonstrated (7, 31, 32). The AB152 antibody against TH has been used reliably on lampreys in many independent studies on DA neurons (24, 33, 34). The specificity of the MAB5300 antibody for DA was tested by ELISA by the manufacturer, and its pattern of labeling in our material corresponded closely to that reported with other DA antibodies in the lamprey (29, 30).

The sections were then observed and photographed using an E600 epifluorescence microscope equipped with a DXM1200 digital camera (Nikon). Combining digital photomicrographs taken with different filter sets and adjusting the levels so that all fluorophores were clearly visible simultaneously was done by using Photoshop CS5 (Adobe). To avoid double counting as a result of the sectioning of the tissue, cells were counted on only half the sections, skipping one in between. The cell counts provided are thus close to half of the actual total neuronal counts, except for TH-containing neurons of the PT projecting to both the striatum and the MLR, in which case all neurons from all sections were counted because of their rarity.

Semi-intact Preparation. To simultaneously record the activity of reticulospinal cells and locomotor movements, a semi-intact preparation was used. We used 13 larval animals for these experiments. The procedure was as described elsewhere (10, 35, 36). To expose the brain and the rostral segments of the spinal cord, skin, muscles, and surrounding tissues were removed from the rostral part of the animal, down to the caudal gills. The dorsal surface of the cranium was opened to obtain free access to the reticulospinal neurons in the MRRN. A transverse section was performed at the level of the habenula to eliminate the inputs from the basal ganglia and other rostral areas to the MLR. A dorsal midsagittal transection was per-

formed at the level of the diencephalon to provide access to the PT. The preparation was then transferred into the recording chamber. The cartilage containing the brain was pinned down to the bottom of a recording chamber covered with Sylgard (Dow Corning), whereas the intact body was left to swim freely in a video monitored adjacent chamber. The preparation was continually perfused with cold oxygenized Ringer solution (4 mL/min) and cooled to a temperature of 8 to 10 °C. A recovery time of at least 1 h after surgery was given before recording. When bath-applying DA onto the brain, the recording chamber was partitioned at the level of the caudal rhombencephalon with petroleum jelly, and the two partitions were independently perfused. Electrical stimulation of the PT (10-s train, 4–5 Hz, 4–30 μA, 2-ms pulses) elicited swimming movements during the experiments. At the end of the experiment, an electrolytic lesion (5 s, DC current, 10 μA) was performed to histologically control the location of the stimulation site (Fig. 3*D*).

Kinematic Recordings and Analysis. Locomotor movements of body were recorded (30 frames per second) by a video camera (HDR-XR200; Sony) positioned 1 m above the recording chamber. Locomotor movements were tracked and analyzed by using custom written scripts in Matlab (MathWorks) previously used in our laboratory (11, 35). Briefly, tracking markers were equidistantly distributed along the midline of the body by using geometrical analysis of the body. Swimming movements were monitored frame-by-frame through local measurement of the angle between the longitudinal axis of nonmoving parts of the body and the line drawn by two successive markers (35). The local curvature angles were determined throughout the whole body. This allowed us to observe that a mechanical wave was traveling rostrocaudally along the body, as expected during forward swimming. For further analysis, monitoring the body curvature of a single pair of markers at a specific point along the body (at 50% of body length) was sufficient to monitor the locomotor frequency, the number of locomotor cycles, and the duration of the locomotor bouts (35).

Isolated Brain Preparation. For experiments in an isolated brain preparation (10 larval animals for voltammetry experiments; 5 newly transformed and 1 larval animal for patch experiments), the same dissection procedure as described for the semi-intact preparation was performed, but the caudal body parts were removed after a complete transversal cut at the level of the first spinal cord segment.

Electrophysiological Recordings and Stimulation. Intracellular recordings of reticulospinal neurons in the MRRN region were performed as described elsewhere with the use of sharp microelectrodes (80–110 MΩ) filled with a 4 M potassium acetate solution (35–37). The signals were amplified by an Axoclamp 2A amplifier (sampling rate of 2–10 kHz; Axon Instruments) and acquired through a Digidata 1200 series interface coupled with Clampex 9.0 software (Axon Instruments) or AxoGraph X 1.4.4 (John Clements). Only reticulospinal neurons with a stable membrane potential, held for 5 min after impalement and lower than −60 mV, were included in the study. Extracellular recordings of reticulospinal neurons were performed by using a glass microelectrode filled with Ringer solution (tip diameter, 5 μm) and amplified with a microelectrode AC amplifier (bandwidth 100–500 Hz; model 1800; A-M Systems).

Homemade glass-coated tungsten microelectrodes (4–5 MΩ with 10-μm exposed tip) and a Grass S88 stimulator coupled to a Grass PSIU6 photoelectric isolation unit for controlling the stimulation intensity (Astro Med) were used for unilateral electrical stimulation of the PT. The stimulation site was chosen on the basis of previous anatomical and physiological studies (3, 10, 11). Electrical square pulses (2-ms duration) were applied with a frequency of 4 to 5 Hz for 10 s for train stimulation. A pause of 3 to 5 min was allowed between two train stimulations. Single stimuli at 0.1 Hz were used for eliciting excitatory postsynaptic currents. The stimulation intensities ranged from 4 to 35 μA. This would theoretically correspond to a maximum spread of the injected current ranging from 80 to 354 μm around the stimulation site (reviewed in ref. 38). In all types of preparations used in the present study, an electrolytic lesion was made at the end of the experiment to control histologically the location of the electrode (Fig. 3*D* shows semi-intact preparation; Fig. S2 *G–I* shows patch and voltammetry experiments in the isolated brain preparation).

Patch clamp was coupled with retrograde labeling to record targeted MLR neurons projecting to reticulospinal neurons on the basis of the protocol described elsewhere to record MLR cells projecting to respiratory networks (11). A surgery was made 24 h before the experiment. The animals were anesthetized with tricaine methanesulfonate (MS 222; 100 mg/L) and then transferred in a cold oxygenated Ringer solution (8–10 °C, 100% O_2). A 2-mm^2 flap window was opened on the top of the head to expose the caudal brainstem. MLR neurons were retrogradely labeled from an injection of Texas red–dextran amines [molecular weight (MW) of 3,000 Da; Molecular Probes] in the MRRN region. The incision was closed with Vetbond after the injection procedure. The animal was then returned to a nursery aquarium filled with oxygenated Ringer solution at room temperature. After maintaining the animal for 24 h to allow retrograde labeling of MLR cells, the brain was extracted and prepared for patch recordings. To access the MLR cells, the dorsal part of the isthmus and caudal mesencephalon was removed with a Vibratome in a cold Ringer solution (1–3 °C). The giant reticulospinal cell I1 was used as landmark to locate the MLR. Neurons were recorded under whole-cell patch clamp. Pipettes were pulled to a tip resistance of 4 to 6 MΩ. Bright-field and fluorescence imaging of the traced neurons were combined to allow targeted whole-cell patch recording of MLR cells projecting to the reticular formation. Patch pipette solution contained (in millimolar): cesium methane sulfonate 102.5, NaCl 1, $MgCl_2$ 1, EGTA 5, Hepes 5, ATP 0.3, GTP 0.1, and biocytin at 0.05%. Biocytin allowed us to identify the recorded cell. The pH was adjusted to 7.2 with CsOH, and the osmolarity to 240 mOsm with H_2O. Positive pressure was applied to the pipettes to allow tissue penetration by the electrode. Pressure was removed to allow a seal against the fluorescently labeled neurons. Recordings were made with a patch-clamp amplifier 2400 (A-M Systems).

Data analysis was performed by using ClampFit 10.0 (Axon Instruments), Spike2 5.19 (Cambridge Electronic Design), or Matlab 7.8 (MathWorks).

Voltammetry Recordings. DA concentration evoked by PT stimulation (10-s train, 5 Hz, 14–25 μA, 2-ms pulses) was locally measured by using fast-scan cyclic voltammetry with glass-insulated, Nafion-coated, carbon-fiber microelectrodes. As previously described (12), electrodes were made from individual carbon fibers (7-μm diameter; Goodfellow). Fibers were aspirated into glass pipettes (0.6 mm o.d., 0.4 mm i.d.; A-M Systems) and pulled on a vertical puller (Narishige). The glass seal was evaluated under light microscopy and the carbon fiber was cut to a length of 75 to 100 μm by using a scalpel. Following construction, the electrode was coated in Nafion (LQ-1105; Ion Power) and baked at 75 °C for 10 min. The electrodes were placed in the MLR and held at −0.4 V against Ag/AgCl between voltammetric scans and then driven to +1.3 V and back at 400 $V{\cdot}s^{-1}$ every 100 ms. Electroactive species within this voltage range oxidize and reduce at different points along the voltage scan and can be identified on the basis of their background-subtracted current by voltage (i.e., cyclic voltammogram) plots (12). Data were acquired and analyzed by using software written in LabVIEW 7.1 (National instruments). Stimulation artifacts were manually removed by interpolation. An electrolytic lesion (5 s, DC current, 10 μA) was performed in the recording site at the end of the experiment to verify histologically the location of the electrode (Fig. S2 *J* and *K*).

Drug Application. All drugs were purchased from Sigma and were diluted to their final concentration in Ringer solution. In some experiments, DA was bath-applied at a concentration of 10 μM. In other experiments, DA (5 mM) or the D1 receptor antagonist SCH 23390 (500 μM) were microinjected locally in the MLR, and D-glutamate (5 mM) was microinjected locally in the PT. As previously done in our laboratory (7, 8, 10, 11, 35, 37, 39), the microinjections were performed through a glass micropipette (tip diameter, 10–20 μm) by applying pressure pulses (3–4 psi) of various durations (20–100 ms) with a Picospritzer (General Valve) ipsilaterally to the stimulation and intracellular recording sites. Fast Green was added to the drug solution for visualizing the injection site as described elsewhere (e.g., refs. 10, 11, 37). The injected volumes were estimated by measuring the diameter of a droplet ejected in air from the tip of the pipette after applying a single pressure pulse. The volume of the droplet was calculated by using the equation of a sphere. The total volume of each microinjection was then estimated by multiplying this volume by the number of pulses used per microinjection, as previously done in our laboratory (e.g., refs. 7, 39). For each drug, the number of moles ejected was calculated. The size of the injections was also controlled visually under the microscope by measuring the spread of Fast Green at the level of the injection site in the brain tissue. The spread did not exceed 300 μm in diameter for any of these injections. This was also confirmed in four larval lampreys by measuring the spread of HRP [10% (wt/vol)] microinjection into the brain tissue (Fig. S2 *J* and *L*), as previously done by us (39). For bath applications and local drug injections, the drugs were washed out for a period of 1 h.

Statistics. Data in the text are presented as the mean ± SEM. The statistical analysis was performed by using Sigma Plot 11.0 (Systat) or Origin 7.0 (OriginLab). Statistical differences were assumed to be significant at $P < 0.05$. One-tailed paired Student *t* tests were used for comparing means between two groups. Correlations between variables were calculated using the Pearson product–moment correlation test.

ACKNOWLEDGMENTS. We thank Danielle Veilleux for technical assistance, Jean-François Gariépy for help with some of the experiments, and Frédéric Bernard for help with graphics. This work was supported by Canadian Institutes of Health Research Grants 15129 and 15176 (to R.D.), Parkinson Society Canada Grant 2011-11 (to R.D.), Fonds de la Recherche en Santé du Québec Groupe de Recherche sur le Système Nerveux Central (GRSNC) Grant 5249, Natural Sciences and Engineering Research Council of Canada Grant 217435 (to R.D.), National Institutes of Health Grant R01 MH 084874 (to S.A); Fonds de la Recherche en Santé du Québec fellowships (to D.R.); and a GRSNC Jasper Fellowship (to D.R.).

1. Kravitz AV, et al. (2010) Regulation of parkinsonian motor behaviours by optogenetic control of basal ganglia circuitry. *Nature* 466(7306):622–626.
2. Stephenson-Jones M, Samuelsson E, Ericsson J, Robertson B, Grillner S (2011) Evolutionary conservation of the basal ganglia as a common vertebrate mechanism for action selection. *Curr Biol* 21(13):1081–1091.
3. Pombal MA, El Manira A, Grillner S (1997) Afferents of the lamprey striatum with special reference to the dopaminergic system: A combined tracing and immunohistochemical study. *J Comp Neurol* 386(1):71–91.
4. Le Ray D, Juvin L, Ryczko D, Dubuc R (2011) Chapter 4—supraspinal control of locomotion: The mesencephalic locomotor region. *Prog Brain Res* 188:51–70.
5. Rolland AS, et al. (2009) Evidence for a dopaminergic innervation of the pedunculopontine nucleus in monkeys, and its drastic reduction after MPTP intoxication. *J Neurochem* 110(4): 1321–1329.
6. Beckstead RM, Domesick VB, Nauta WJ (1979) Efferent connections of the substantia nigra and ventral tegmental area in the rat. *Brain Res* 175(2):191–217.
7. Le Ray D, et al. (2003) Nicotinic activation of reticulospinal cells involved in the control of swimming in lampreys. *Eur J Neurosci* 17(1):137–148.
8. Smetana R, Juvin L, Dubuc R, Alford S (2010) A parallel cholinergic brainstem pathway for enhancing locomotor drive. *Nat Neurosci* 13(6):731–738.
9. Ménard A, Auclair F, Bourcier-Lucas C, Grillner S, Dubuc R (2007) Descending GABAergic projections to the mesencephalic locomotor region in the lamprey Petromyzon marinus. *J Comp Neurol* 501(2):260–273.
10. Derjean D, et al. (2010) A novel neural substrate for the transformation of olfactory inputs into motor output. *PLoS Biol* 8(12):e1000567.
11. Gariépy JF, et al. (2012) Specific neural substrate linking respiration to locomotion. *Proc Natl Acad Sci USA* 109(2):E84–E92.
12. Roitman MF, Wheeler RA, Wightman RM, Carelli RM (2008) Real-time chemical responses in the nucleus accumbens differentiate rewarding and aversive stimuli. *Nat Neurosci* 11(12):1376–1377.
13. Surmeier DJ, Ding J, Day M, Wang Z, Shen W (2007) D1 and D2 dopamine-receptor modulation of striatal glutamatergic signaling in striatal medium spiny neurons. *Trends Neurosci* 30(5):228–235.
14. Le Crom S, Kapsimali M, Barôme PO, Vernier P (2003) Dopamine receptors for every species: Gene duplications and functional diversification in Craniates. *J Struct Funct Genomics* 3(1-4):161–176.
15. Ericsson J, et al. (2013) Dopamine differentially modulates the excitability of striatal neurons of the direct and indirect pathways in lamprey. *J Neurosci* 33(18):8045–8054.
16. Blin M, Norton W, Bally-Cuif L, Vernier P (2008) NR4A2 controls the differentiation of selective dopaminergic nuclei in the zebrafish brain. *Mol Cell Neurosci* 39(4): 592–604.
17. Rink E, Wullimann MF (2001) The teleostean (zebrafish) dopaminergic system ascending to the subpallium (striatum) is located in the basal diencephalon (posterior tuberculum). *Brain Res* 889(1-2):316–330.
18. Marín O, Smeets WJ, González A (1997) Basal ganglia organization in amphibians: Catecholaminergic innervation of the striatum and the nucleus accumbens. *J Comp Neurol* 378(1):50–69.
19. Yamamoto K, Vernier P (2011) The evolution of dopamine systems in chordates. *Front Neuroanat* 5:21.
20. Puelles L, Verney C (1998) Early neuromeric distribution of tyrosine-hydroxylase-immunoreactive neurons in human embryos. *J Comp Neurol* 394(3):283–308.
21. Ericsson J, Silberberg G, Robertson B, Wikström MA, Grillner S (2011) Striatal cellular properties conserved from lampreys to mammals. *J Physiol* 589(pt 12):2979–2992.
22. Ericsson J, et al. (2013) Evolutionarily conserved differences in pallial and thalamic short-term synaptic plasticity in striatum. *J Physiol* 591(pt 4):859–874.
23. Pombal MA, El Manira A, Grillner S (1997) Organization of the lamprey striatum - transmitters and projections. *Brain Res* 766(1-2):249–254.
24. Robertson B, et al. (2012) The dopamine D2 receptor gene in lamprey, its expression in the striatum and cellular effects of D2 receptor activation. *PLoS ONE* 7(4):e35642.
25. Stephenson-Jones M, Ericsson J, Robertson B, Grillner S (2012) Evolution of the basal ganglia: Dual-output pathways conserved throughout vertebrate phylogeny. *J Comp Neurol* 520(13):2957–2973.
26. Grillner S, Robertson B, Stephenson-Jones M (2013) The evolutionary origin of the vertebrate basal ganglia and its role in action-selection. *J Physiol* 2013(Feb):25.
27. Schultz W, Dayan P, Montague PR (1997) A neural substrate of prediction and reward. *Science* 275(5306):1593–1599.
28. Thompson RH, Ménard A, Pombal M, Grillner S (2008) Forebrain dopamine depletion impairs motor behavior in lamprey. *Eur J Neurosci* 27(6):1452–1460.
29. Abalo XM, Villar-Cheda B, Anadón R, Rodicio MC (2005) Development of the dopamine-immunoreactive system in the central nervous system of the sea lamprey. *Brain Res Bull* 66(4-6):560–564.
30. Pierre J, Mahouche M, Suderevskaya EI, Repérant J, Ward R (1997) Immunocytochemical localization of dopamine and its synthetic enzymes in the central nervous system of the lamprey Lampetra fluviatilis. *J Comp Neurol* 380(1):119–135.
31. Pombal MA, Marín O, González A (2001) Distribution of choline acetyltransferase-immunoreactive structures in the lamprey brain. *J Comp Neurol* 431(1):105–126.
32. Quinlan KA, Buchanan JT (2008) Cellular and synaptic actions of acetylcholine in the lamprey spinal cord. *J Neurophysiol* 100(2):1020–1031.
33. Villar-Cerviño V, et al. (2006) Presence of glutamate, glycine, and gamma-aminobutyric acid in the retina of the larval sea lamprey: Comparative immunohistochemical study of classical neurotransmitters in larval and postmetamorphic retinas. *J Comp Neurol* 499(5): 810–827.
34. Barreiro-Iglesias A, Villar-Cerviño V, Villar-Cheda B, Anadón R, Rodicio MC (2008) Neurochemical characterization of sea lamprey taste buds and afferent gustatory fibers: Presence of serotonin, calretinin, and CGRP immunoreactivity in taste bud bi-ciliated cells of the earliest vertebrates. *J Comp Neurol* 511(4):438–453.
35. Brocard F, et al. (2010) The transformation of a unilateral locomotor command into a symmetrical bilateral activation in the brainstem. *J Neurosci* 30(2):523–533.
36. Sirota MG, Di Prisco GV, Dubuc R (2000) Stimulation of the mesencephalic locomotor region elicits controlled swimming in semi-intact lampreys. *Eur J Neurosci* 12(11): 4081–4092.
37. Brocard F, Dubuc R (2003) Differential contribution of reticulospinal cells to the control of locomotion induced by the mesencephalic locomotor region. *J Neurophysiol* 90(3): 1714–1727.
38. Ranck JB, Jr. (1975) Which elements are excited in electrical stimulation of mammalian central nervous system: a review. *Brain Res* 98(3):417–440.
39. Brocard F, Bardy C, Dubuc R (2005) Modulatory effect of substance P to the brain stem locomotor command in lampreys. *J Neurophysiol* 93(4):2127–2141.

5.2. Nigral glutamatergic neurons control the speed of locomotion

Ryczko, D., Grätsch, S., Schläger, L., Keuyalian, A., Boukhatem, Z., Garcia, C., Auclair, F., Büschges, A., and Dubuc, R.

Published 2017 in *Journal of Neuroscience*, 37(40):9759-9770.

Author contributions

Designed research:
Dimitri Ryczko, Swantje Grätsch, François Auclair, and Réjean Dubuc.

Performed research:
Dimitri Ryczko, Swantje Grätsch, Laura Schläger, Avo Keuyalian, Zakaria Boukhatem, Claudia Garcia, and François Auclair.

Analyzed data:
Dimitri Ryczko, Swantje Grätsch, Laura Schläger, Avo Keuyalian, Zakaria Boukhatem, Claudia Garcia, François Auclair, and Réjean Dubuc.

Wrote the paper:
Dimitri Ryczko, Ansgar Büschges, and Réjean Dubuc.

Systems/Circuits

Nigral Glutamatergic Neurons Control the Speed of Locomotion

Dimitri Ryczko,[1,2] Swantje Grätsch,[1,3] Laura Schläger,[1] Avo Keuyalian,[1] Zakaria Boukhatem,[1] Claudia Garcia,[1] François Auclair,[1] Ansgar Büschges,[3] and Réjean Dubuc[1,4]

[1]Groupe de Recherche sur le Système Nerveux Central, Département de Neurosciences, Université de Montréal, Montréal, Québec H3C 3J7, Canada, [2]Département de Pharmacologie-Physiologie, Université de Sherbrooke, Sherbrooke, Québec J1H 5N4, Canada,[3]Department of Animal Physiology, Biocenter Cologne, University of Cologne, 50674 Cologne, Germany, and [4]Groupe de Recherche en Activité Physique Adaptée, Département des Sciences de l'Activité Physique, Université du Québec à Montréal, Montréal, Québec, H3C 3P8, Canada

The mesencephalic locomotor region (MLR) plays a crucial role in locomotor control. In vertebrates, stimulation of the MLR at increasing intensities elicits locomotion of growing speed. This effect has been presumed to result from higher brain inputs activating the MLR like a dimmer switch. Here, we show in lampreys (*Petromyzon marinus*) of either sex that incremental stimulation of a region homologous to the mammalian substantia nigra pars compacta (SNc) evokes increasing activation of MLR cells with a graded increase in the frequency of locomotor movements. Neurons co-storing glutamate and dopamine were found to project from the primal SNc to the MLR. Blockade of glutamatergic transmission largely diminished MLR cell responses and locomotion. Local blockade of D_1 receptors in the MLR decreased locomotor frequency, but did not disrupt the SNc-evoked graded control of locomotion. Our findings revealed the presence of a glutamatergic input to the MLR originating from the primal SNc that evokes graded locomotor movements.

Key words: **dopamine; glutamate; lamprey; locomotion; mesencephalic locomotor region; substantia nigra pars compacta**

Significance Statement

The mesencephalic locomotor region (MLR) plays a crucial role in the control of locomotion. It projects downward to reticulospinal neurons that in turn activate the spinal locomotor networks. Increasing the intensity of MLR stimulation produces a growing activation of reticulospinal cells and a progressive increase in the speed of locomotor movements. Since the discovery of the MLR some 50 years ago, it has been presumed that higher brain regions activate the MLR in a graded fashion, but this has not been confirmed yet. Here, using a combination of techniques from cell to behavior, we provide evidence of a new glutamatergic pathway activating the MLR in a graded fashion, and consequently evoking a progressive increase in locomotor output.

Introduction

In the brainstem, the mesencephalic locomotor region (MLR) plays a crucial role in locomotor control. First discovered in cats by a Russian team (Shik et al., 1966), the MLR was found in all vertebrates tested afterward (lamprey: Sirota et al., 2000; salamander: Cabelguen et al., 2003; stingray: Bernau et al., 1991; bird: Sholomenko et al., 1991; rat: Garcia-Rill et al., 1987; mouse: Lee et al., 2014; Roseberry et al., 2016; rabbit: Musienko et al., 2008; guinea-pig: Marlinsky and Voitenko, 1991; monkey: Eidelberg et al., 1981; Karachi et al., 2010; Goetz et al., 2016). The MLR projects downward to reticulospinal neurons, which activate the spinal locomotor networks (cat: Orlovskiĭ, 1970; Steeves and Jordan, 1980; Garcia-Rill and Skinner, 1987a,b; Noga et al., 1991; Musienko et al., 2012; rat: Bachmann et al., 2013; bird: Sholomenko et al., 1991; lamprey: Buchanan and Grillner, 1987; Brocard et al., 2010; mouse: Bretzner and Brownstone, 2013; salamander: Ryczko et al., 2016a). One salient feature of the MLR lies in its ability to finely control locomotor output. Increasing MLR stimulation intensity produces a growing activation of reticulospinal cells and a progressive increase in the speed of locomotor movements.

Since the discovery of the MLR (Shik et al., 1966), it was presumed that the MLR is activated incrementally (i.e., like a dimmer switch) by higher brain regions, but the source of the rheostat-like inputs remained unknown. The MLR receives projections from the cortex, basal ganglia, periaqueductal gray, lat-

Received June 28, 2017; revised Aug. 8, 2017; accepted Aug. 26, 2017.

Author contributions: D.R., S.G., F.A., and R.D. designed research; D.R., S.G., L.S., A.K., Z.B., C.G., and F.A. performed research; D.R., S.G., L.S., A.K., Z.B., C.G., F.A., A.B., and R.D. analyzed data; D.R., A.B., and R.D. wrote the paper.

This work was supported by the Canadian Institutes of Health Research (15129); the Fonds de la Recherche en Santé du Québec (Groupe de Recherche sur le Système Nerveux Central, GRSNC, 5249); the Natural Sciences and Engineering Research Council of Canada Grant 217435 (R.D.); the Great Lakes Fishery Commission Grants 54011 and 54021 (R.D.); fellowships from the Fonds de la Recherche en Santé du Québec (D.R.) and the GRSNC Jasper fellowship (D.R.); and scholarships from the University of Cologne and the German Academic Exchange Service (S.G.). We thank Arlette Kolta for providing access to her electrophysiology setup for some experiments, Danielle Veilleux for her technical assistance, and Frédéric Bernard for his help with the graphics.

The authors declare no competing financial interests.

Correspondence should be addressed to Dr. Réjean Dubuc, Groupe de Recherche en Activité Physique Adaptée, Département des Sciences de l'Activité Physique, Université du Québec à Montréal, C.P. 8888, Section Centre-ville, Montréal, QC H3C 3P8, Canada. E-mail: rejean.dubuc@gmail.com.

DOI:10.1523/JNEUROSCI.1810-17.2017

 0270-6474/17/379759-12$15.00/0

eral hypothalamus (for review, see Ryczko and Dubuc, 2013), and from dopamine neurons of the substantia nigra pars compacta (SNc; Ryczko et al., 2013, 2016b). The physiological role of these different inputs to the MLR is not fully understood. The tonic inhibition sent by the output stations of the basal ganglia (lamprey: Stephenson-Jones et al., 2011, 2012; Ménard et al., 2007; cat: Takakusaki et al., 2003; mouse: Kravitz et al., 2010; Roseberry et al., 2016) is considered to be involved in action selection and therefore locomotion initiation or suppression, rather than fine control of locomotion (Albin et al., 1989; Redgrave et al., 1999; Grillner et al., 2013; Grillner and Robertson, 2016). The lamprey homolog of the mammalian motor cortex (i.e., pallium) was shown to elicit reticulospinal responses and locomotion (Ocaña et al., 2015), but its contribution to the graded control of MLR activity and locomotion is unknown.

So far, only one source of input to the MLR called the posterior tuberculum (PT) was characterized physiologically. This diencephalic region, which is considered homologous to the mammalian SNc (Pombal et al., 1997; Stephenson-Jones et al., 2011; Ryczko et al., 2013, 2016b), provides a strong excitatory input to MLR cells and robustly evokes locomotion (Derjean et al., 2010; Gariépy et al., 2012a; Ryczko et al., 2013). The PT sends a descending dopaminergic projection to the MLR (Ryczko et al., 2013; Pérez-Fernández et al., 2014) where it releases dopamine that increases locomotor output through a D_1 receptor-dependent mechanism (Ryczko et al., 2013). Interestingly, the PT also contains glutamatergic neurons (Villar-Cerviño et al., 2011, 2013), and data suggest that their descending projections could control MLR activity. The PT sends non-dopaminergic (thus potentially glutamatergic) projections to the MLR (Ryczko et al., 2013). PT stimulation elicits fast synaptic responses in MLR cells (Gariépy et al., 2012a; Ryczko et al., 2013). Blockade of MLR glutamatergic receptors disrupts reticulospinal responses elicited by stimulation of the olfactory bulbs, which project to the PT (Derjean et al., 2010). Glutamate application in the MLR elicits locomotion (Brocard et al., 2010; Gariépy et al., 2012a). However, there is no direct evidence for descending glutamatergic inputs from the PT to the MLR, and it is unknown whether such input can progressively increase MLR activation and the speed of the locomotor movements. Here, using neural tracing, immunofluorescence, calcium imaging, patch-clamp recordings, and intracellular recordings during locomotion in lampreys, we show that a descending glutamatergic pathway originating from the primal SNc controls MLR activity and locomotor movements like a dimmer switch.

Materials and Methods

Ethics statement. All procedures conformed to the guidelines of the Canadian Council on Animal Care and were approved by the animal care and use committees of the Université de Montréal (Quebec, Canada) and Université du Québec à Montréal (Quebec, Canada). A total of 47 sea lampreys (*Petromyzon marinus*) were used, with $n = 36$ larvae for physiology experiments and $n = 4$ transformed and $n = 7$ adults for anatomy experiments. Sex of the individuals used was not taken into account in the present study. Care was taken to minimize the number of animals used and their suffering.

Semi-intact and isolated brain preparations. Larval sea lampreys were anesthetized with tricaine methanesulphonate (MS 222, 200 mg/L; Sigma-Aldrich) dissolved in a Ringer's solution (in mM: 130 NaCl, 2.1 KCl, 2.6 $CaCl_2$, 1.8 $MgCl_2$, 4.0 HEPES, 4.0 dextrose, and 1.0 $NaHCO_3$ at pH 7.4). The animals were anesthetized for 8–10 min and then transferred into oxygenated cold Ringer's solution. To expose the brain, the skin and muscles were removed from the rostral part of the animal. The dorsal cranium was opened to obtain *ad libitum* access to the PT and to reticulospinal neurons in the middle rhombencephalic reticular nucleus (MRRN). Brain tissue rostral to the PT was removed by a transverse section between the diencephalon and the telencephalon. The rostral spinal segments were exposed and the caudal body parts were left intact. The brain was pinned down dorsal side up in the recording chamber, and the body was free to move in a video monitored chamber. To provide access to the PT, a dorsal midsagittal transection was performed at the level of the diencephalon. Recovery time lasted 1 h before the recording experiments began. For isolated brain preparations, the same dissection procedure was used, but the body was removed.

Electrophysiology and stimulation. Intracellular recordings were performed with sharp glass microelectrodes (80–110 MΩ) filled with potassium acetate (4 M). The signals were amplified with an Axoclamp 2A (Molecular Devices). Only cells with a membrane potential < -60 mV and held stable for 15 min after impalement were included in the study.

Extracellular recordings of reticulospinal neurons were performed using glass micropipettes (diameter 5 μm) filled with Ringer's solution and the recordings were amplified with a model 1800 amplifier (bandwidth 100–500 Hz; A-M Systems). Signals were acquired (sampling rate of 5–10 kHz) through a Digidata 1200 series interface coupled with Clampex 9.0 (Brocard et al., 2010; Ryczko et al., 2013).

Targeted patch-clamp recordings of MLR cells were done using the protocol previously developed in the laboratory (Gariépy et al., 2012a; Ryczko et al., 2013). Briefly, MLR cells were first retrogradely labeled *in vivo* from an injection of Texas Red dextran amines (MW 3000 Da; Invitrogen) in the MRRN. The following day, the animal was killed and the brain was isolated and placed in a cold Ringer's solution (1–3 °C). To provide access to MLR cells, the dorsal part of the brain was removed with a vibratome. The giant reticulospinal cell I1 (Rovainen, 1967) was used as a landmark to locate the MLR (Brocard et al., 2010; Ryczko et al., 2013). Retrogradely labeled MLR cells were visualized under a microscope (Nikon Instruments or Olympus) equipped for fluorescence and targeted for whole-cell patch-clamp. Patch pipette (4–6 MΩ) were filled with a solution containing the following (in mM): 102.5 cesium methane sulfonate, 1 NaCl, 1 $MgCl_2$, 5 EGTA, 5 HEPES, 0.3 ATP, and 0.1 GTP. The pH was adjusted to 7.2 with CsOH, and the osmolarity to 240 mOsm with H_2O. The cellular electrophysiological signals were recorded with a model 2400 amplifier (A-M Systems). To measure the drug effects on the amplitude of synaptic responses, 20 excitatory postsynaptic potentials (EPSPs) were recorded for each cell and for each drug condition.

Glass-coated tungsten microelectrodes (0.7–3.1 MΩ with 10–40 μm exposed tip) and a Grass S88 stimulator (Astro Med) coupled to a Grass PSIU6 photoelectric isolation unit for controlling stimulation intensity (Astro Med) were used for electrical stimulation. The stimulation site was chosen on the basis of previous anatomical and physiological studies (Derjean et al., 2010; Gariépy et al., 2012a; Ryczko et al., 2013) and confirmed by subsequent histology (see Fig. 2*B*,*C*). The electrical stimulation consisted of square pulses (2 ms duration) applied with a frequency of 4–5 Hz for 10 s to elicit swimming. A pause of 3–5 min was made between two stimulations. Single pulses applied at a frequency of 0.1 Hz were used to evoke excitatory postsynaptic currents (EPSCs). High-frequency doublet pulses (20 Hz) were used to test for monosynaptic connectivity. The stimulation intensity ranged from 1 to 32 μA.

Ca^{2+} imaging. MLR cells were retrogradely labeled by placing crystal of the Ca^{2+} indicator Ca^{2+} green-dextran amines (MW 3000, Invitrogen) at the level of the MRRN, immediately after a complete transverse transection of the brainstem at the level of the MRRN. The preparation was then transferred for 18–24 h in a chamber perfused with cooled (8–10°C), oxygenated Ringer's solution to allow the tracer to migrate to fill the MLR cell bodies. The next day, the brain tissue rostral to the PT was removed following a transverse section. As for the patch-clamp recording experiments described above, the dorsal part of the brain was cut away with a vibratome to provide access to MLR cells. The preparation was then pinned down to the bottom of a recording chamber perfused with cooled (8–10°C), oxygenated Ringer's solution (4 ml/min). Changes in fluorescence were recorded as previously (Brocard et al., 2010; Ryczko et al., 2016a,b) with a Nikon epifluorescent microscope coupled with a CCD video camera (Photometrics CoolSNAP HQ, Roper Scientific). To measure the changes in fluorescence, regions-of-interest were manually delineated around the MLR cell bodies labeled with the Ca^{2+} dye. Changes

in fluorescence of MLR neurons to PT stimulation were acquired at a rate of 2 Hz using MetaFluor (Universal Imaging). The Ca^{2+} responses were expressed as the relative changes in fluorescence ($\Delta F/F$). The baseline was defined as the averaged fluorescence before stimulation. Data analysis was performed using MetaFluor, Clampfit (Molecular Devices) and MATLAB (MathWorks). To measure drug effects on Ca^{2+} responses, 4–6 responses were recorded for each cell and for each drug condition.

Drug application. Chemicals were purchased from Sigma-Aldrich and diluted to their final concentration in Ringer's solution. In some experiments, bath application of a Ringer's solution containing the AMPA/Kainate antagonist 6-cyano-7-nitroquinoxaline-2,3-dione (CNQX; 25 μM) and the NMDA antagonist (2R)-amino-5-phosphonovaleric acid (AP5; 100 μM) was used. In some other experiments, a Ringer's solution containing CNQX (1 mM) and AP5 (0.5 mM; Gariépy et al., 2012a; Ryczko et al., 2016a) or the D_1 receptor antagonist SCH 23390 (0.5 mM; Ryczko et al., 2013) was microinjected in the MLR. In some experiments, a Ringer's solution containing D,L-glutamate (2.5 mM) was also microinjected in the PT. The microinjection procedure was as previously described (Brocard and Dubuc, 2003; Le Ray et al., 2003; Derjean et al., 2010; Gariépy et al., 2012a, 2012b; Ryczko et al., 2013, 2016a,b). The microinjections were done with a glass micropipette (tip diameter of 10–20 μm) using pressure pulses (3–4 psi) of variable duration (10–80 ms) applied with a Picospritzer (General Valve). Fast green was added to the injected solution to monitor the extent of the injection site. The injected volumes were estimated by measuring the diameter of a droplet ejected in air from the tip of the pipette multiplied by the number of pressure pulses, and the resulting number of moles ejected was calculated for each drug (Le Ray et al., 2003; Ryczko et al., 2013, 2016a,b).

Kinematics. Locomotor movements were monitored with a video camera (Sony HDR-XR200; 30 frames/s) positioned 1 m above the recording chamber. Data were analyzed offline using homemade software (Brocard et al., 2010; Gariépy et al., 2012a; Ryczko et al., 2013; Juvin et al., 2016). Briefly, tracking markers were equidistantly distributed along the body and monitored over time. Swimming was identified through the presence of mechanical waves traveling from head to tail (Fig. 1; Sirota et al., 2000; Ryczko et al., 2013). To quantify the frequency of swimming movements a single couple of markers located in the middle part of the body was used.

Anatomical tracing and immunofluorescence. These experiments were performed on isolated brain preparations (see above). Biocytin (Sigma-Aldrich) was used for retrograde labeling of PT cells as previously described (Gariépy et al., 2012a,b, Ryczko et al., 2013, 2016a,b). First, a pulled glass micropipette was used to perform a lesion at the injection site in the MLR and crystals of biocytin were immediately placed in the lesion, allowing the dissolving tracer to be picked up by cut axons. After 10–15 min, the injection site was thoroughly rinsed and the brain was transferred to a chamber perfused with cold oxygenated Ringer's solution overnight to allow retrograde transport of the tracer. The injection site was chosen based on previous studies on the MLR (Derjean et al., 2010; Ryczko et al., 2013; for review see Ryczko and Dubuc, 2013) and verified by histology. The next day, the brain was transferred to a fixative solution according to the immunofluorescence procedure to follow. It is safe to presume that not all axons crossing the injection site were filled by the tracer. Consequently, the labeled cells in the PT constitute an underestimation of the actual number of cells projecting to the MLR in each preparation.

For tyrosine-hydroxylase (TH) immunofluorescence, the whole brain was immersed for 24 h in 4% (w/v) paraformaldehyde in PBS and then transferred to PB containing 20% (w/v) sucrose, both steps at 4°C. The next day, the brain was sectioned at 25 μm thickness with a cryostat. The sections collected on Color-Frost Plus slides (Fisher Scientific) were air-dried overnight at 37°C, after which they were rinsed three times 10 min in PBS and blocked in PBS containing 5% normal goat serum and 0.3% Triton X-100 for 60 min. The sections were then incubated overnight in the blocking solution containing the TH antibody. The next day, they were rinsed three times 10 min with PBS, incubated in the blocking solution containing the secondary antibody for 60 min, and rinsed again three times 10 min in PBS. The slides were immediately coverslipped using Vectashield (with or without DAPI, H-1200, H-1000; Vector Laboratories) as mounting medium.

The presence of dopamine (DA) and glutamate was detected by immunofluorescence concurrently or separately. The brain was immersed for 17–18 h in a 0.05 M Tris buffered 0.1% sodium metabisulfite and 0.8% NaCl (TBSM; pH 7.4) solution containing 2% glutaraldehyde. The brain was then transferred to TBSM containing 20% (w/v) sucrose overnight. The last two steps were performed at 4°C. The next day, the brain was cut on a cryostat. Sections of 25 μm thickness were collected on slides and air-dried overnight. The sections were then rinsed three times 10 min and incubated in TBSM containing 1% sodium borohydride for 30 min. After three rinses in TBSM, the sections were incubated in TBSM containing 5% normal goat serum and 0.3% Triton X-100 for 60 min. The sections were then incubated overnight at 4°C in the blocking solution containing the DA and/or the glutamate primary antibodies. The next day, the sections were rinsed three times 10 min with TBSM, incubated in the blocking solution containing the appropriate secondary antibodies (see below) for 60 min, and rinsed again three times 10 min in TBSM. The slides were then immediately coverslipped as described for TH.

For TH immunofluorescence, a rabbit anti-TH primary antibody was used (diluted 1:400; AB152; Millipore) followed by a donkey anti-rabbit AlexaFluor 594 (diluted 1:400; A21207; Invitrogen) or a goat anti-rabbit AlexaFluor 488 (1:400; A11008; Invitrogen). TH immunofluorescence was sometimes used in the present study as an alternative to DA immunofluorescence to visualize the DA neurons in the PT, based on studies in lampreys (Pombal et al., 1997; Abalo et al., 2005; Pierre et al., 1997; Ryczko et al., 2013). The AB152 antibody against TH has been used reliably on lampreys in many independent studies by different research groups on DA neurons (Villar-Cerviño et al., 2006; Barreiro-Iglesias et al., 2008; Robertson et al., 2012; Ryczko et al., 2013). For DA immunofluorescence, a mouse anti-DA primary antibody was used (diluted 1:400; MAB5300; Millipore) followed by a either a goat anti-mouse AlexaFluor 488 (diluted 1:400; A11001; Invitrogen) or a goat anti-mouse DyLight 594 (diluted 1:400; 115-515-146; Jackson ImmunoResearch). The specificity of the MAB5300 antibody for DA was tested by ELISA by the manufacturer, and its pattern of labeling in our material corresponded closely to that reported with other DA antibodies in the lamprey (Abalo et al., 2005; Pierre et al., 1997). We have also independently confirmed that the TH-immunoreactive neurons in the PT use DA as neurotransmitter (Ryczko et al., 2013). For glutamate immunofluorescence, a rabbit polyclonal primary antibody directed against glutamate was used (diluted 1:5000; IG1007, lot 3603, ImmunoSolution) followed by either a goat anti-rabbit AlexaFluor 594 antibody (diluted 1:400; A11012, Invitrogen) or a goat anti-rabbit AlexaFluor 488 (diluted 1:400; A11008, Invitrogen). The IG1007 glutamate antibody has been used successfully to label glutamatergic neurons in the lamprey brain (Barreiro-Iglesias et al., 2008; Villar-Cerviño et al., 2011; Fernández-López et al., 2012) and in salamanders (Ryczko et al., 2016a). The specificity of the antibody was confirmed by dot blots performed by the supplier, which revealed no immunoreaction against a variety of amino acid conjugates such as aspartate. Western blots did not yield staining of lamprey brain proteins extracts (Barreiro-Iglesias et al., 2008; Villar-Cerviño et al., 2011). The staining is similar to that obtained with a mouse monoclonal antibody directed against glutamate (Fernández-López et al., 2012). Brain regions stained by the antibody used in the present study also contained neurons expressing the vesicular transporter for glutamate mRNA (Villar-Cerviño et al., 2011).

In double DA/glutamate immunofluorescence experiments, the primary antibodies, and the secondary antibodies, were mixed together. The specific labeling obtained under these conditions was in every ways similar to the labeling obtained when the antibodies were each used separately. Biocytin was visualized with streptavidin Alexa Fluor594, 488, or 350 (diluted 1:400; Life Technologies), which was added to the secondary antibodies' solution without altering the immunofluorescence labeling.

In all cases, omitting the primary antibody from the procedures resulted in the absence of specific labeling on the brain sections.

The sections were then observed and photographed using an E600 epifluorescence microscope equipped with a DXM1200 digital camera (Nikon). For some sections, a confocal microscope was used (FV1000, Olympus). Photoshop CS5 (Adobe) was used to combine digital photomicrographs taken with different filter sets and to adjust the levels so that all fluorophores were clearly visible simultaneously.

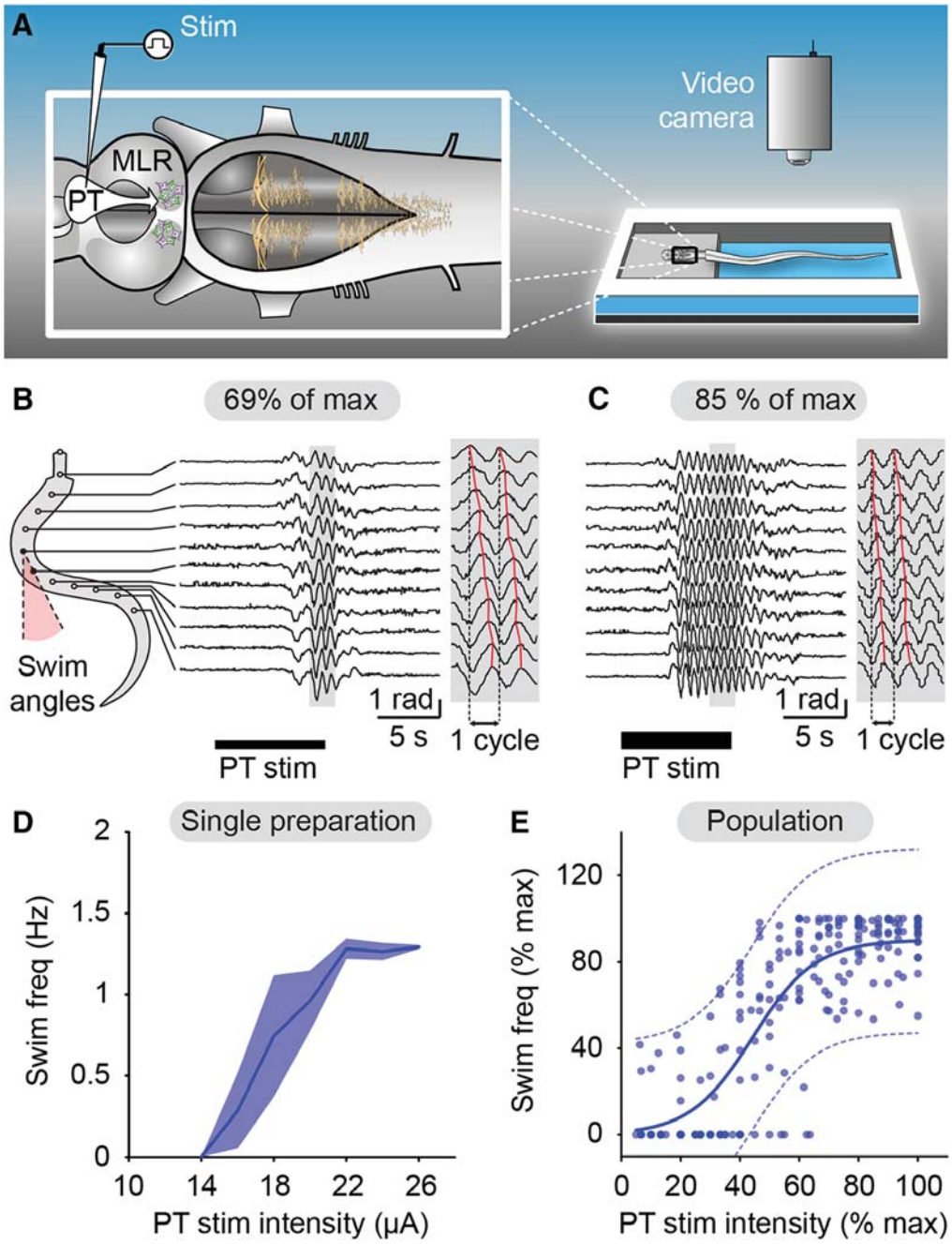

Figure 1. Incremental stimulation of the PT evokes gradual increase in swimming frequency. ***A***, In a semi-intact preparation, the PT was stimulated electrically and locomotion was quantified by placing equidistant markers along the body (see Materials and Methods). Angular variations (radians) of the body curvature were measured over time. ***B***, ***C***, PT stimulation elicited swimming as illustrated by head-to-tail mechanical waves (***B*** and ***C***, gray insets, where red solid lines indicate the maximal bending curvature for each marker). Increasing PT stimulation intensity (18–22 μA, i.e., 69–85% of the maximal stimulation intensity used in this preparation) increased swimming frequency. ***D***, Plot illustrating swimming frequency (mean ± SEM; 2–3 trials per stimulation intensity) as a function of PT stimulation intensity for the preparation shown in ***B*** and ***C***. ***E***, Relationship between swimming frequency (blue dots; $n = 213$ trials pooled from 17 preparations) and PT stimulation intensity (1–32 μA, 10 s train, 2 ms pulses, 4–5 Hz). Data followed a sigmoidal function (blue solid line; $R^2 = 0.69$, $p < 0.0001$). The dotted lines illustrate the 95% prediction intervals. Locomotor frequency and stimulation intensity were expressed as a percentage of their maximal values.

Statistics. Data in the text are presented as the mean ± SEM. For Ca^{2+} imaging, measurements of the area under the curve from the beginning of the response to the return to baseline were calculated using a calculation script in Clampfit (Molecular Devices). The values were expressed in $\Delta F/F \times s$. Correlations between variables and their significance as well as 95% confidence intervals were calculated using Sigma-Aldrich Plot 11.0. No statistical method was used to predetermine sample sizes. The sample sizes in the present study are in general similar to those used in the field. No randomization or blinding procedure was used. Parametric analyses were used when assumptions for normality and equal variance were respected, otherwise nonparametric analyses were used. Two-tailed paired Student's *t* tests were performed for comparing means between two dependent groups. For more than two dependent groups, a parametric one-way ANOVA for repeated measures or a nonparametric Friedman ANOVA on ranks for repeated measures was used. When two factors were tested, a two-way ANOVA for repeated measures on ranks was performed. Both ANOVA analyses were followed by a Student–Newman–Keuls *post hoc* test for multiple comparisons between groups. Statistical differences were assumed to be significant when $p < 0.05$.

Data availability. All relevant data are available from the authors.

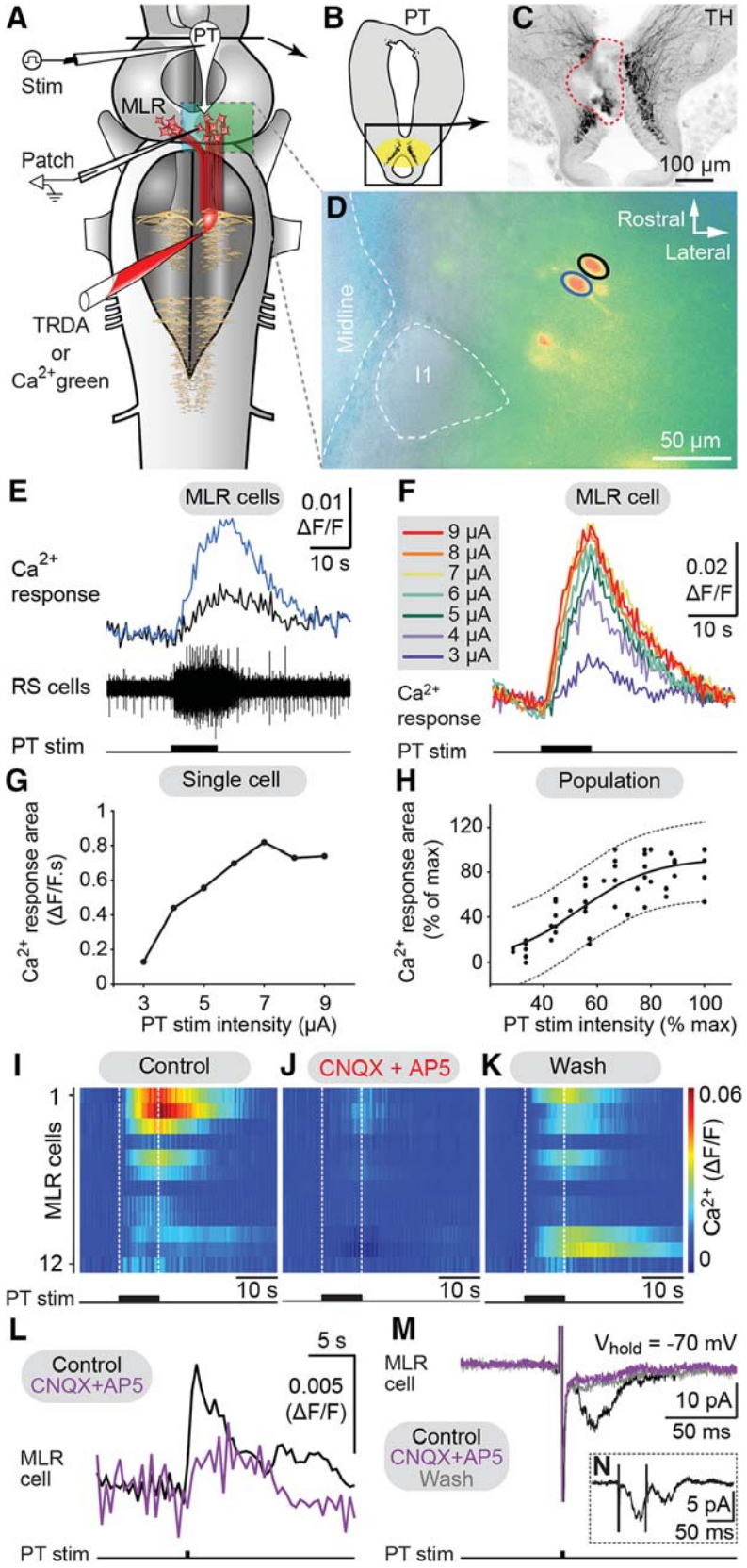

Figure 2. Incremental stimulation of the PT gradually increases MLR cell responses. ***A***, Retrogradely labeled MLR cells were recorded using calcium (Ca^{2+}) imaging or patch-clamp electrodes in an isolated brainstem preparation. ***B***, ***C***, The stimulation site in the PT (enclosed by a red dashed line) was located within TH-immunoreactive cells (black). ***D***, Two MLR cells (blue and black circles) labeled with Ca^{2+} green dextran amines. The giant reticulospinal (RS) cell I1, a MLR landmark, is enclosed by a white dashed circle. ***E***, Chemical stimulation of the PT with glutamate (2.5 mM, 2 Hz, 50 ms pulses, 24 pulses) elicited Ca^{2+} rise in MLR cells together with activation of RS cells recorded extracellularly. ***F***, Ca^{2+} increases ($\Delta F/F$) in a MLR cell in response to incremental electrical PT stimulations (10 s train, 5 Hz, 2 ms pulses). ***G***, Plot of Ca^{2+} response versus PT stimulation intensity in the MLR cell in ***F***. ***H***, Relationship between MLR cell Ca^{2+} response area ($n = 56$ trials, 10 cells from 4 preparations) and PT stimulation intensity (2–10 μA, 10 s train, 5 Hz, 2 ms pulses) both expressed as a percentage of their maximal values. ***I–K***, Color plots illustrating MLR Ca^{2+} responses ($\Delta F/F$) in response to PT stimulation (5–10 μA,10 s train, 5 Hz, 2 ms pulses) in control condition, following 7–22 min bath application of CNQX (25 μM) and AP5 (100 μM), and 60–77 min after wash out. Each line illustrates the response of individual MLR cells ($n = 12$ cells from 4 preparations). White dotted lines indicate onset and offset of PT stimulation. Warmer colors (red) indicate larger Ca^{2+} responses. ***L***, Ca^{2+} responses ($\Delta F/F$) elicited by single-pulse stimulation of the PT (0.1 Hz, 15 μA, 2 ms pulses) in MLR neurons were abolished by bath application of CNQX (25 μM) and AP5 (100 μM). Each trace is the average of the pooled Ca^{2+} responses obtained in three MLR neurons. In each neuron, five trials were recorded for each condition. ***M***, EPSCs evoked by PT stimulation (0.1 Hz, 5–9 μA, 2 ms pulses) in voltage-clamped MLR neurons were reduced by bath-applied CNQX (25 μM) and AP5 (100 μM). Each trace is the average of 10 EPSCs. Only a partial washout was obtained for this cell. ***N***, EPSCs (average of 60 trials) induced in a MLR neuron by high-frequency doublets (20 Hz) applied to the PT. TRDA, Texas Red dextran amines.

Results

We first confirmed that electrical stimulation of the PT robustly evokes swimming (Fig. 1*A*,*B*) in a lamprey semi-intact preparation in which the brain is exposed for stimulation, while the body swims in the chamber (Derjean et al., 2010; Gariépy et al., 2012a; Ryczko et al., 2013). We then examined whether PT stimulation could evoke graded locomotor output. A progressive increase in the PT stimulation intensity (1–32 μA, 4–5 Hz, 2 ms pulses, 10 s trains) elicited a graded increase in swimming frequency (Fig. 1*B–D*; $n = 17$ preparations). The recorded swimming frequencies (0.3–3.6 Hz) are in the range observed in freely moving lampreys (Islam and Zelenin, 2008). Data were pooled by expressing the locomotor frequency as a percentage of the maximal locomotor frequency. The PT stimulation intensity was expressed as a percentage of maximal stimulation intensity, that was defined when the locomotor response reached a plateau and did not grow further as the stimulation intensity was increased, as previously done in lampreys (Brocard et al., 2010) and salamanders (Ryczko et al., 2016a). The relationship between PT stimulation intensity and locomotor frequency followed a sigmoidal function, with swimming frequencies reaching a plateau at higher stimulation intensities (Fig. 1*E*; $R^2 = 0.69$, $p < 0.0001$, $n = 213$ trials pooled 17 preparations). These findings establish that incremental PT stimulation evokes graded intensification of swimming frequency.

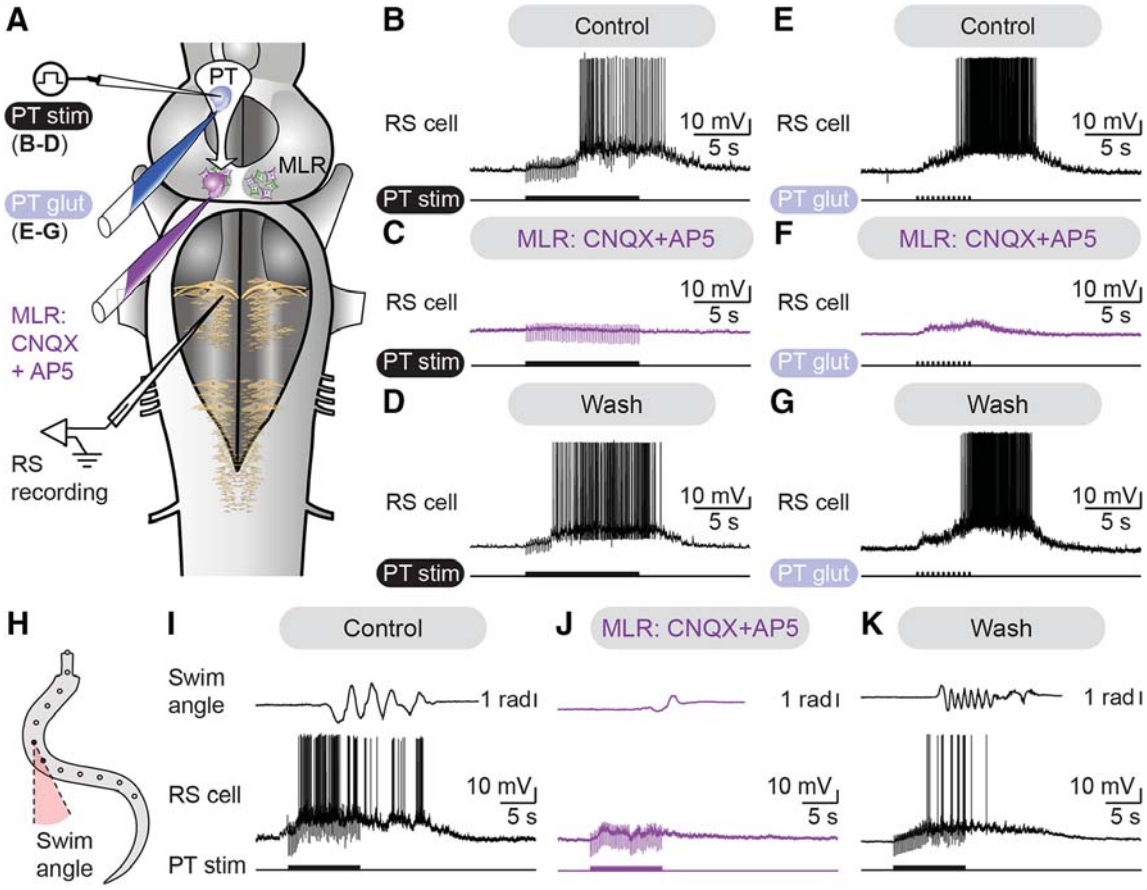

Figure 3. The descending glutamatergic drive from the PT to the MLR evokes reticulospinal activity and locomotion. ***A***, In isolated brainstem preparations, glutamatergic antagonists were microinjected in the MLR. RS activity was recorded extracellularly in response to electrical (2 ms pulses, 5 Hz, 10 s train, 8–12 μA) or chemical stimulation (glutamate 2.5 mM, 20–80 ms pulses, 2 Hz, 9–11 pulses) of the PT. ***B–D***, Microinjection of 36.4–78.4 pmol of CNQX (1 mM) and 18.2–39.2 pmol of AP5 in the MLR (0.5 mM) dramatically decreased RS activity elicited by PT stimulation (7 μA, 10 s train, 2 ms pulses, 4 Hz). Recovery was obtained after 62–108 min of washout. ***E–G***, Microinjection of 51.5–119.9 pmol of CNQX (1 mM) and 25.7–156.4 pmol of AP5 (0.5 mM) in the MLR reduced RS activity elicited by PT chemical stimulation with 1.0–19.1 pmol of glutamate (illustrated case: 50 ms pulses, 2 Hz, 11 pulses). Responses recovered after 88–135 min of wash out. ***H***, In a semi-intact preparation where RS neurons were recorded intracellularly to monitor the activity of brainstem locomotor circuits, glutamatergic antagonists were microinjected in the MLR. Angular variations (radians) of the curvature of a mid-body segment were measured over time during swimming. ***I–K***, Microinjections of 34.8–68.4 pmol of CNQX (1 mM) and 17.4–34.2 pmol of AP5 (0.5 mM) in the MLR dramatically reduced RS activity and swimming movements elicited by PT stimulation (illustrated case: 10 μA, 10 s train, 2 ms pulses, 5 Hz). These effects were reversed after 48–135 min of washout. Data from ***B–D***, ***E–G***, and ***I–K*** are from three different preparations.

Then, we examined whether MLR cells are directly controlled in a graded fashion by descending inputs from the PT. We performed Ca^{2+} imaging of MLR cells in isolated brain preparations. MLR cells were retrogradely labeled with a Ca^{2+} indicator injected in the dendritic field of reticulospinal neurons. The dorsal part of the brain (i.e., the tectum) was removed to provide access to MLR cells for Ca^{2+} imaging (Fig. 2*A*). Reticulospinal cells were recorded extracellularly to monitor the activity of brainstem locomotor networks downstream the MLR. Stimulation of the PT (Fig. 2*B*,*C*) elicited Ca^{2+} responses in MLR cells together with reticulospinal activity (Fig. 2*D*,*E*). Increasing the intensity of the PT stimulation increased the size of the Ca^{2+} response in MLR cells (Fig. 2*F*,*G*). The relationship between normalized Ca^{2+} responses in the MLR and PT stimulation intensity also followed a sigmoidal function (Fig. 2*H*; $R^2 = 0.71$, $p < 0.0001$, $n = 56$ trials, 10 cells pooled from 4 preparations). These results indicate that incremental increase in PT stimulation evokes graded intensification of MLR cell activation.

We then examined whether glutamatergic transmission was involved. Bath application of glutamatergic antagonists (CNQX 25 μM, AP5 100 μM) dramatically decreased the area of the Ca^{2+} responses evoked in MLR cells by trains of PT stimulation (reduced by 86.5 ± 5.1%, $p < 0.05$ vs control, Student–Newman–Keuls test, $n = 12$ cells pooled from 4 preparations; Fig. 2*I*,*J*). The responses returned to 76.4 ± 16.1% of control after wash out ($p < 0.05$ vs CNQX/AP5, Student–Newman–Keuls test; Fig. 2*K*). Similarly, bath applied glutamatergic antagonists also significantly decreased the responses evoked by single-pulse stimulation in MLR cells recorded either with Ca^{2+} imaging (reduced by 90.7 ± 23.1%, $p < 0.01$ vs control, paired *t* test, $n = 3$ cells; Fig. 2*L*) or patch-clamp recordings (reduced by 64.7 ± 1.6% in cell 1, $p < 0.05$ vs control, Student–Newman–Keuls test; reduced by 38.3 ± 4.1% in cell 2, $p < 0.001$ vs control, Student–Newman–Keuls test; Fig. 2*M*). The PT to MLR connection is likely monosynaptic as MLR cell responses followed high-frequency (20 Hz) stimulation doublets applied to the PT ($n = 5$ cells of 5 tested, data pooled from 3 preparations; Fig. 2*N*). Altogether, this shows that glutamatergic transmission is involved in the PT-evoked responses in MLR cells.

Next, we investigated whether the descending glutamatergic drive from the PT to the MLR was responsible for the activation of the locomotor circuits downstream the MLR. Electrical stimulation of the PT elicited reticulospinal discharges in isolated brain preparations. Microinjection in the MLR of the glutamatergic antagonists CNQX (1 mM) and AP5 (0.5 mM) dramatically decreased the discharge frequency elicited in reticulospinal neu-

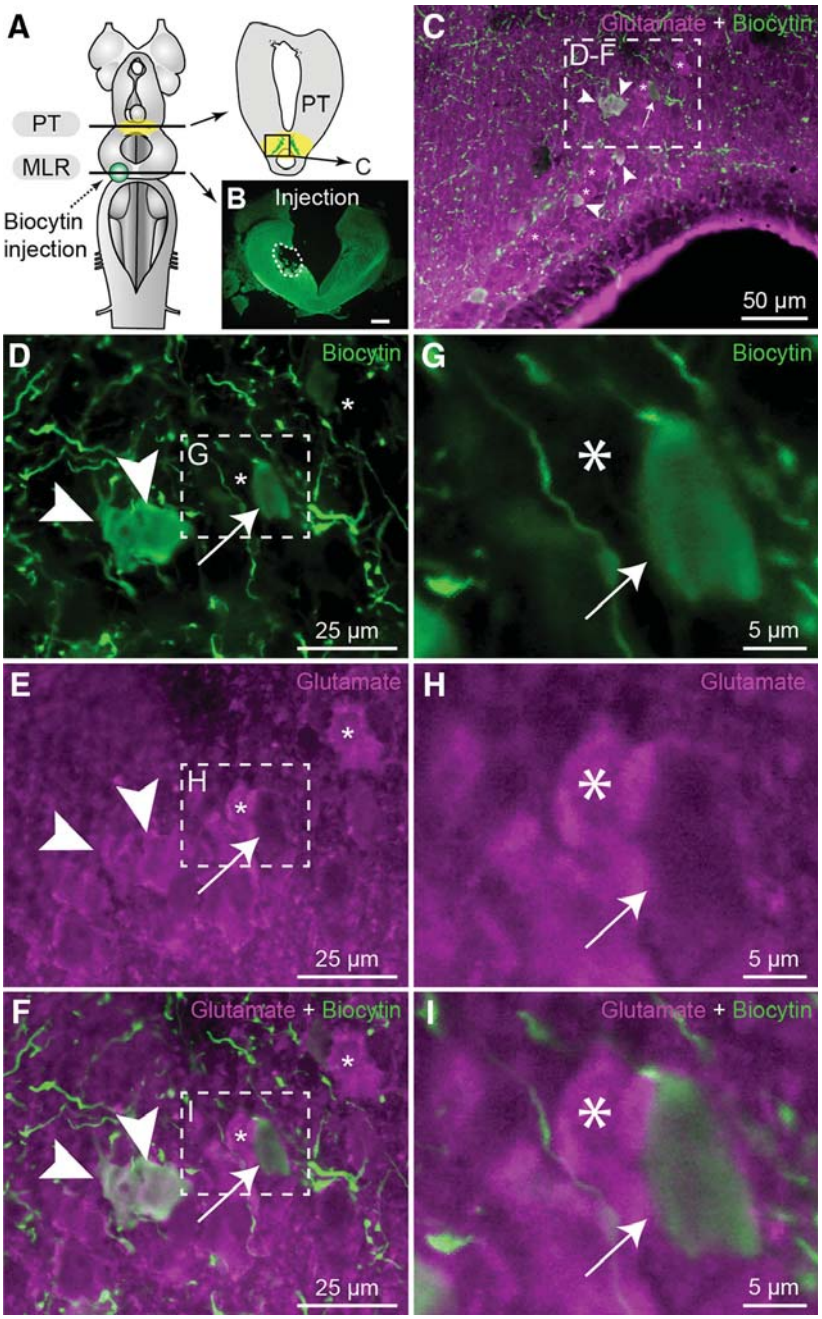

Figure 4. Glutamatergic neurons of the PT send descending projections to the MLR. ***A***, Schematic dorsal view of a lamprey brain. The diagram on the right illustrates a cross section at the level of the PT (homologous to the mammalian substantia nigra pars compacta) with the approximate location of the micrographs shown in ***C–F***. ***B***, The photomicrograph illustrates the tracer (biocytin, green) injection site (enclosed by a white dashed line) in the MLR. Scale bar, 300 μm. ***C***, Cells labeled in the PT following biocytin (green) injection in the MLR and immunofluorescence against glutamate (magenta). ***D–F***, Magnification of the dashed rectangle in ***C***. ***G–I***, Magnifications of the dashed rectangles in ***D–F***. ***C–I***, White arrowheads indicate retrogradely labeled cells that were immunopositive for glutamate in the PT. Asterisks denote cells positive for glutamate but not retrogradely labeled. The white arrow points to a cell retrogradely labeled but not immunopositive for glutamate.

rons by electrical PT stimulation (reduced by 92.3 ± 4.9%, $p <$ 0.001 vs control, Student–Newman–Keuls test, $n = 15$ trials pooled from 3 preparations; Fig. 3*A–C*). After wash out, the responses recovered with spiking frequency returning to 86.7 ± 12.8% of control ($p < 0.001$ vs CNQX/AP5, Student–Newman–Keuls test; Fig. 3*D*). Because electrical stimulation can recruit fibers of passage in addition to local cell bodies, electrical stimulation was replaced with chemical stimulation (Fig. 3*A*, *E–G*). Such chemical stimulation likely activates local cell bodies that are dopaminergic, glutamatergic and possibly from other types. Microinjections of glutamate (2.5 mM) onto the PT elicited discharges in reticulospinal cells similar to those evoked by electrical stimulation. Local microinjections of CNQX (1 mM) and AP5 (0.5 mM) in the MLR decreased the discharge frequency of reticulospinal neurons (reduced by 84.0 ± 4.2%, $p < 0.05$ vs control, Student–Newman–Keuls test, $n = 20$ trials pooled from 4 preparations). Recovery was obtained after wash out of the glutamatergic antagonists, with spiking frequency increasing back to 97.8 ± 15.4% of control ($p < 0.05$ vs CNQX/AP5, Student–Newman–Keuls test). In semi-intact preparations (Fig. 3*H*), microinjections of CNQX (1 mM) and AP5 (0.5 mM) in the MLR dramatically decreased the frequency of locomotor movements evoked by PT stimulation (reduced by 61.3 ± 10.3%, $p < 0.001$ vs control, Student-Newman–Keuls test; Fig. 3*I*, *J*). Recovery was obtained after wash out with the locomotor frequency returning to 96.4 ± 6.4% of control ($p < 0.001$ vs CNQX/AP5, Student–Newman–Keuls test, $n = 18$ trials per condition pooled from 3 preparations; Fig. 3*K*). Similar results were obtained in semi-intact preparations for the discharge frequency of reticulospinal neurons following microinjections of glutamatergic antagonists in the MLR (reduced by 93.0 ± 3.0%, $p < 0.001$ vs control, Student–Newman–Keuls test). These effects were also reversed after washout with frequency returning to 71.5 ± 7.6% of control ($p < 0.001$ vs CNQX/AP5, Student–Newman–Keuls test). Altogether, these results show that the descending glutamatergic pathway from the PT to the MLR plays an important role in the activation of locomotor circuits downstream the MLR.

We then looked for the anatomical substrate of these effects. We examined whether glutamatergic PT neurons send a descending projection to the MLR with anatomical techniques. Glutamatergic neurons were found in the PT ($n = 9$ preparations). We injected an axonal tracer in the MLR to label retrogradely neurons in the PT (Fig. 4*A*, *B*) and we observed that several of those were immunoreactive for glutamate (Fig. 4*C–I*; $n = 7$ preparations). Because a descending dopaminergic pathway originating from the PT to the MLR was previously reported (Ryczko et al., 2013; Pérez-Fernández et al., 2014), we examined whether PT glutamatergic cells were a separate population from the PT dopaminergic ones. Using double-labeling experiments, we found that several PT neurons were colabeled for dopamine and glutamate (Fig. 5*A–I*; $n = 6$ preparations). To determine whether PT neurons co-storing dopamine and glutamate sent descending projections to the MLR, we added a retro-

grade tracer injection in the MLR (Fig. 6*A*,*B*) in a series of triple labeling experiments. We found that several PT cells projecting down to the MLR were colabeled for dopamine and glutamate ($n = 4$ preparations; Fig. 6*C–K*). PT neurons storing only dopamine or glutamate were also found to send descending projections to the MLR. Altogether, these results provide direct evidence of a glutamatergic pathway from the PT to the MLR, in parallel with the previously characterized dopaminergic pathway (Ryczko et al., 2013; Pérez-Fernández et al., 2014). There is thus an anatomical substrate for interaction between these two transmitters at the level of the MLR.

Next, we examined the role of the interactions between glutamatergic and dopaminergic inputs from the PT to the MLR in the graded control of locomotor movements. We previously showed that PT-evoked dopamine release in the MLR increases swimming frequency through the activation of D_1 receptors (Ryczko et al., 2013). Here we examined in semi-intact preparations whether the activation of D_1 receptors in the MLR is needed to evoke graded swimming when stimulating the PT with increasing intensities. When the D_1 antagonist SCH 23390 (0.5 mM) was microinjected in the MLR, the locomotor frequency of PT-evoked swimming was decreased as expected, but graded control of swimming was still possible when stimulating the PT with increasing intensities (Fig. 7*A*). Similar observations were made when pooling the data by expressing stimulation intensity and locomotor frequency as a function of their maximal values (Fig. 7*B–D*). In control conditions, the relationship between stimulation intensity and swimming frequency followed a sigmoid function ($R^2 = 0.78$, $p < 0.0001$, $n = 81$ trials pooled from 6 preparations) that persisted in the presence of the D_1 antagonist injected in the MLR ($R^2 = 0.76$, $p < 0.0001$, $n = 81$ trials pooled from 6 preparations), indicating that progressive increase in stimulation intensity still elicited graded increase in swimming. After wash out of the drug, the sigmoid relation was still present ($R^2 = 0.83$, $p < 0.0001$, $n = 81$ trials pooled from 6 preparations). Statistical analysis confirmed that the D_1 antagonist reversibly decreased locomotor frequency especially at maximal PT stimulation intensities (Fig. 7*E*). This might be explained by a "floor effect" at lower intensities, where the range of evoked swimming frequencies could be too narrow to detect significant differences between drug conditions. In the presence of the D_1 antagonist, the locomotor frequencies reached a plateau that was lower than under control conditions at 50, 60, 70, 80, 90, and 100% of maximal stimulation intensities ($p < 0.05$ to $p < 0.001$ against control, Student–Newman–Keuls test after a two-way ANOVA on ranks for repeated measures, $p < 0.001$; Fig. 7*E*). This effect was abolished after wash out at 50, 60, 70, 90, and 100% of maximal stimulation intensities ($p < 0.05$ to $p < 0.001$ against drug injection, Student–Newman–Keuls test). Because we previously demonstrated that a small number of dopamine cells in the PT send descending projections to the contralateral MLR (Ryczko et al., 2013), microinjections of the D_1 antagonist were performed on both sides of the MLR ($n = 5$ preparations). The effects were very similar to those observed with a unilateral injection of the drug.

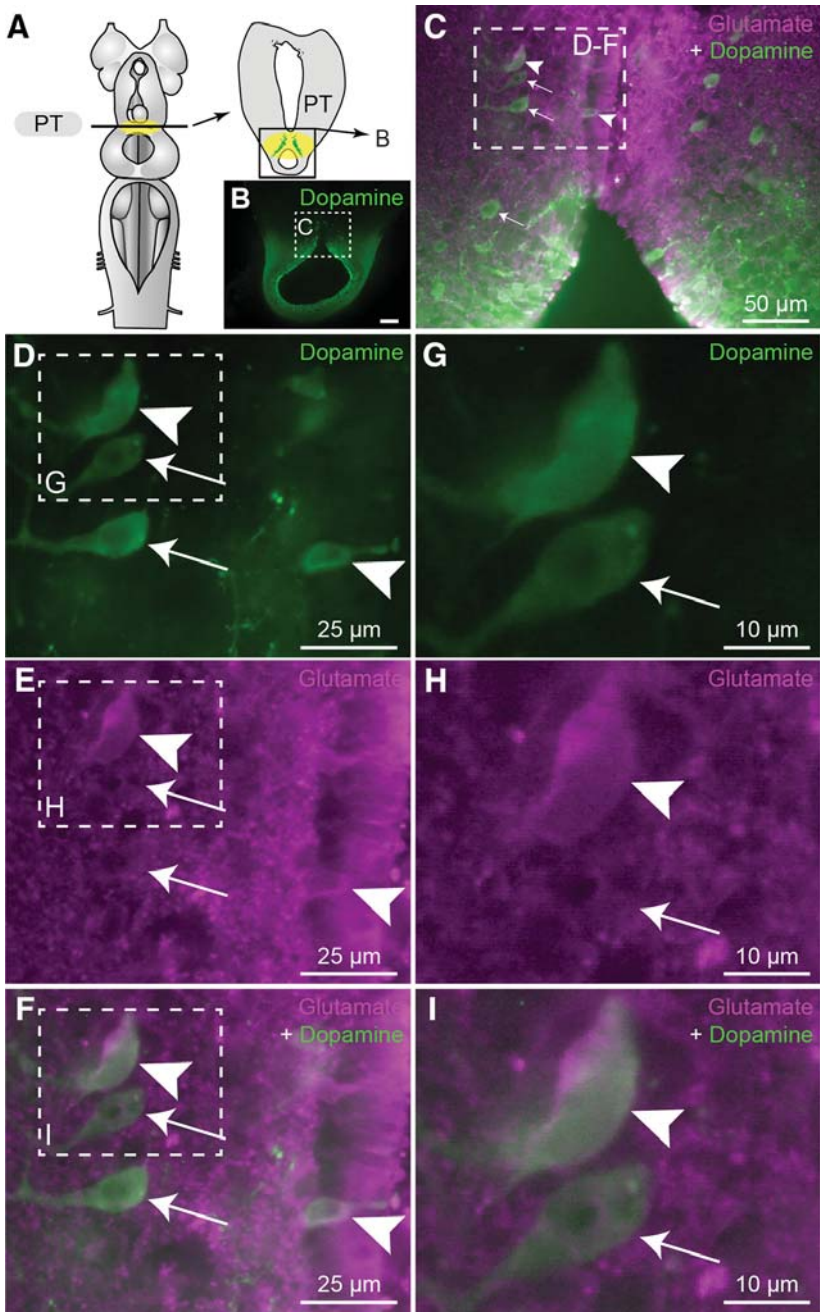

Figure 5. Colabeling of dopamine and glutamate in neurons of the PT. ***A***, Schematic dorsal view of a lamprey brain. The diagram on the right illustrates a cross section at the level of the PT (homologous to the mammalian substantia nigra pars compacta) with the approximate location of the micrograph in ***B***. ***B***, Transverse section of the PT showing dopaminergic neurons (green), and the location of the micrograph shown in ***C***. ***C***, Magnification of the dashed rectangle in ***B***, merged with immunofluorescence against glutamate (magenta). ***D–F***, Magnification of the dashed rectangle in ***C***. ***G–I***, Magnifications of the dashed rectangles in ***D–F***. ***C–I***, White arrowheads illustrate cells showing immunofluorescence against glutamate (magenta) and dopamine (green). White arrows point to cells immunopositive for dopamine but not for glutamate.

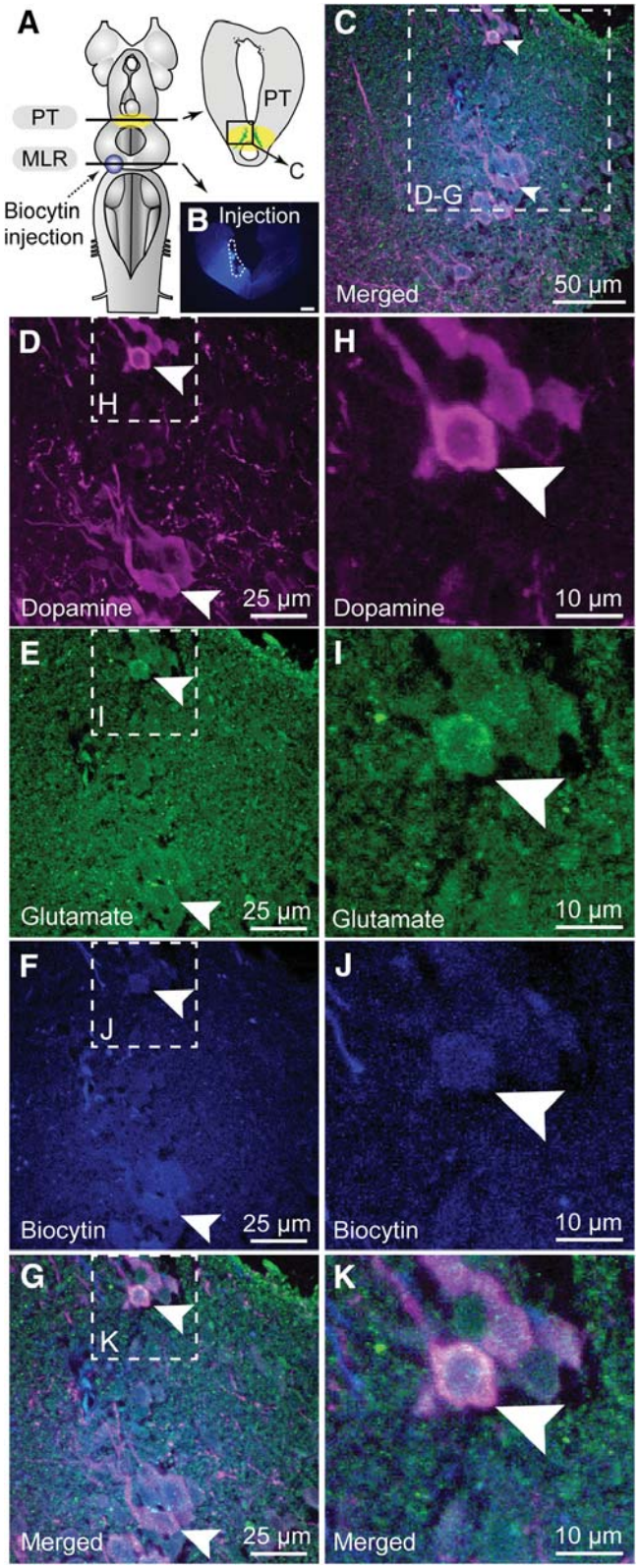

Figure 6. Neurons colabeled for dopamine and glutamate in the PT send descending projections to the MLR. ***A***, Schematic dorsal view of a lamprey brain. The diagram in the top right corner illustrates a cross section at the level of the PT (homologous to the mammalian substantia nigra pars compacta) with the approximate location of the micrograph shown in ***C***. ***B***, The photomicrograph illustrates the tracer (biocytin, blue) injection site (enclosed by white dashed lines) in the MLR. Scale bar, 300 μm. ***C***, The three micrographs were merged to show the three markers with dopamine in magenta, glutamate in green, and biocytin in blue. ***D–G***, Transverse sections illustrate an example of triple labeling of PT cells positive for dopamine (magenta) and glutamate (green) that project to the MLR (blue). ***H–K***, Magnification of the dashed rectangle in ***D–G***. ***D***, ***H***, Dopamine-positive neurons (magenta) in the PT. ***E***, ***I***, Glutamate-positive neurons (green) in the PT. ***F***, ***J***, Cells retrogradely labeled in the PT following biocytin (blue) injection in the MLR. ***G***, ***K***, Photomicrographs in ***D–F*** and ***H–J*** merged, respectively, to show the three markers. Arrowheads indicate examples of triple labeled cells.

The swimming frequency was reduced at 40, 50, 60, 70, 80, 90, and 100% of maximal stimulation intensities ($p < 0.05$ to $p < 0.001$ against control, Student–Newman–Keuls test after a two-way ANOVA on ranks for repeated measures, $p < 0.001$) and graded control of locomotor frequency was still present with increasing intensities of PT stimulation (sigmoid fit: $R^2 = 0.62$, $p < 0.0001$, $n = 70$ trials pooled from 5 preparations). Altogether, these results suggest that glutamatergic inputs from the PT to the MLR are necessary for evoking locomotor output in a graded fashion, whereas the dopaminergic inputs amplify the descending glutamatergic command through D_1 receptors without contributing to the rheostat-like effect.

Discussion

Results from the present study show in lamprey that the PT, a structure homologous to the mammalian SNc, sends a descending glutamatergic input that controls MLR cell activity and swimming in a graded fashion. We found PT neurons labeled for both dopamine and glutamate that projected to the MLR, indicating a close interaction between these transmitters in the generation of the locomotor command. Blockade of D_1 receptors in the MLR resulted in a reduced frequency of swimming movements without disrupting the graded control of locomotion by the PT, whereas blockade of glutamatergic receptors in the MLR nearly abolished locomotor output.

To our knowledge, results from the present study provide the first demonstration that the MLR can be activated incrementally by a higher brain region to control the speed of the locomotor movements. The substrate underlying this phenomenon consists of glutamatergic and dopaminergic inputs acting in parallel. We now show that the glutamatergic input is essential to elicit MLR activity and locomotion in a graded fashion, whereas the dopaminergic one provides additional excitation, but is not essential to evoke locomotion. In the presence of a D_1 blocker, the relationship between stimulation intensity and swimming frequency was shifted to the right, indicating that a stronger stimulus was necessary to generate the same swimming frequency. This is consistent with our previous observation that dopamine application over the brainstem reduced the threshold of the current applied to the PT needed to elicit swimming (Ryczko et al., 2013). This suggests that D_1 activation either increases the strength of glutamatergic inputs to the MLR or increases MLR cell excitability through modulation of their intrinsic properties.

We found that some PT cells projecting to the MLR colocalize dopamine and glutamate. There is accumulating evidence that neurons with multiple transmitters are present in several neural circuits from lamprey to mammals (for review, see Granger et al., 2017). In zebrafish, catecholaminergic neurons were also found to coexpress either glutamate or GABA markers, including in the PT, where dopaminergic neurons preferentially use glutamate as a second transmitter (Filippi et al., 2014). In mammals, neurons co-storing dopamine and glutamate were found in the SNc and ventral tegmental area (Sulzer et al., 1998; Chuhma et al., 2004; Dal Bo et al., 2004; Kawano et al., 2006; Hnasko et al., 2010; Stuber et al., 2010; Fortin et al., 2012; for review, see Morales and Root, 2014). A future avenue would consist in determining

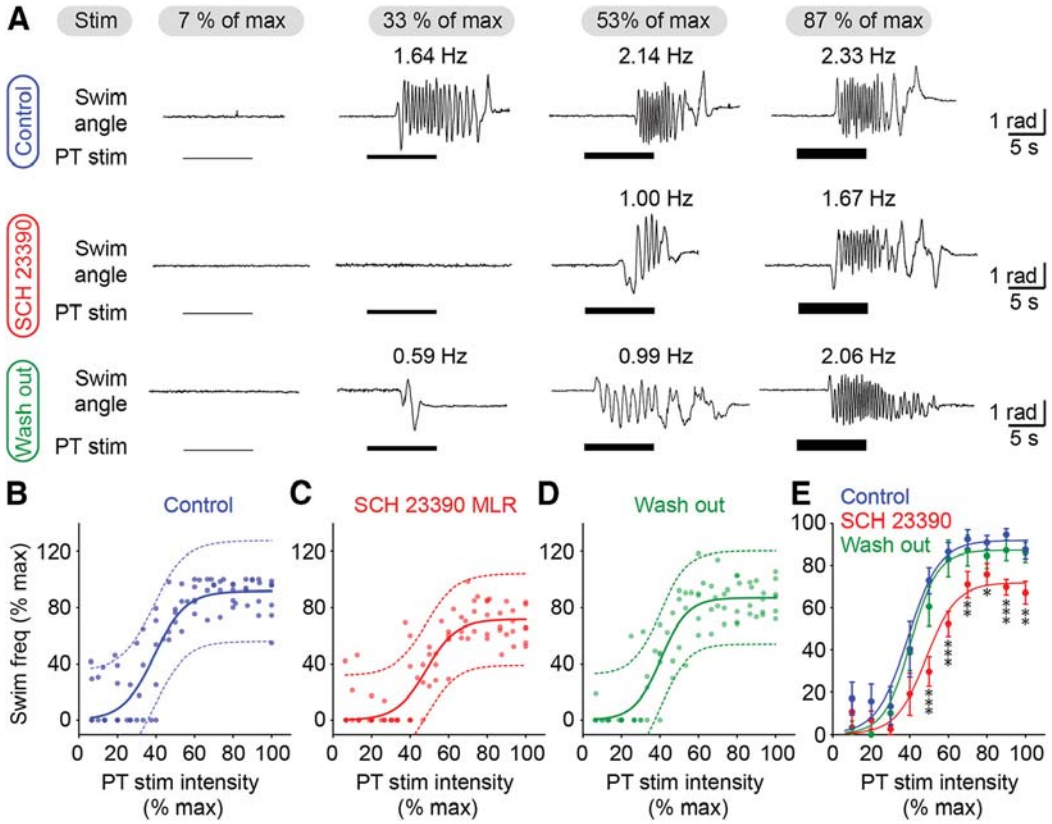

Figure 7. Effect of D_1 receptor blockade in the MLR on the graded control of swimming evoked by the PT. In a semi-intact preparation, the PT was stimulated electrically with increasing intensities. The D_1 antagonist SCH 23390 was microinjected in the MLR with a Picospritzer (pipette diameter 15–20 μm; pressure: 3–4 psi; pulses: 20; duration 20–50 ms). To quantify swimming frequency, the angular variations (radians) of the body curvature were measured over time. ***A***, From left to right, incremental PT stimulation (1–15 μA) elicited graded increase in swimming frequencies in control conditions (top), after microinjections of the D_1 receptor antagonist SCH 23390 in the MLR (middle), and after a wash out period of ~1 h (bottom). The average swimming frequency is indicated for each trial. ***B–D***, Relationships for each condition between swimming frequency and PT stimulation intensity (1–16 μA; in each condition, $n = 81$ trials pooled from 6 preparations). Data followed a sigmoidal function in control condition (***B***, blue solid line; $R^2 = 0.78$, $p < 0.0001$, frequency range 0.3–3.0 Hz), following microinjection of 0.4–1.5 pmol of SCH 23390 (0.5 mM) in the MLR (***C***, red solid line; $R^2 = 0.76$, $p < 0.0001$, frequency range 0.3–2.4 Hz) and after wash out (***D***, green solid line; $R^2 = 0.83$, $p < 0.0001$, frequency range 0.5–2.9 Hz). In each condition the dotted lines illustrate the 95% prediction intervals. Locomotor frequency and stimulation intensity were expressed as a percentage of their maximal values. ***E***, Pooled data were binned as a function of stimulation intensity, with a bin size of 10%. Normalized frequencies were compared for each bin using a two-way ANOVA on ranks. *$p < 0.05$ against control, **$p < 0.01$ against control, ***$p < 0.001$ against control; Student-Newman–Keuls test after a two-way ANOVA on ranks for repeated measures, $p < 0.001$. For convenience the sigmoid fits obtained from ***B–D*** are illustrated for each condition.

whether the release of each transmitter is activity-dependent and targets different cell populations within the MLR.

The mechanisms underlying the interplay between dopaminergic and glutamatergic inputs from the primal SNc in the graded activation of MLR cells remain to be investigated. In mammals, D_1 receptor activation increases AMPA (Cepeda et al., 1993; Hernández-Echeagaray et al., 2004; Tseng and O'Donnell, 2004; Han and Whelan, 2009) and NMDA-mediated responses (Cepeda et al., 1993; Tseng and O'Donnell, 2004). D_2 receptors are also present in lampreys (Robertson et al., 2012; Ericsson et al., 2013; Pérez-Fernández et al., 2014). In mammals D_2 receptor activation decreases both AMPA- and NMDA-mediated components of glutamatergic responses (Cepeda et al., 1993; Hernández-Echeagaray et al., 2004; Tseng and O'Donnell, 2004). Dopamine could also modulate glutamatergic transmission presynaptically as shown in mammals (for review, see Tritsch and Sabatini, 2012) and lamprey spinal cord (Svensson et al., 2003a,b). There is also a possibility that dopamine acts directly on MLR cell intrinsic properties as shown in the lamprey striatum (Ericsson et al., 2013).

It is noteworthy that other forebrain regions send input to brainstem motor networks. The pallium (homologous to the mammalian cortex) sends projections to the MLR and reticulospinal neurons (Ocaña et al., 2015). Pallium stimulation elicits reticulospinal responses and sometimes elicits swimming in lampreys (Ocaña et al., 2015), but whether incremental pallium activation can control MLR cell responses and locomotor movements is not known. In mammals, motor cortex stimulation is rather linked to voluntary modification of limb trajectory during ongoing locomotion (Bretzner and Drew, 2005). Moreover, another locomotor center, called the diencephalic locomotor region (considered to be equivalent to the subthalamic locomotor region in mammals), sends direct input to reticulospinal neurons (El Manira et al., 1997; Ménard and Grillner, 2008). The possibility that our present results might be explained by the recruitment of descending fibers originating from these two regions is unlikely, because the activation of the MLR was also obtained when stimulating the PT with local injections of glutamate, thus circumventing axonal recruitment. Future studies should seek to determine how these different inputs from supra-MLR regions are integrated by brainstem motor centers to shape motor output.

At the functional level, the dual inputs could tune the activity of MLR cells for the animal to appropriately approach targets or avoid threats, an essential function for survival. In this context, it is noteworthy that the olfactory bulb sends direct inputs to the PT (Derjean et al., 2010). Olfactory information could thus generate different levels of PT activity to control locomotor output in order for the animal to reach or avoid olfactory targets. Future

studies should examine whether and how olfactory information controls the activity of cell populations in the PT.

The lamprey is considered as a blueprint of the vertebrate brain (Robertson et al., 2014), suggesting that the descending glutamatergic pathway from the SNc to brainstem locomotor networks reported here could be present in all vertebrates. In line with this possibility, we recently provided evidence that the descending dopaminergic pathway from the SNc to the MLR is conserved in amphibians, mammals, and likely humans (Ryczko et al., 2016b; for review, see Ryczko and Dubuc, 2017). Furthermore, the present study suggests that a dysfunction in the regulation of the interaction between glutamate and dopamine in the MLR could translate into abnormal activation of the locomotor system, and thus result in locomotor deficits such as those reported in Parkinson's disease and other locomotor disorders.

References

Abalo XM, Villar-Cheda B, Anadón R, Rodicio MC (2005) Development of the dopamine-immunoreactive system in the central nervous system of the sea lamprey. Brain Res Bull 66:560–564. CrossRef Medline

Albin RL, Young AB, Penney JB (1989) The functional anatomy of basal ganglia disorders. Trends Neurosci 12:366–375. CrossRef Medline

Bachmann LC, Matis A, Lindau NT, Felder P, Gullo M, Schwab ME (2013) Deep brain stimulation of the midbrain locomotor region improves paretic hindlimb function after spinal cord injury in rats. Sci Transl Med 5:208ra146. CrossRef Medline

Barreiro-Iglesias A, Villar-Cerviño V, Villar-Cheda B, Anadón R, Rodicio MC (2008) Neurochemical characterization of sea lamprey taste buds and afferent gustatory fibers: presence of serotonin, calretinin, and CGRP immunoreactivity in taste bud bi-ciliated cells of the earliest vertebrates. J Comp Neurol 511:438–453. CrossRef Medline

Bernau NA, Puzdrowski RL, Leonard RB (1991) Identification of the midbrain locomotor region and its relation to descending locomotor pathways in the Atlantic stingray, *Dasyatis sabina*. Brain Res 557:83–94. CrossRef Medline

Bretzner F, Brownstone RM (2013) Lhx3-Chx10 reticulospinal neurons in locomotor circuits. J Neurosci 33:14681–14692. CrossRef Medline

Bretzner F, Drew T (2005) Contribution of the motor cortex to the structure and the timing of hindlimb locomotion in the cat: a microstimulation study. J Neurophysiol 94:657–672. CrossRef Medline

Brocard F, Dubuc R (2003) Differential contribution of reticulospinal cells to the control of locomotion induced by the mesencephalic locomotor region. J Neurophysiol 90:1714–1727. CrossRef Medline

Brocard F, Ryczko D, Fénelon K, Hatem R, Gonzales D, Auclair F, Dubuc R (2010) The transformation of a unilateral locomotor command into a symmetrical bilateral activation in the brainstem. J Neurosci 30:523–533. CrossRef Medline

Buchanan JT, Grillner S (1987) Newly identified "glutamate interneurons" and their role in locomotion in the lamprey spinal cord. Science 236:312–314. CrossRef Medline

Cabelguen JM, Bourcier-Lucas C, Dubuc R (2003) Bimodal locomotion elicited by electrical stimulation of the midbrain in the salamander *Notophthalmus viridescens*. J Neurosci 23:2434–2439. Medline

Cepeda C, Buchwald NA, Levine MS (1993) Neuromodulatory actions of dopamine in the neostriatum are dependent upon the excitatory amino acid receptor subtypes activated. Proc Natl Acad Sci U S A 90:9576–9580. CrossRef Medline

Chuhma N, Zhang H, Masson J, Zhuang X, Sulzer D, Hen R, Rayport S (2004) Dopamine neurons mediate a fast excitatory signal via their glutamatergic synapses. J Neurosci 24:972–981. CrossRef Medline

Dal Bo G, St-Gelais F, Danik M, Williams S, Cotton M, Trudeau LE (2004) Dopamine neurons in culture express VGLUT2 explaining their capacity to release glutamate at synapses in addition to dopamine. J Neurochem 88:1398–1405. CrossRef Medline

Derjean D, Moussaddy A, Atallah E, St-Pierre M, Auclair F, Chang S, Ren X, Zielinski B, Dubuc R (2010) A novel neural substrate for the transformation of olfactory inputs into motor output. PLoS Biol 8:e1000567. CrossRef Medline

Eidelberg E, Walden JG, Nguyen LH (1981) Locomotor control in macaque monkeys. Brain 104:647–663. CrossRef Medline

El Manira A, Pombal MA, Grillner S (1997) Diencephalic projection to reticulospinal neurons involved in the initiation of locomotion in adult lampreys *Lampetra fluviatilis*. J Comp Neurol 389:603–616. CrossRef Medline

Ericsson J, Stephenson-Jones M, Pérez-Fernández J, Robertson B, Silberberg G, Grillner S (2013) Dopamine differentially modulates the excitability of striatal neurons of the direct and indirect pathways in lamprey. J Neurosci 33:8045–8054. CrossRef Medline

Fernández-López B, Villar-Cerviño V, Valle-Maroto SM, Barreiro-Iglesias A, Anadón R, Rodicio MC (2012) The glutamatergic neurons in the spinal cord of the sea lamprey: an *in situ* hybridization and immunohistochemical study. PloS One 7:e47898. CrossRef Medline

Filippi A, Mueller T, Driever W (2014) *vglut2* and *gad* expression reveal distinct patterns of dual GABAergic versus glutamatergic cotransmitter phenotypes of dopaminergic and noradrenergic neurons in the zebrafish brain. J Comp Neurol 522:2019–2037. CrossRef Medline

Fortin GM, Bourque MJ, Mendez JA, Leo D, Nordenankar K, Birgner C, Arvidsson E, Rymar VV, Bérubé-Carrière N, Claveau AM, Descarries L, Sadikot AF, Wallén-Mackenzie Å, Trudeau LÉ (2012) Glutamate corelease promotes growth and survival of midbrain dopamine neurons. J Neurosci 32:17477–17491. CrossRef Medline

Garcia-Rill E, Skinner RD (1987a) The mesencephalic locomotor region: I. Activation of a medullary projection site. Brain Res 411:1–12. CrossRef Medline

Garcia-Rill E, Skinner RD (1987b) The mesencephalic locomotor region: II. Projections to reticulospinal neurons. Brain Res 411:13–20. CrossRef Medline

Garcia-Rill E, Houser CR, Skinner RD, Smith W, Woodward DJ (1987) Locomotion-inducing sites in the vicinity of the pedunculopontine nucleus. Brain Res Bull 18:731–738. CrossRef Medline

Gariépy JF, Missaghi K, Chevallier S, Chartré S, Robert M, Auclair F, Lund JP, Dubuc R (2012a) Specific neural substrate linking respiration to locomotion. Proc Natl Acad Sci U S A 109:E84–E92. CrossRef Medline

Gariépy JF, Missaghi K, Chartré S, Robert M, Auclair F, Dubuc R (2012b) Bilateral connectivity in the brainstem respiratory networks of lampreys. J Comp Neurol 520:1442–1456. CrossRef Medline

Goetz L, Piallat B, Bhattacharjee M, Mathieu H, David O, Chabardès S (2016) On the role of the pedunculopontine nucleus and mesencephalic reticular formation in locomotion in nonhuman primates. J Neurosci 36:4917–4929. CrossRef Medline

Granger AJ, Wallace ML, Sabatini BL (2017) Multi-transmitter neurons in the mammalian central nervous system. Curr Opin Neurobiol 45:85–91. CrossRef Medline

Grillner S, Robertson B (2016) The basal ganglia over 500 million years. Curr Biol 26:R1088–R1100. CrossRef Medline

Grillner S, Robertson B, Stephenson-Jones M (2013) The evolutionary origin of the vertebrate basal ganglia and its role in action selection. J Physiol 591:5425–5431. CrossRef Medline

Han P, Whelan PJ (2009) Modulation of AMPA currents by D_1-like but not D_2-like receptors in spinal motoneurons. Neuroscience 158:1699–1707. CrossRef Medline

Hernández-Echeagaray E, Starling AJ, Cepeda C, Levine MS (2004) Modulation of AMPA currents by D2 dopamine receptors in striatal medium-sized spiny neurons: are dendrites necessary? Eur J Neurosci 19:2455–2463. CrossRef Medline

Hnasko TS, Chuhma N, Zhang H, Goh GY, Sulzer D, Palmiter RD, Rayport S, Edwards RH (2010) Vesicular glutamate transport promotes dopamine storage and glutamate corelease *in vivo*. Neuron 65:643–656. CrossRef Medline

Islam SS, Zelenin PV (2008) Modifications of locomotor pattern underlying escape behavior in the lamprey. J Neurophysiol 99:297–307. Medline

Juvin L, Grätsch S, Trillaud-Doppia E, Gariépy JF, Büschges A, Dubuc R (2016) A specific population of reticulospinal neurons controls the termination of locomotion. Cell Rep 15:2377–2386. CrossRef Medline

Karachi C, Grabli D, Bernard FA, Tandé D, Wattiez N, Belaid H, Bardinet E, Prigent A, Nothacker HP, Hunot S, Hartmann A, Lehéricy S, Hirsch EC, François C (2010) Cholinergic mesencephalic neurons are involved in gait and postural disorders in Parkinson disease. J Clin Invest 120:2745–2754. CrossRef Medline

Kawano M, Kawasaki A, Sakata-Haga H, Fukui Y, Kawano H, Nogami H, Hisano S (2006) Particular subpopulations of midbrain and hypothalamic dopamine neurons express vesicular glutamate transporter 2 in the rat brain. J Comp Neurol 498:581–592. CrossRef Medline

Kravitz AV, Freeze BS, Parker PR, Kay K, Thwin MT, Deisseroth K, Kreitzer AC (2010) Regulation of parkinsonian motor behaviours by optogenetic control of basal ganglia circuitry. Nature 466:622–626. CrossRef Medline

Lee AM, Hoy JL, Bonci A, Wilbrecht L, Stryker MP, Niell CM (2014) Identification of a brainstem circuit regulating visual cortical state in parallel with locomotion. Neuron 83:455–466. CrossRef Medline

Le Ray D, Brocard F, Bourcier-Lucas C, Auclair F, Lafaille P, Dubuc R (2003) Nicotinic activation of reticulospinal cells involved in the control of swimming in lampreys. Eur J Neurosci 17:137–148. CrossRef Medline

Marlinsky VV, Voitenko LP (1991) The effect of procaine injection into the medullary reticular formation on forelimb muscle activity evoked by mesencephalic locomotor region and vestibular stimulation in the decerebrated guinea-pig. Neuroscience 45:753–759. CrossRef Medline

Ménard A, Grillner S (2008) Diencephalic locomotor region in the lamprey: afferents and efferent control. J Neurophysiol 100:1343–1353. CrossRef Medline

Ménard A, Auclair F, Bourcier-Lucas C, Grillner S, Dubuc R (2007) Descending GABAergic projections to the mesencephalic locomotor region in the lamprey *Petromyzon marinus*. J Comp Neurol 501:260–273. CrossRef Medline

Morales M, Root DH (2014) Glutamate neurons within the midbrain dopamine regions. Neuroscience 282:60–68. CrossRef Medline

Musienko PE, Zelenin PV, Lyalka VF, Orlovsky GN, Deliagina TG (2008) Postural performance in decerebrated rabbit. Behav Brain Res 190:124–134. CrossRef Medline

Musienko PE, Zelenin PV, Lyalka VF, Gerasimenko YP, Orlovsky GN, Deliagina TG (2012) Spinal and supraspinal control of the direction of stepping during locomotion. J Neurosci 32:17442–17453. CrossRef Medline

Noga BR, Kriellaars DJ, Jordan LM (1991) The effect of selective brainstem or spinal cord lesions on treadmill locomotion evoked by stimulation of the mesencephalic or pontomedullary locomotor regions. J Neurosci 11:1691–1700. Medline

Ocaña FM, Suryanarayana SM, Saitoh K, Kardamakis AA, Capantini L, Robertson B, Grillner S (2015) The lamprey pallium provides a blueprint of the mammalian motor projections from cortex. Curr Biol 25:413–423. CrossRef Medline

Orlovskiĭ GN (1970) Work of reticulo-spinal neurons during locomotion (in Russian). Biofizika 15:728–737. Medline

Pérez-Fernández J, Stephenson-Jones M, Suryanarayana SM, Robertson B, Grillner S (2014) Evolutionarily conserved organization of the dopaminergic system in lamprey: SNc/VTA afferent and efferent connectivity and D2 receptor expression. J Comp Neurol 522:3775–3794. CrossRef Medline

Pierre J, Mahouche M, Suderevskaya EI, Repérant J, Ward R (1997) Immunocytochemical localization of dopamine and its synthetic enzymes in the central nervous system of the lamprey *Lampetra fluviatilis*. J Comp Neurol 380:119–135. CrossRef Medline

Pombal MA, El Manira A, Grillner S (1997) Afferents of the lamprey striatum with special reference to the dopaminergic system: a combined tracing and immunohistochemical study. J Comp Neurol 386:71–91. CrossRef Medline

Redgrave P, Prescott TJ, Gurney K (1999) The basal ganglia: a vertebrate solution to the selection problem? Neuroscience 89:1009–1023. CrossRef Medline

Robertson B, Huerta-Ocampo I, Ericsson J, Stephenson-Jones M, Pérez-Fernández J, Bolam JP, Diaz-Heijtz R, Grillner S (2012) The dopamine D2 receptor gene in lamprey, its expression in the striatum and cellular effects of D2 receptor activation. PloS One 7:e35642. CrossRef Medline

Robertson B, Kardamakis A, Capantini L, Pérez-Fernández J, Suryanarayana SM, Wallén P, Stephenson-Jones M, Grillner S (2014) The lamprey blueprint of the mammalian nervous system. Prog Brain Res 212:337–349. CrossRef Medline

Roseberry TK, Lee AM, Lalive AL, Wilbrecht L, Bonci A, Kreitzer AC (2016) Cell-type-specific control of brainstem locomotor circuits by basal ganglia. Cell 164:526–537. CrossRef Medline

Rovainen CM (1967) Physiological and anatomical studies on large neurons of central nervous system of the sea lamprey (*Petromyzon marinus*): I. Müller and Mauthner cells. J Neurophysiol 30:1000–1023. Medline

Ryczko D, Dubuc R (2013) The multifunctional mesencephalic locomotor region. Curr Pharm Des 19:4448–4470. CrossRef Medline

Ryczko D, Grätsch S, Auclair F, Dubé C, Bergeron S, Alpert MH, Cone JJ, Roitman MF, Alford S, Dubuc R (2013) Forebrain dopamine neurons project down to a brainstem region controlling locomotion. Proc Natl Acad Sci U S A 110:E3235–3242. CrossRef Medline

Ryczko D, Auclair F, Cabelguen JM, Dubuc R (2016a) The mesencephalic locomotor region sends a bilateral glutamatergic drive to hindbrain reticulospinal neurons in a tetrapod. J Comp Neurol 524:1361–1383. CrossRef Medline

Ryczko D, Cone JJ, Alpert MH, Goetz L, Auclair F, Dubé C, Parent M, Roitman MF, Alford S, Dubuc R (2016b) A descending dopamine pathway conserved from basal vertebrates to mammals. Proc Natl Acad Sci U S A 113:E2440–2449. CrossRef Medline

Ryczko D, Dubuc R (2017) Dopamine and the brainstem locomotor networks: from lamprey to human. Front Neurosci 11:295. CrossRef Medline

Shik ML, Severin FV, Orlovskiĭ GN (1966) Control of walking and running by means of electric stimulation of the midbrain (in Russian). Biofizika 11:659–666. Medline

Sholomenko GN, Funk GD, Steeves JD (1991) Avian locomotion activated by brainstem infusion of neurotransmitter agonists and antagonists: II. γ-Aminobutyric acid. Exp Brain Res 85:674–681. CrossRef Medline

Sirota MG, Di Prisco GV, Dubuc R (2000) Stimulation of the mesencephalic locomotor region elicits controlled swimming in semi-intact lampreys. Eur J Neurosci 12:4081–4092. CrossRef Medline

Steeves JD, Jordan LM (1980) Localization of a descending pathway in the spinal cord which is necessary for controlled treadmill locomotion. Neurosci Lett 20:283–288. CrossRef Medline

Stephenson-Jones M, Samuelsson E, Ericsson J, Robertson B, Grillner S (2011) Evolutionary conservation of the basal ganglia as a common vertebrate mechanism for action selection. Curr Biol 21:1081–1091. CrossRef Medline

Stephenson-Jones M, Ericsson J, Robertson B, Grillner S (2012) Evolution of the basal ganglia: dual-output pathways conserved throughout vertebrate phylogeny. J Comp Neurol 520:2957–2973. CrossRef Medline

Stuber GD, Hnasko TS, Britt JP, Edwards RH, Bonci A (2010) Dopaminergic terminals in the nucleus accumbens but not the dorsal striatum corelease glutamate. J Neurosci 30:8229–8233. CrossRef Medline

Sulzer D, Joyce MP, Lin L, Geldwert D, Haber SN, Hattori T, Rayport S (1998) Dopamine neurons make glutamatergic synapses *in vitro*. J Neurosci 18:4588–4602. Medline

Svensson E, Wikström MA, Hill RH, Grillner S (2003a) Endogenous and exogenous dopamine presynaptically inhibits glutamatergic reticulospinal transmission via an action of D2-receptors on N-type Ca2+ channels. Eur J Neurosci 17:447–454. CrossRef Medline

Svensson E, Woolley J, Wikström M, Grillner S (2003b) Endogenous dopaminergic modulation of the lamprey spinal locomotor network. Brain Res 970:1–8. CrossRef Medline

Takakusaki K, Habaguchi T, Ohtinata-Sugimoto J, Saitoh K, Sakamoto T (2003) Basal ganglia efferents to the brainstem centers controlling postural muscle tone and locomotion: a new concept for understanding motor disorders in basal ganglia dysfunction. Neuroscience 119:293–308. CrossRef Medline

Tritsch NX, Sabatini BL (2012) Dopaminergic modulation of synaptic transmission in cortex and striatum. Neuron 76:33–50. CrossRef Medline

Tseng KY, O'Donnell P (2004) Dopamine-glutamate interactions controlling prefrontal cortical pyramidal cell excitability involve multiple signaling mechanisms. J Neurosci 24:5131–5139. CrossRef Medline

Villar-Cerviño V, Abalo XM, Villar-Cheda B, Meléndez-Ferro M, Pérez-Costas E, Holstein GR, Martinelli GP, Rodicio MC, Anadón R (2006) Presence of glutamate, glycine, and gamma-aminobutyric acid in the retina of the larval sea lamprey: comparative immunohistochemical study of classical neurotransmitters in larval and postmetamorphic retinas. J Comp Neurol 499:810–827. CrossRef Medline

Villar-Cerviño V, Barreiro-Iglesias A, Mazan S, Rodicio MC, Anadón R (2011) Glutamatergic neuronal populations in the forebrain of the sea lamprey, *Petromyzon marinus*: an in situ hybridization and immunocytochemical study. J Comp Neurol 519:1712–1735. CrossRef Medline

Villar-Cerviño V, Barreiro-Iglesias A, Fernández-López B, Mazan S, Rodicio MC, Anadón R (2013) Glutamatergic neuronal populations in the brainstem of the sea lamprey, *Petromyzon marinus*: an in situ hybridization and immunocytochemical study. J Comp Neurol 521:522–557. CrossRef Medline

5.3. A specific population of reticulospinal neurons controls the termination of locomotion

Juvin. L.,* Grätsch, S.,* Trillaud-Doppia, E., Gariépy, J.F., Büschges, A., and Dubuc, R.

* co-first authors

Published 2016 in *Cell Reports*, 15(11):2377-86.

Author contributions

Designed research:

Laurent Juvin, Swantje Grätsch, and Réjean Dubuc.

Performed research:

Laurent Juvin, Swantje Grätsch, Emilie Trillaud-Doppia, and Jean-François Gariépy.

Analyzed data:

Laurent Juvin, Swantje Grätsch, Emilie Trillaud-Doppia, and Jean-François Gariépy.

Wrote the paper:

Laurent Juvin, Swantje Grätsch, Ansgar Büschges, and Réjean Dubuc.

Report

Cell Reports

A Specific Population of Reticulospinal Neurons Controls the Termination of Locomotion

Graphical Abstract

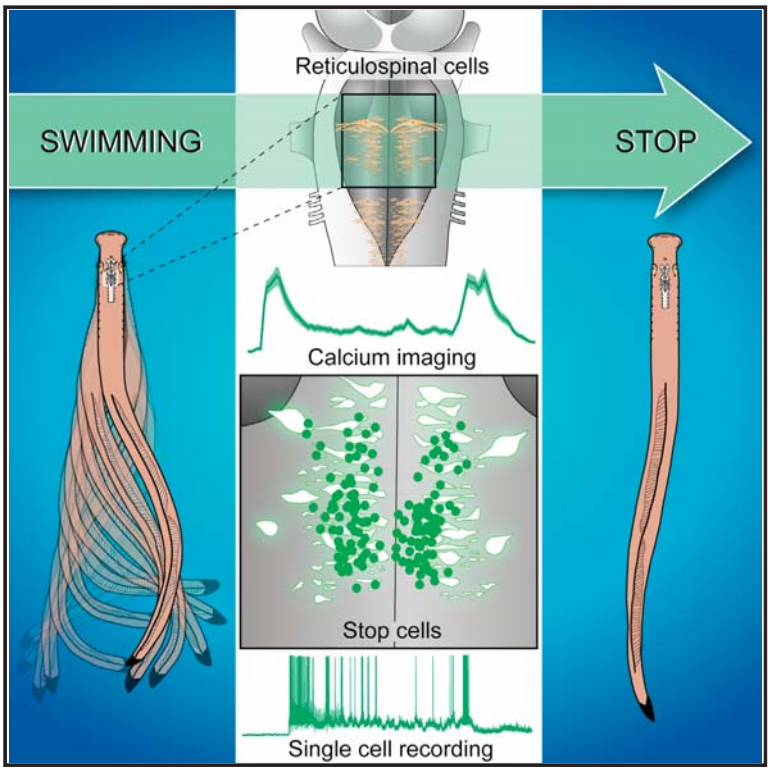

Authors

Laurent Juvin, Swantje Grätsch, Emilie Trillaud-Doppia, Jean-François Gariépy, Ansgar Büschges, Réjean Dubuc

Correspondence

rejean.dubuc@gmail.com

In Brief

Reticulospinal neurons are known to control locomotion in vertebrates. Juvin et al. find a population of reticulospinal neurons in lampreys that are activated at the end of a locomotor bout. Pharmacological activation and inactivation of these cells reveals that they play a crucial role in stopping locomotion.

Highlights

- Lamprey reticulospinal neurons display three patterns of activity during locomotion
- The patterns are compatible with starting, maintaining, and stopping locomotion
- Pharmacological activation of one reticulospinal population terminates locomotion
- Reducing activity of the same cell population impairs the termination of locomotion

Juvin et al., 2016, Cell Reports *15*, 2377–2386
June 14, 2016
http://dx.doi.org/10.1016/j.celrep.2016.05.029

Cell Reports
Report

A Specific Population of Reticulospinal Neurons Controls the Termination of Locomotion

Laurent Juvin,[1,4] Swantje Grätsch,[1,2,3,4] Emilie Trillaud-Doppia,[1] Jean-François Gariépy,[1] Ansgar Büschges,[3] and Réjean Dubuc[1,2,*]
[1]Department of Neuroscience, Université de Montréal, Montréal, QC H3C 3J7, Canada
[2]Department of Sciences de l'Activité Physique, Université du Québec à Montréal, Montréal, QC H3C 3P8, Canada
[3]Department of Animal Physiology, Biocenter Cologne, University of Cologne, 50674 Cologne, Germany
[4]Co-first author
*Correspondence: rejean.dubuc@gmail.com
http://dx.doi.org/10.1016/j.celrep.2016.05.029

SUMMARY

Locomotion requires the proper sequencing of neural activity to start, maintain, and stop it. Recently, brainstem neurons were shown to specifically stop locomotion in mammals. However, the cellular properties of these neurons and their activity during locomotion are still unknown. Here, we took advantage of the lamprey model to characterize the activity of a cell population that we now show to be involved in stopping locomotion. We find that these neurons display a burst of spikes that coincides with the end of swimming activity. Their pharmacological activation ends ongoing swimming, whereas the inactivation of these neurons dramatically impairs the rapid termination of swimming. These neurons are henceforth referred to as stop cells, because they play a crucial role in the termination of locomotion. Our findings contribute to the fundamental understanding of motor control and provide important details about the cellular mechanisms involved in locomotor termination.

INTRODUCTION

Locomotion is a basic motor function vital for survival. In vertebrates, central pattern generators (CPGs) in the spinal cord are responsible for generating the rhythmic muscle synergies underlying body propulsion, whereas supraspinal structures play a crucial role in starting, maintaining, and stopping locomotion (for review, see Grillner et al., 1998). Brainstem reticulospinal (RS) cells project directly to spinal CPG neurons. They are in turn activated by the mesencephalic locomotor region (MLR), which initiates and maintains locomotion and controls the intensity of the locomotor output like a rheostat (for review, see Dubuc et al., 2008; Ryczko and Dubuc, 2013). In lampreys, unilateral stimulation of the MLR induces bilaterally symmetrical swimming with similar activation of RS cells on both sides (Brocard et al., 2010). The MLR inputs activate RS cells via both cholinergic and glutamatergic receptors (Brocard and Dubuc, 2003; Le Ray et al., 2003). The MLR also activates muscarinoceptive cells in the lower brainstem that provide additional excitation to RS cells through a parallel connection (Smetana et al., 2010).

How locomotion is initiated and maintained was examined intensively in the past, and some of the underlying neural mechanisms are well understood (for review, see Dubuc et al., 2008). The termination of locomotion has remained far more elusive (for review, see Mullins et al., 2011). Recently, a genetically identified group of V2a cells in mice was described as halting locomotion when activated optogenetically (Bouvier et al., 2015). Blocking the synaptic output of these V2a stop neurons dramatically impaired the termination of locomotion in free-walking animals. Because these cells were not yet accessible for intracellular recordings, no details relative to their cellular activity and membrane properties were provided.

Using calcium imaging, electrophysiological, and kinematic techniques, we identify a specific population of lamprey RS cells that showed functional features similar to those of mouse V2a stop neurons. Using strengths of the lamprey model, we were able to describe the cellular activity and membrane properties of these cells. We thus demonstrate that these neurons produce a transient burst of spikes when locomotion terminates. This termination burst was present when locomotion was elicited by MLR stimulation, was sensory evoked, or occurred spontaneously. Pharmacological activation of these neurons with D-glutamate halted ongoing locomotor activity, whereas inactivation of these cells dramatically impaired locomotor termination. In line with these findings, we have named this RS cell population stop cells.

RESULTS

RS Neurons in the MRRN Show Three Distinct Patterns of Activity

In lampreys, RS neurons from the middle rhombencephalic reticular nucleus (MRRN) have been identified as command cells and were shown to be essential for the initiation and control of locomotion (Brocard and Dubuc, 2003). They have been described as key elements of a neural circuit controlling locomotor speed and swimming direction (Smetana et al., 2010; Deliagina et al., 2008). Despite the key role played by these neurons in locomotion, the activity of only a small number of lamprey RS cells, namely, the large MRRN cells (Müller and Mauthner cells), was

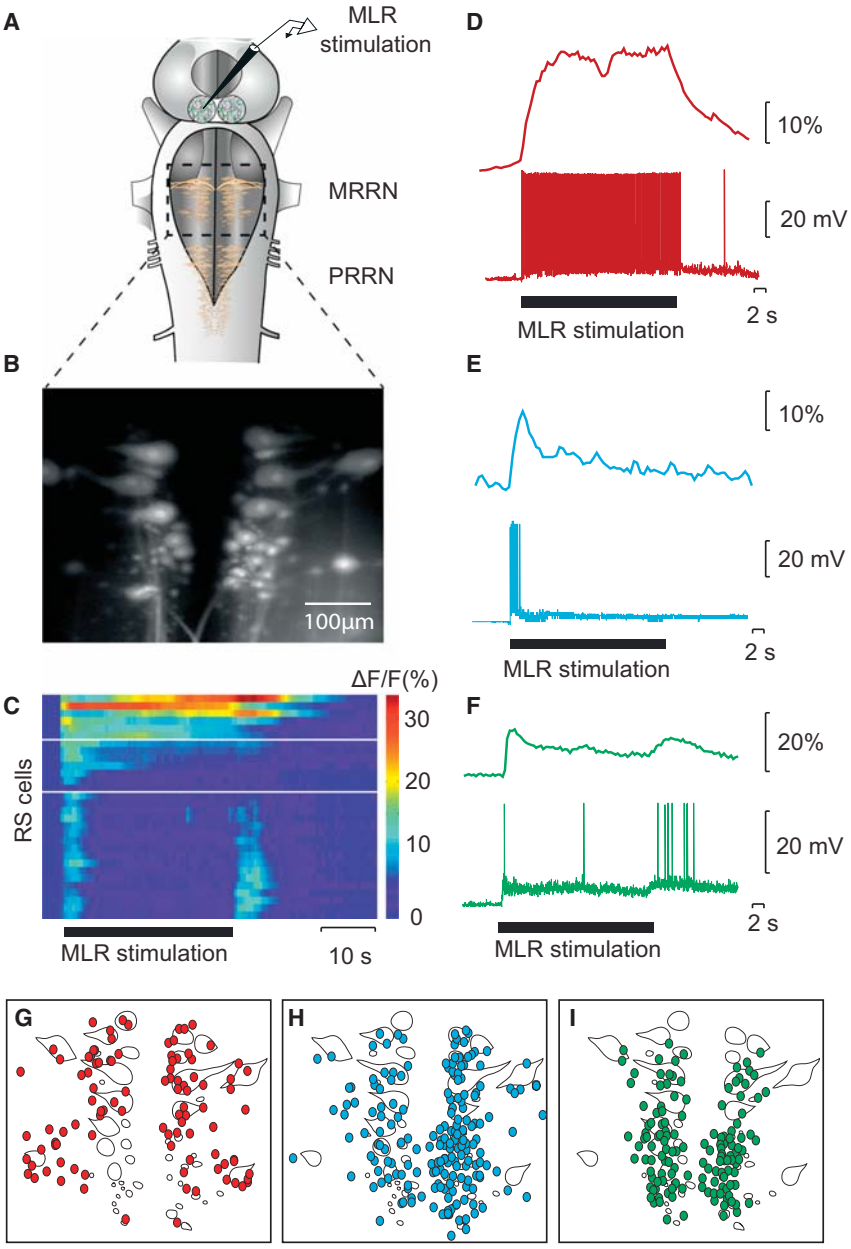

Figure 1. RS Neurons Show Three Patterns of Calcium Responses during MLR Stimulation

(A) Schematic representation of the in vitro brainstem preparation illustrating the localization of the stimulation and recording sites.

(B) Dorsal view of MRRN RS neurons backfilled with calcium green-dextran amines.

(C) Color-coded calcium responses in the backfilled RS neurons during MLR stimulation.

(D–F) Calcium responses (top) and corresponding membrane potential responses (bottom) to MLR stimulation of maintain cells (D, red traces), start cells (E, blue traces), and stop cells (F, green traces).

(G–I) Localization of maintain cells (G, red), start cells (H, blue), and stop cells (I, green) on a schematic representation of the MRRN.

documented in the context of locomotor activity. To examine the activity of a larger proportion of RS cells, we calcium imaged MRRN RS cells during MLR stimulation (Figure 1A). Using this approach, it was possible to record activity of 14–45 neurons at the same time (n = 417 cells in 21 preparations; Figure 1B). In an isolated in vitro brainstem preparation, electrical stimulation of the MLR (30 s trains of 2 ms stimuli at 5 Hz) induced changes in intracellular calcium concentrations (expressed as ΔF/F) in RS neurons. RS cells displayed three distinct patterns of calcium responses to MLR stimulation (Figure 1C) that were matched by membrane potential changes recorded intracellularly (Figures 1D–1F). On the basis of their activity, RS neurons were then divided into three populations. One population of RS neurons showed a sustained calcium response and membrane depolarization with action potential firing during the entire MLR stimulation (Figure 1D). This pattern of activity is consistent with that previously described in large MRRN RS cells known to control locomotor speed and direction (Deliagina et al., 2008; Dubuc et al., 2008). A second group of neurons showed a transient calcium response and a brief burst of spikes that occurred at the onset of MLR stimulation and decreased over time (Figure 1E). A last group of neurons displayed two transient calcium responses, as well as two bursts of action potentials: a first response at the beginning and a second at the end of MLR stimulation (Figure 1F). Calcium imaging experiments showed that cells of the three RS populations were not uniformly distributed in the MRRN (Figures 1G–1I). Most neurons that produced a sustained calcium response were located in the medio-rostral and latero-caudal part of the MRRN (n = 103 cells from the 417 recorded neurons, 24.7% of the cells; Figure 1G). RS neurons active at the beginning of MLR stimulation were distributed all over the reticular nucleus (n = 170 cells, 40.7% of the cells; Figure 1H), whereas RS neurons with two transient bursts of activity were located mainly in the medio-caudal part of the MRRN (n = 144 cells, 34.5% of the cells; Figure 1I).

One interesting observation was that RS cells in the three cell populations were all activated at the beginning of MLR stimulation. Differences in spiking activity occurred after this initial burst. To distinguish the three populations, they were named according to their activity pattern: Cells active throughout MLR stimulation were named maintain cells. Cells active only at the beginning of the stimulation were referred to as start cells. Cells that showed a

second burst of discharge at the end of the MLR stimulation were named stop cells. The name of the final cell group was chosen because of their activity pattern and their further investigated function, described later.

The Termination Burst Is Present during Active Swimming

As stated earlier, the presence of maintain cells and start cells had already been described (for review, see Mullins et al., 2011). In contrast, RS cells displaying a late burst (stop cells) had not been described previously in vertebrates. We hypothesized that this cell population could be involved in locomotor termination. We tested this in semi-intact preparations (Figure 2A) in which intracellular recordings of RS stop cells (Figure 2B, bottom) could be correlated with swimming movements of the intact body (Figure 2B, top) using kinematic analysis. An anatomical approach was used to identify the recorded neurons as RS cells and to monitor their specific location within the MRRN. The recorded RS cells were injected with biocytin, and retrograde tracing was done after the electrophysiological experiment by applying Texas red-dextran amines to the cut spinal cord (Figure 2C). Double-labeled neurons indicated that the recorded cells directly project to the spinal cord. As indicated earlier, stop cells were mainly found in the caudal MRRN (five of six labeled cells).

Examining spiking activity of stop cells during swimming, we found that the first burst of spikes occurred at the beginning of the locomotor bout, whereas the second burst (termination burst) occurred when locomotion ended (Figures 2B and 2D). When the duration of MLR stimulation was modified (7 s, 10 s, and 20 s), the length of swimming episodes changed accordingly (Figure 2D). Under those conditions, the termination burst remained strongly linked to the end of swimming but not to the end of MLR stimulation.

To examine the changes in discharge patterns during MLR-evoked locomotion, the mean spiking frequency of stop cells was calculated at the start and termination of swimming (n = 7; Figure 3A). As illustrated in the left panel, the frequency of neural activity rapidly increased before and during swimming onset (Figure 3A, left, shaded areas) and then decreased dramatically and remained low throughout the ongoing locomotor bout. The second transient burst of spikes then occurred right before termination of locomotion, which was defined as the end of the last locomotor cycle (Figure 3A, right, shaded area). Altogether, our results indicate that cellular activity of stop cells increases right before termination of locomotion, suggesting a role of these neurons in locomotion ending.

Sensory-Evoked and Spontaneous Locomotion also Evoke Stop Cell Response

So far, we described the stop cell discharge pattern only in response to MLR stimulation. Under natural conditions, however, locomotion is initiated by sensory or internal cues (Di Prisco et al., 1997, 2000). We recorded stop cell activity during both conditions to assess whether the termination burst was associated only to MLR-evoked locomotion or it was expressed in various types of locomotion. Bouts of sensory-evoked locomotion were initiated by a gentle pinch of the dorsal fin of the lamprey body (n = 7; Figure 3B, middle), and in a few experiments, we were able to record stop cells during spontaneous locomotor activity (n = 3; Figure 3B, right). It was found that stop cells displayed an activity pattern similar to that previously described for MLR-induced swimming (Figure 3B, left). To compare stop cell activity during MLR and sensory-evoked locomotion, the cell activity was aligned to the termination of locomotion (Figure 3C; every horizontal line in the raster plots represents the stop cell discharge for one locomotor bout). The stop cell spiking markedly increased right before locomotor termination for MLR-induced swimming (n = 45 bouts; Figure 3C, left), as well as for sensory-evoked swimming (n = 50 bouts; Figure 3C, right). These results indicate that the termination burst is associated with the end of locomotion rather than with MLR or sensory stimulation.

Intrinsic membrane properties are crucial in regulating the activity pattern of RS neurons in response to synaptic inputs (Di Prisco et al., 1997). To determine whether membrane properties played a role in the biphasic response of stop cells, they were characterized using whole-cell patch recordings (Figure S1). We found that the termination burst is unlikely to be mediated by intrinsic properties such as voltage-gated conductances, spike frequency adaptation, or intrinsic rebound properties and that a specific synaptic drive is more likely to be involved.

Glutamatergic Activation of Stop Cells Halts Ongoing Swimming

The preceding described results indicate that stop cells might play a crucial role in terminating locomotion. Consequently, if these cells halt locomotion, then experimentally activating them should terminate an ongoing locomotor bout. To test this, stop cells were pharmacologically stimulated during ongoing MLR-induced locomotor activity by locally pressure-ejecting D-glutamate (5 mM) over them (Jackson et al., 2007). D-glutamate was ejected either bilaterally or unilaterally, and a colorant (fast green) was added to the solution to estimate the site and volume of the ejections. To test the ejections specificity, three distinct sites were examined (Figure 4A): (1) the rostral part of the MRRN (rMRRN), where most maintain cells are located (Figure 4C); (2) the caudal part of the MRRN (cMRRN), where stop cells are prevalently located (Figure 4D); and (3) the rostral part of the posterior rhombencephalic reticular nucleus (PRRN) (rPRRN), a nucleus recruited during fast swimming (Figure 4E; Brocard and Dubuc, 2003). In comparison to control (no injection; Figure 4B), the duration of swimming bouts was not significantly modified by D-glutamate ejections over either the rMRRN or the rPRRN (control: 50.66 ± 9.19 s; rMRRN: 47.19 ± 9.40 s; rPRRN: 46.5 ± 7.24 s; n = 7; Figure 4F). However, D-glutamate ejection over the cMRRN decreased tail muscle activity (Figure S2A) and stopped locomotor activity within 5 s (Figure 4D). The duration of MLR-induced swimming bouts was significantly decreased in comparison to the control condition (control: 50.66 ± 9.19 s; cMRRN: 16.55 ± 1.03 s; n = 7; $p < 0.01$; Figure 4F). Moreover, regardless of whether D-glutamate was ejected unilaterally or bilaterally, the body axis did not change when locomotion was halted pharmacologically (one-way ANOVA; n = 9; $F_{8,171} = 0.55$; $p > 0.05$; Figure S2C). In addition, the slowdown of swimming was associated with a progressive decrease

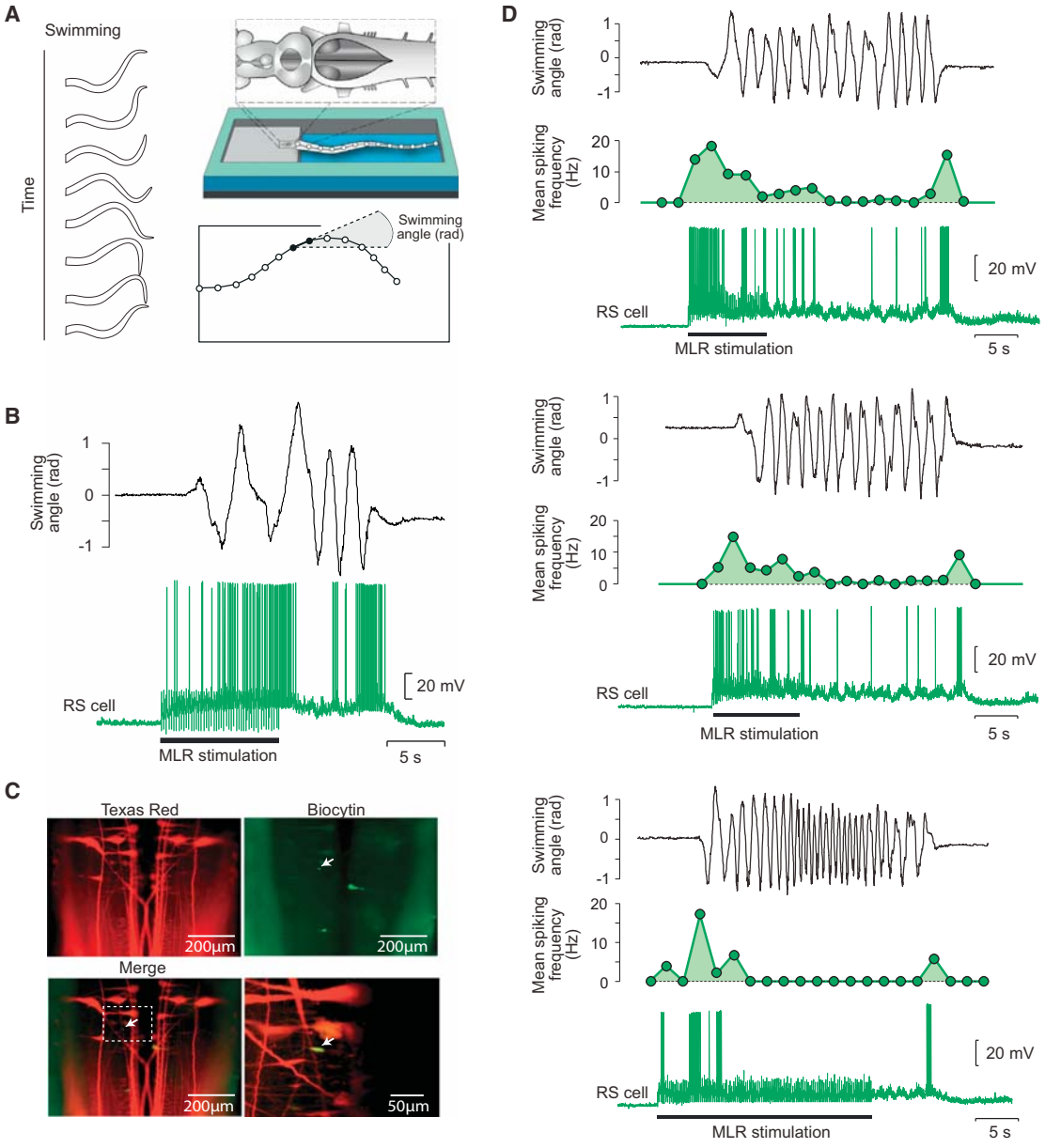

Figure 2. Stop Cells Show a Burst of Discharge Related to the Termination of Swimming

(A) Schematic representation of the body movements during a locomotor cycle (left). Semi-intact preparation in the recording chamber (top, right). Equally spaced white dots were added to the video using homemade software. Angle displacement (in radians, rad) of a mid-body segment was measured over time during locomotion (bottom, right).

(B) Swimming angle of a mid-body segment (top) combined with an intracellular recording of a stop cell (bottom) during a MLR-induced swimming bout.

(C) Dorsal view of RS neurons of the MRRN backfilled with Texas red-dextran amines (top, left) and one RS cell (recorded in B) labeled with the intracellular dye biocytin (top, right). Merged images at low magnification (bottom, left) and high magnification (bottom, right).

(D) Intracellular recordings of a stop cell during MLR-induced swimming bouts. The duration of the MLR stimulation was increased from 7 s (top), to 10 s (middle), to 20 s (bottom). The stop cell reliably generated a termination burst at the end of each locomotor bout.

See also Figure S1.

in the firing frequency of maintain cells (Figures S2A and S2B). This could result from decreased ascending excitatory input from the spinal locomotor networks to RS cells (Antri et al., 2009), whereby active stop cells would decrease the activity of spinal networks, which consequently provide less excitation to maintain cells. Taken together, the D-glutamate experiments show that the activation of stop cells is sufficient to halt ongoing locomotion.

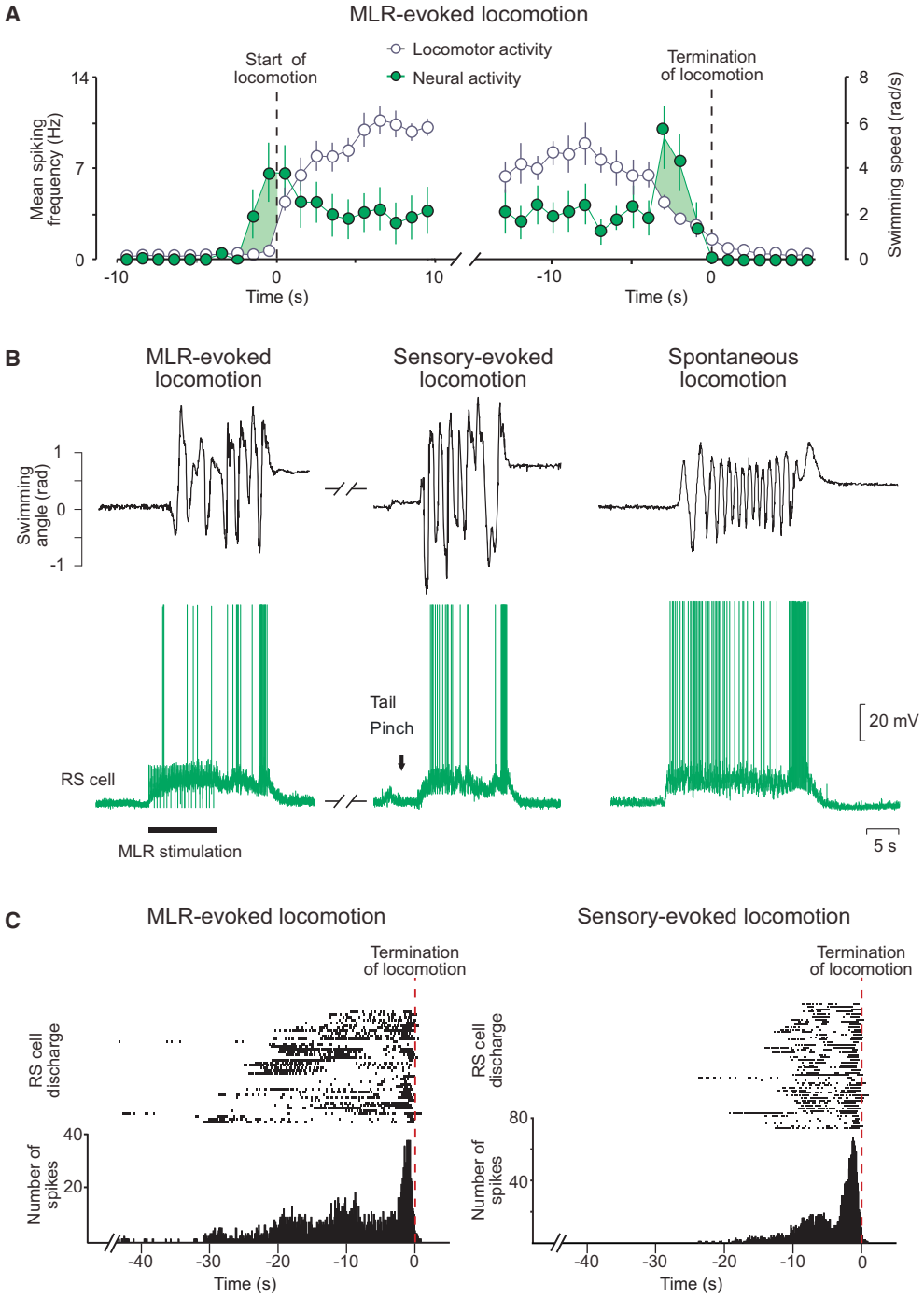

Figure 3. The Termination Burst is Present during Sensory-Evoked and Spontaneous Locomotion

(A) Mean spiking frequency of stop cells (n = 7; green circles) and swimming speed of a mid-body segment (empty circles) at the onset (left, dotted line, as indicated) and termination (right, dotted line, as indicated) of MLR-induced locomotion.

(B) Swimming angle of a mid-body segment combined with an intracellular recording of stop cell discharge in response to MLR stimulation (left), sensory-evoked locomotion (middle), and spontaneous locomotor activity (right).

(C) Raster plot (top) illustrating individual stop cell discharges after MLR stimulation (n = 45; left). The raster plots are aligned on the termination of swimming. The graph (below) illustrates the summation of the raster plots (bin width: 100 ms). The same representation is shown for stop cell discharges during sensory-evoked locomotion (n = 50; right).

All averages represent means ± SEM; rad, radian. See also Figure S1.

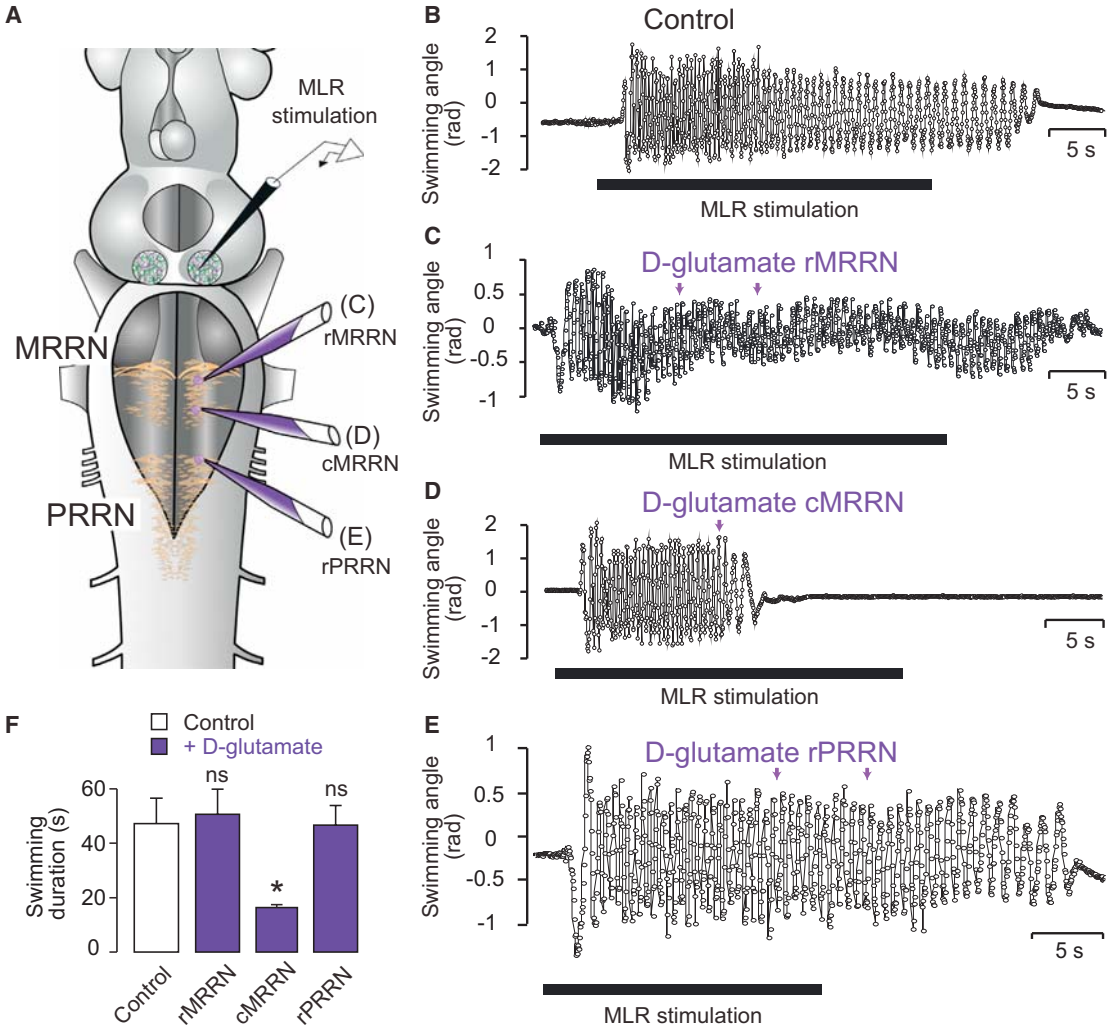

Figure 4. Activation of RS Neurons in the Caudal MRRN Induces Earlier Termination of Swimming

(A) Schematic representation showing the experimental setup (semi-intact preparation).

(B) Swimming angle of a body segment during MLR-induced locomotion in the control condition.

(C–E) Swimming activity during ejection of D-glutamate over the rMRRN (C), the cMRRN (D), or the rPRRN (E). Only ejection of D-glutamate over the cMRRN stopped locomotor activity.

(F) Histogram (n = 7 preparations) showing the duration of MLR-induced swimming (30 s stimulation at 5 Hz) in control (empty bar) and when D-glutamate was ejected over the rMRRN (filled bar, left), the cMRRN (filled bar, middle), or the rPRRN (filled bar, right).

All averages represent means ± SEM; *$p < 0.05$; rad, radian; ns, not significantly different. See also Figure S2.

Inactivation of Stop Cells Impairs Swimming Termination

In another series of experiments, we inactivated stop cells pharmacologically by ejecting glutamate receptor antagonists over them (6-cyano-7-nitroquinoxaline-2,3-dione [CNQX] at 1.25 mM and 2-amino-5-phosphonovaleric acid [AP5] at 5 mM; Figure 5A). The antagonists did not significantly change the speed of swimming induced by MLR stimulation (Student's t test; 5.90 ± 0.91 rad/s versus 6.31 ± 2.83 rad/s; n = 5; t4 = −0.17; $p > 0.05$). The duration of MLR-evoked swimming bouts did not change either (Student's t test; 51.79 ± 12.63 s versus 40.65 ± 6.89 s; n = 6; t5 = 1.409; $p > 0.05$; Figure 5C). However, the rapid slowdown of locomotor activity seen under the control condition (Figures 5B, top, and 5D, empty circles) changed to swimming activity that ended far more gradually and slowly (Figures 5B, bottom, and 5D, orange circles). These results indicate that stop cells are likely involved in producing rapid locomotor termination and that inactivating them results in slower termination of swimming.

DISCUSSION

Our findings provide insight into the neural mechanisms underlying the termination of locomotion in vertebrates. We describe

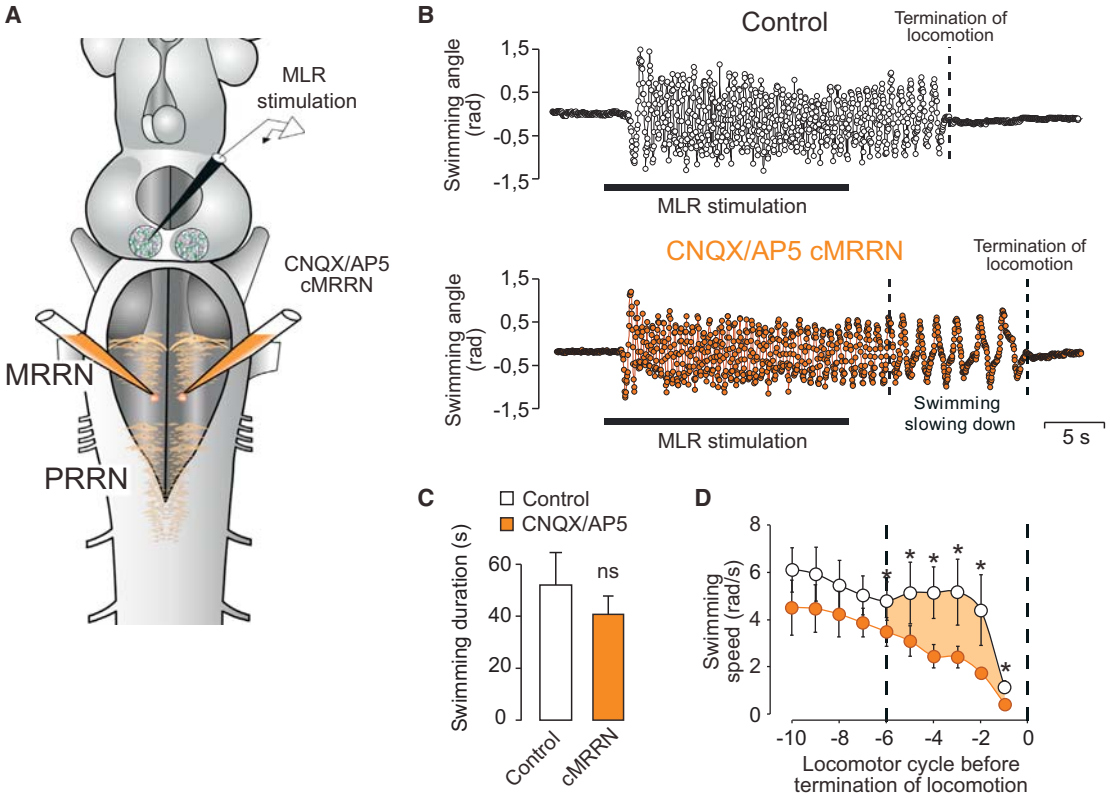

Figure 5. Inactivation of RS Neurons in the Caudal MRRN Impairs the Termination of Locomotion

(A) Schematic representation showing the experimental setup (semi-intact preparation).

(B) Swimming angle of a mid-body segment during locomotion in the control condition (top) and following the bilateral ejection of CNQX/AP5 (1.25/5 mM) over the cMRRN (bottom).

(C) Histogram of the duration of swimming activity before and after CNQX/AP5.

(D) Angular speed of a mid-body segment during the last swimming cycles that precede locomotor termination in the control condition (empty) and following the CNQX/AP5 ejection (orange).

All averages represent means ± SEM; *p < 0.05; rad, radian; ns, not significantly different.

cellular activity and properties of RS cells (stop cells) that appear to play a crucial role in the termination of locomotion.

We show that stop cells produce a transient burst of activity at the end of a locomotor bout. Similar activity patterns have been observed in another vertebrate species in the context of locomotor termination, e.g., *Xenopus* tadpole (Perrins et al., 2002). However, the cells were exclusively activated by a sensory signal originating from the rostral part of the head. In freely walking crayfish (Kagaya and Takahata, 2010, 2011) and crickets (Kai and Okada, 2013) cells with spiking activity at the end of locomotion were also found. We now show in lampreys that a termination burst occurs independent of the type of locomotion under way, i.e., after MLR stimulation, during sensory-evoked locomotion, and during spontaneous swimming (Figure 3B). From this, we conclude that this activity pattern is likely to be present when the animal moves in its natural environment.

The source of the termination burst observed in stop cells is still unknown. Intrinsic properties or synaptic inputs from higher brain centers could generate this stop signal. We found that stop cells do not have intrinsic properties that can explain their activity at the end of locomotor bouts (Figure S1). However, the stop signal could originate directly from the MLR through a gating mechanism specifically activating stop cells at the end of a locomotor bout but not other RS cells, such as maintain cells or start cells. It was recently reported in mice that the MLR provides a signal that halts locomotion (Roseberry et al., 2016), but the activity of the MLR neurons involved was not characterized. It would be of interest to determine whether stop cells described in the present study receive specific inputs from the MLR that could eventually trigger a termination burst in RS cells.

In this study, we performed pharmacological activation and inactivation experiments and concluded that stop cells play a key role in the termination process of locomotion. It was proposed that an inhibitory medullary reticular region controlled the termination of locomotion in the cat (Takakusaki et al., 2003). Electrical stimulation of this region stopped motor activity and led to inhibition of hindlimb motoneurons. However, specific cells responsible for ending locomotion were not identified. Similarly, in a recent study in mice, the optogenetic activation of V2a neurons located in the rostral medulla and caudal pons was shown to control locomotor termination (Bouvier et al., 2015). Although we did not use an optogenetic approach in this study,

pharmacological activation or inactivation still provides an excellent tool to manipulate cell activity. This has been used and continues to be used extensively in several animal models (Mentis et al., 2005; Petzold et al., 2009). We do not consider pharmacological manipulation of the stop cells to be as selective as the optogenetic approach. The localization of the three populations of RS cells described in our study showed some anatomical overlap. Ejections of D-glutamate over the cMRRN could then activate stop cells, as well as start cells or interneurons in the vicinity. Nevertheless, our results consistently demonstrated a powerful impact of the drug ejection on swimming activity associated with the termination of locomotion. This could result from the presence of a larger number of stop cells in the vicinity or a gating mechanism, whereby stop cells could be activated at the end of the locomotor bout, whereas start cells would be in a state of low excitability. Briefly, the significant halting effects we obtained by pharmacologically activating the cMRRN and the absence of effects in our control experiments indicate that stop cells are sufficient to terminate ongoing locomotion.

When stop cells were inactivated by local CNQX/AP5 ejection, locomotor duration was not significantly modified. Yet in the control condition, the deceleration process of swimming preceding locomotor termination lasted only a few seconds and swimming speed decreased abruptly (Figure 5). After CNQX/AP5 ejection, however, the duration of the deceleration process increased and instead of an abrupt reduction of swimming speed, a slower and gradual decrease occurred. These results suggest that stop cells might not provide the sole command for locomotor termination, but they would be needed to swiftly halt locomotion. Similarly, blocking the synaptic output of V2a stop neurons increased mobility in freely behaving mice (Bouvier et al., 2015). Stopping episodes were still present and could arise from another pathway.

So far, we have not identified the neuronal targets of lamprey stop cells in the spinal cord or the neurotransmitter or neurotransmitters used by those cells. In some studies, inhibitory descending neurons were described to be involved in stopping locomotion. The hindbrain RS neurons were shown to inhibit the spinal locomotor neural network mainly through activation of γ-aminobutyric acid type A ($GABA_A$; *Xenopus* tadpole; Li et al., 2003) and glycinergic receptors (lamprey; Wannier et al., 1995). However, it was recently reported in the mouse that V2a stop neurons are glutamatergic and directly project to the lumbar spinal cord, where they contact inhibitory and excitatory neurons (Bouvier et al., 2015).

We have shown that stop cells discharge both when locomotion is initiated and when it stops. Such an antagonistic activity pattern was previously reported in the leech, where Tr2 neurons can either initiate or stop locomotion (O'Gara and Friesen, 1995). Activation of these neurons initiates an episode of fictive locomotion. However, similar to stop cells, Tr2 neurons cease to fire action potentials once locomotion is started, and their activation terminates ongoing fictive swimming. These results indicate that antagonistic signals could be coded sequentially by one neuron, depending on the state of the network. Onset and offset signals with similar effects have been recorded in dorsal striatum and substantia nigra of monkeys in relation to the control of movement (Jin and Costa, 2010). The dual neural activity was proposed to signal both the initiation and the termination of action sequences. This suggest that neural activity involved in programming movement sequences shares similar mechanisms with that involved in initiation, maintenance, and termination of locomotion.

In the present study, we show that the termination of locomotion in lampreys is encoded by a specific population of RS neurons, the stop cells. Pharmacological activation and inactivation of these cells revealed that they play a crucial role in rapid locomotor termination. So far, we have not identified the origin of the termination burst produced by stop cells, but this will be the subject of upcoming studies. The present results should have importance in the field of motor control, because they reveal the cellular activity of specific brainstem cells involved in halting locomotion.

EXPERIMENTAL PROCEDURES

In Vitro Isolated Brainstem Preparation

Experiments were performed on the isolated brainstem of larval lampreys (*Petromyzon marinus*). Under tricaine methanesulphonate anesthesia (MS 222, 100 mg/L; Sigma Chemical), the animals were decapitated, incised along the ventral midline, and eviscerated in a cold saline solution (Ringer's solution) with the following composition: 130.0 mM NaCl, 2.1 mM KCl, 2.6 mM $CaCl_2$, 1.8 mM $MgCl_2$, 4.0 mM HEPES, 4.0 mM dextrose, and 1.0 mM $NaHCO_3$, adjusted to a pH of 7.4. The dorsal surface of the brain and spinal cord was exposed. Animals were decerebrated and spinalized between the first and the second segments of the spinal cord. The cartilage containing the isolated brainstem was pinned down to the Sylgard bottom of a cooled, 5 ml chamber. The recording chamber was continually superfused with cold oxygenated Ringer's solution (8°C–10°C). All procedures conformed to the guidelines of the Canadian Council on Animal Care and were approved by the University Animal Care and Use Committees. Special care was taken to limit any possible suffering and to limit the number of animals used in the experiments.

Imaging

Calcium imaging experiments were performed in larval lampreys (n = 21) in which the brainstem had been isolated in vitro as described earlier. Crystals of calcium green-dextran amines (3,000 molecular weight [MW]; Invitrogen) were applied over the cut spinal cord (between the first and the second spinal segments) to label RS cells retrogradely. The preparations were perfused with cold Ringer's solution overnight in the dark to allow dye transport (10–24 hr). Calcium responses were measured in labeled RS neurons during electrical stimulation of the MLR using a Nikon epifluorescent microscope equipped with a 20× (0.75 numerical aperture) objective and captured using an intensified charge-coupled device video camera (Photometrics CoolSNAP HQ; Roper Scientific) at a rate of two images per second. The MLR was stimulated using a glass-coated tungsten microelectrode (0.8–2 MΩ). Metafluor imaging software (Molecular Devices) was used to acquire and analyze the data. Calcium responses were expressed as relative changes in fluorescence $\Delta F/F$ after subtraction of background fluorescence immediately adjacent to the recorded neurons. All arithmetic manipulations performed on the image data were linear (background subtraction and alterations in gain) and were applied uniformly across the image under analysis.

Electrophysiology

RS neurons were impaled with glass microelectrodes (80–120 MΩ) filled with potassium acetate (4 M). The signals were amplified (Axoclamp 2A; Axon Instruments) and sampled at a rate of 10 kHz. Only RS neurons with a stable membrane potential (below −70 mV for more than 15 min) were included in the study. In some experiments, patch recordings of RS neurons were made in either whole-cell current clamp mode or voltage clamp mode (−60 to −70 mV) with a model 2400 amplifier (A-M Systems). The cells were targeted under an Eclipse FN-1 microscope (Nikon Instruments) equipped for

fluorescence. The patch pipette solution contained: 102.5 mM cesium methane sulfonate, 1.0 mM NaCl, 1.0 mM $MgCl_2$, 5.0 mM EGTA, 5.0 mM HEPES, and 0.1% biocytin. The pH was adjusted to 7.2 with CsOH, and pipettes were pulled to a tip resistance of 5 MΩ.

Labeling of RS Neurons

Microelectrodes were filled with 4 M potassium acetate and 0.5% biocytin (Sigma), and depolarizing pulses (0.5–1.0 nA) were delivered for 10 min to fill individual neurons iontophoretically. RS cells were retrogradely labeled after the experiment by applying Texas red-dextran amines (Molecular Probes) on the rostral stump of a transversely cut spinal cord, and the preparation was perfused with cold oxygenated Ringer's solution overnight to allow dye transport. The tissue was fixed in 4% paraformaldehyde (Fisher Scientific) for 24 hr at 4°C and was then transferred into a solution of Alexa Fluor 488 conjugated streptavidin (Invitrogen) diluted in Triton X-1000 and PBS (1:200) to reveal the biocytin for 24 hr. The tissue was dehydrated in an ascending series of ethanol solutions (50%, 70%, 85%, 95%, and 100%) and cleared in methyl salicylate (Fisher Scientific). The cleared whole mount was then observed and photographed with an E600 epifluorescence microscope equipped with a DXM 1200 digital camera (Nikon); insets were made with an Olympus FV1000 confocal microscope.

Semi-intact Preparation

For semi-intact preparations (n = 56), the brain and the ten most rostral spinal cord segments were exposed to the Ringer's solution while the remaining body was kept intact. The cranium and the most rostral notochord were pinned down on Sylgard while the body was free to move. At least 2 hr were allowed between the end of the dissection and the beginning of recording session. Locomotor bouts were induced by electrical stimulation of the MLR (10–30 s trains of 2 ms stimuli at 5 Hz) using a glass-coated tungsten microelectrode. In some experiments, locomotion was induced by tactile stimulation of the body or occurred spontaneously. Electromyographic (EMG) recordings were carried out using Teflon-coated stainless steel wires (diameter: 50 μm; California Fine Wire) inserted into the body musculature between segments 20 and 25. The quality of the swimming was assessed visually. The EMG signals were amplified (1,000 times), filtered (bandwidth: 30 Hz to 1 kHz), and acquired with a sampling rate of 5 kHz. Kinematic recordings of body movements were performed using a high-definition video camera (GZ-HD3U; JVC) at a sampling rate of 30 Hz. Body movements were analyzed using a homemade MATLAB R2009A script (MathWorks). Markers were placed offline at equal distances on the body (Figure 2A) and tracked over time to monitor swimming behavior.

Drugs

All drugs were dissolved at their final concentration in the Ringer's solution and injected as described previously (e.g., Smetana et al., 2010; Ryczko et al., 2013). D-glutamate (5 mM; Sigma-Aldrich), and a CNQX/AP5 mixture (CNQX at 1.25 mM and AP5 at 5 mM) was pressure ejected through a glass micropipette with a Picospritzer (General Valve Corporation). The inactive dye fast green was added to the drug solution to monitor the extent of the injection. The injection micropipette was positioned on the surface of the tissue, and injection parameters were set so that a fast green stain of ~100 μm diameter would be visible on the surface of the tissue right after injection. Control injections of fast green dissolved in Ringer's solution did not induce responses in RS neurons.

Data Acquisition and Analysis

Electrophysiological data were acquired through a Digidata 1322A interface with Clampex 8.0 software (Axon Instruments, Molecular Devices) and analyzed with Clampfit 10.2 software. Data were expressed as means ± SEM. Using SigmaPlot 11.0, statistical significance was determined using Student's t tests or one-way ANOVA, followed by Tukey's post hoc test. Correlations were obtained using a Spearman correlation test. $p < 0.05$ was considered statistically significant.

SUPPLEMENTAL INFORMATION

Supplemental Information includes two figures can be found with this article online at http://dx.doi.org/10.1016/j.celrep.2016.05.029.

AUTHOR CONTRIBUTIONS

L.J. and S.G. performed both the experiments and the analyses, wrote sections, and edited the paper. E.T.-D. performed experiments and analyses and edited sections of the paper. J.-F.G. performed experiments. A.B. supervised the project and edited sections of the paper. R.D. supervised the project and wrote and edited sections of the paper.

ACKNOWLEDGMENTS

We thank D. Veilleux for her assistance with experiments, C. Valiquette for his expertise in computer programming, F. Bernard for his help with the figures, and F. Auclair for his help with anatomical work. This work was funded by the Canadian Institutes of Health Research (15129 and 15176), the Natural Sciences and Engineering Research Council of Canada (217435-01), the Great Lakes Fishery Commission (54011, 54021, and 54035). L.J. received a Jasper fellowship from the Groupe de Recherche sur le Système Nerveux Central. S.G. received scholarships from the University of Cologne and the German Academic Exchange Service.

Received: May 22, 2015
Revised: March 23, 2016
Accepted: May 5, 2016
Published: June 2, 2016

REFERENCES

Antri, M., Fénelon, K., and Dubuc, R. (2009). The contribution of synaptic inputs to sustained depolarizations in reticulospinal neurons. J. Neurosci. *29*, 1140–1151.

Bouvier, J., Caggiano, V., Leiras, R., Caldeira, V., Bellardita, C., Balueva, K., Fuchs, A., and Kiehn, O. (2015). Descending command neurons in the brainstem that halt locomotion. Cell *163*, 1191–1203.

Brocard, F., and Dubuc, R. (2003). Differential contribution of reticulospinal cells to the control of locomotion induced by the mesencephalic locomotor region. J. Neurophysiol. *90*, 1714–1727.

Brocard, F., Ryczko, D., Fénelon, K., Hatem, R., Gonzales, D., Auclair, F., and Dubuc, R. (2010). The transformation of a unilateral locomotor command into a symmetrical bilateral activation in the brainstem. J. Neurosci. *30*, 523–533.

Deliagina, T.G., Beloozerova, I.N., Zelenin, P.V., and Orlovsky, G.N. (2008). Spinal and supraspinal postural networks. Brain Res. Brain Res. Rev. *57*, 212–221.

Di Prisco, G.V., Pearlstein, E., Robitaille, R., and Dubuc, R. (1997). Role of sensory-evoked NMDA plateau potentials in the initiation of locomotion. Science *278*, 1122–1125.

Di Prisco, G.V., Pearlstein, E., Le Ray, D., Robitaille, R., and Dubuc, R. (2000). A cellular mechanism for the transformation of a sensory input into a motor command. J. Neurosci. *20*, 8169–8176.

Dubuc, R., Brocard, F., Antri, M., Fénelon, K., Gariépy, J.F., Smetana, R., Ménard, A., Le Ray, D., Viana Di Prisco, G., Pearlstein, E., et al. (2008). Initiation of locomotion in lampreys. Brain Res. Brain Res. Rev. *57*, 172–182.

Grillner, S., Ekeberg, O., El Manira, A., Lansner, A., Parker, D., Tegnér, J., and Wallén, P. (1998). Intrinsic function of a neuronal network—a vertebrate central pattern generator. Brain Res. Brain Res. Rev. *26*, 184–197.

Jackson, A.W., Pino, F.A., Wiebe, E.D., and McClellan, A.D. (2007). Movements and muscle activity initiated by brain locomotor areas in semi-intact preparations from larval lamprey. J. Neurophysiol. *97*, 3229–3241.

Jin, X., and Costa, R.M. (2010). Start/stop signals emerge in nigrostriatal circuits during sequence learning. Nature *466*, 457–462.

Kagaya, K., and Takahata, M. (2010). Readiness discharge for spontaneous initiation of walking in crayfish. J. Neurosci. *30*, 1348–1362.

Kagaya, K., and Takahata, M. (2011). Sequential synaptic excitation and inhibition shape readiness discharge for voluntary behavior. Science *332*, 365–368.

Kai, K., and Okada, J. (2013). Characterization of locomotor-related spike activity in protocerebrum of freely walking cricket. Zoolog. Sci. *30*, 591–601.

Le Ray, D., Brocard, F., Bourcier-Lucas, C., Auclair, F., Lafaille, P., and Dubuc, R. (2003). Nicotinic activation of reticulospinal cells involved in the control of swimming in lampreys. Eur. J. Neurosci. *17*, 137–148.

Li, W.C., Perrins, R., Walford, A., and Roberts, A. (2003). The neuronal targets for GABAergic reticulospinal inhibition that stops swimming in hatchling frog tadpoles. J. Comp. Physiol. A Neuroethol. Sens. Neural Behav. Physiol. *189*, 29–37.

Mentis, G.Z., Alvarez, F.J., Bonnot, A., Richards, D.S., Gonzalez-Forero, D., Zerda, R., and O'Donovan, M.J. (2005). Noncholinergic excitatory actions of motoneurons in the neonatal mammalian spinal cord. Proc. Natl. Acad. Sci. USA *102*, 7344–7349.

Mullins, O.J., Hackett, J.T., Buchanan, J.T., and Friesen, W.O. (2011). Neuronal control of swimming behavior: comparison of vertebrate and invertebrate model systems. Prog. Neurobiol. *93*, 244–269.

O'Gara, B.A., and Friesen, W.O. (1995). Termination of leech swimming activity by a previously identified swim trigger neuron. J. Comp. Physiol. A Neuroethol. Sens. Neural Behav. Physiol. *177*, 627–636.

Perrins, R., Walford, A., and Roberts, A. (2002). Sensory activation and role of inhibitory reticulospinal neurons that stop swimming in hatchling frog tadpoles. J. Neurosci. *22*, 4229–4240.

Petzold, G.C., Hagiwara, A., and Murthy, V.N. (2009). Serotonergic modulation of odor input to the mammalian olfactory bulb. Nat. Neurosci. *12*, 784–791.

Roseberry, T.K., Lee, A.M., Lalive, A.L., Wilbrecht, L., Bonci, A., and Kreitzer, A.C. (2016). Cell-type-specific control of brainstem locomotor circuits by basal ganglia. Cell *164*, 526–537.

Ryczko, D., and Dubuc, R. (2013). The multifunctional mesencephalic locomotor region. Curr. Pharm. Des. *19*, 4448–4470.

Ryczko, D., Grätsch, S., Auclair, F., Dubé, C., Bergeron, S., Alpert, M.H., Cone, J.J., Roitman, M.F., Alford, S., and Dubuc, R. (2013). Forebrain dopamine neurons project down to a brainstem region controlling locomotion. Proc. Natl. Acad. Sci. USA *110*, E3235–E3242.

Smetana, R., Juvin, L., Dubuc, R., and Alford, S. (2010). A parallel cholinergic brainstem pathway for enhancing locomotor drive. Nat. Neurosci. *13*, 731–738.

Takakusaki, K., Kohyama, J., and Matsuyama, K. (2003). Medullary reticulospinal tract mediating a generalized motor inhibition in cats: III. Functional organization of spinal interneurons in the lower lumbar segments. Neuroscience *121*, 731–746.

Wannier, T., Orlovsky, G., and Grillner, S. (1995). Reticulospinal neurones provide monosynaptic glycinergic inhibition of spinal neurones in lamprey. Neuroreport *6*, 1597–1600.

6. Study under review

6.1. A brainstem neural substrate for stopping locomotion

Grätsch, S., Auclair, F., Demers, O., Auguste, E., Hanna, A., Büschges, A., and Dubuc, R.

Submitted to and reviewed by *Current Biology*.

Author contributions

Designed research:

Swantje Grätsch, François Auclair, Ansgar Büschges, and Réjean Dubuc.

Performed research:

Swantje Grätsch, François Auclair, Olivier Demers, Emmanuella Auguste, and Amer Hanna.

Analyzed data:

Swantje Grätsch, François Auclair, Olivier Demers, Emmanuella Auguste, Amer Hanna, Ansgar Büschges, and Réjean Dubuc.

Wrote the paper:

Swantje Grätsch, Ansgar Büschges, and Réjean Dubuc.

A Brainstem Neural Substrate for Stopping Locomotion

Swantje Grätsch[1, 2, 3], François Auclair[1], Olivier Demers[2], Emmanuella Auguste[2], Amer Hanna[1], Ansgar Büschges[3], and Réjean Dubuc[1, 2, 4*]

[1] Dept. Neuroscience; Université de Montréal; Montréal, Québec, H3C 3J7; Canada

[2] Dept. Sciences de l'Activité Physique; Université du Québec à Montréal; Montréal, Québec, H3C 3P8; Canada

[3] Biocenter Cologne; Dept. Animal Physiology; University of Cologne; Cologne, D-50674; Germany

[4] Lead contact

*Correspondence to: rejean.dubuc@gmail.com

GRAPHICAL ABSTRACT

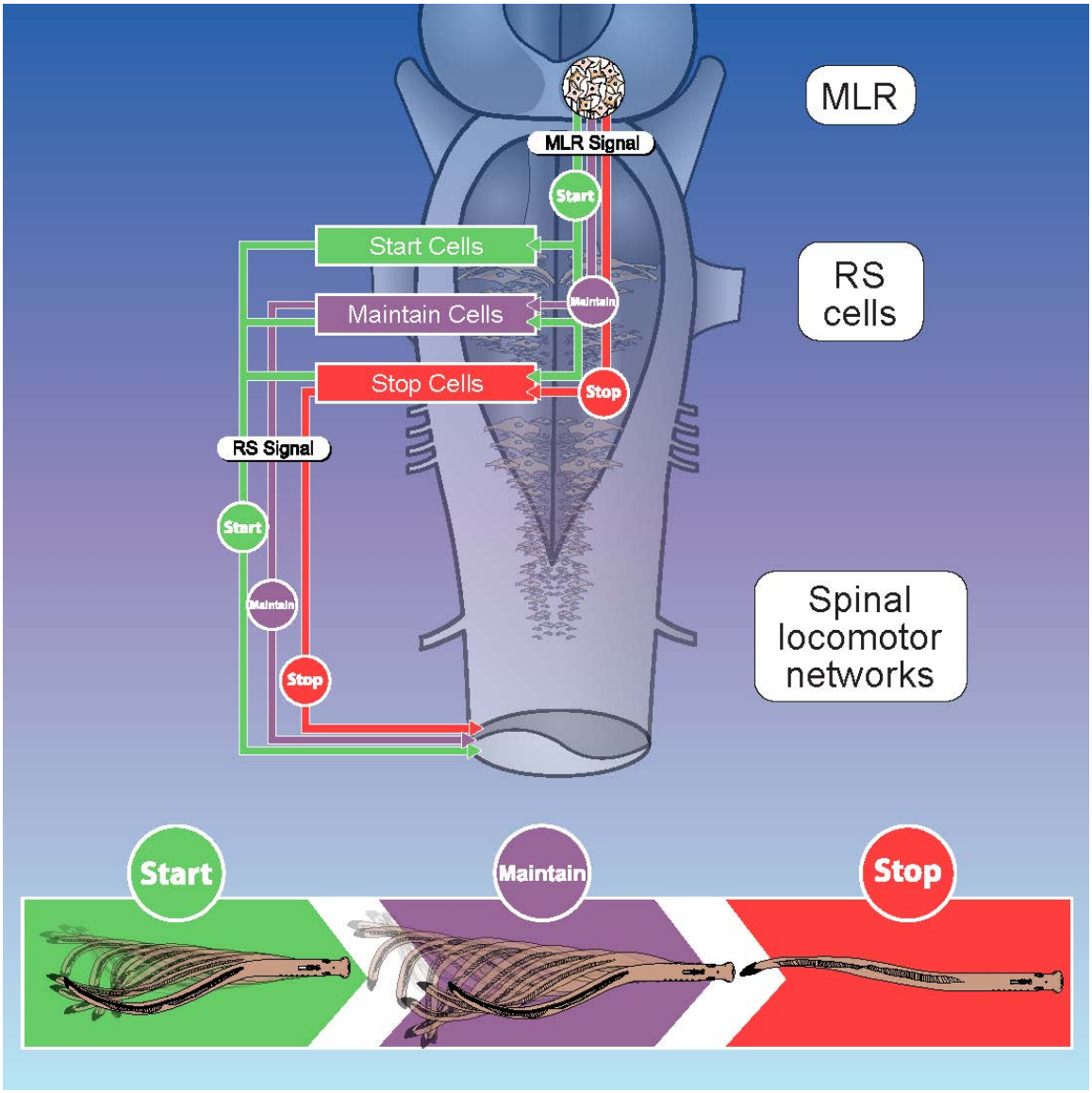

SUMMARY

Locomotion is a basic motor function crucial for survival. Daily activities consist of locomotor bouts that need to be started, maintained, and stopped. The neural substrate underlying starting and maintaining locomotion is partly known, but there is little knowledge concerning stopping. Recently, reticulospinal (RS) neurons (stop cells) that control locomotor termination were identified. The inputs that activate the stop cells are unknown. The mesencephalic locomotor region (MLR) is classically described as a major input to RS cells as it is involved in starting and maintaining locomotion. We now show in the lamprey, that the MLR also produces locomotor termination that is accompanied by a burst of discharge in stop cells. Our results suggest the presence of a monosynaptic pathway from MLR to stop cells. These results fill an important gap in knowledge relative to the neural mechanisms controlling the termination of locomotion.

KEYWORDS

locomotion; locomotor termination; brainstem; mesencephalic locomotor region; reticulospinal neurons; stop cells; lamprey.

eTOC BLURB

Grätsch et al. describe a neural substrate involved in terminating locomotion. The mesencephalic locomotor region is well known for initiating and controlling locomotion. The authors demonstrate that it also controls the termination of locomotion through inputs to reticulospinal cells (stop cells) that play a crucial role in stopping of locomotion.

HIGHLIGHTS

MLR stimulation not only initiates and maintains locomotion, it also stops it

Both electrical and chemical stimulation of the MLR can stop locomotion

RS stop cells display a termination burst in response to MLR stimulation

MLR stimulation also stops sensory-evoked and spontaneous locomotion

INTRODUCTION

Goal-directed locomotion is essential for individuals to survive and interact in their environment. To successfully achieve this, the central nervous system must generate locomotor bouts that can be efficiently started, maintained, and stopped. In vertebrates, the spinal cord contains the neural networks (central pattern generators; CPGs) that produce the muscle synergies essential for body propulsion (for review, see [1]). These spinal networks are controlled by brainstem reticulospinal (RS) neurons, which are activated by upstream-located locomotor centers, such as the mesencephalic locomotor region (MLR) [2] (for review, see [3-5]).

RS cells are command neurons displaying activity that is strongly correlated to motor behavior [6-10]. They are not activated uniformly during locomotion but encode different motor outputs, *e.g.* slow and fast locomotion [7, 11, 12], forward and backward swimming [13], or turning movements [8, 14]. Three subpopulations of RS cells were recently identified in the brainstem of the lamprey, a basal vertebrate, and their activity was correlated to different phases of locomotion [15]. Start cells discharge transiently at the beginning of a locomotor episode, whereas maintain cells fire action potentials throughout the locomotor bout. Stop cells respond with a burst of action potentials at the beginning and another at the end of a locomotor episode (termination burst). Pharmacological activation of these RS stop cells stops ongoing swimming activity and their inactivation slows down the termination process. These results were recently corroborated by mammalian studies. Glutamatergic brainstem neurons (V2a 'stop neurons') were identified and shown to control stopping of locomotion in the mouse [16]. Optogenetic activation of these neurons halts ongoing movements, whereas blocking their synaptic output results in increased mobility and reduced stopping behavior. Inhibitory brainstem neurons in the mouse have also been described [12]. When optogenetically activated, ongoing locomotion stops. These glycinergic neurons were identified in multiple brainstem regions and shown to project directly to the spinal cord. As of now, it has not been resolved how command cells that provide a stop signal to the spinal CPGs are activated. We have examined the membrane properties of RS stop cells in the lamprey and concluded that synaptic inputs rather than intrinsic properties are responsible for generating the termination burst [15]. Because the MLR projects extensively to RS cells [7, 17- 20] (for review, see [5]), it is a likely candidate for activating the stop cells. Indeed, the MLR controls locomotion in all vertebrate species tested to date (*e.g.* cat: [2]; rat: [21]; mouse: [22]; salamander: [23]; birds: [24]; lamprey: [25]). Located at the border between the mid- and hindbrain, it initiates motor behavior when activated electrically, pharmacologically, or optogenetically [2, 22, 26-29]. There is still a controversy relative to the exact motor output produced by stimulation of the MLR. In mammals, it is a large area and stimulation of different MLR sub-regions was shown to elicit diverse motor behaviors *e.g.* appetitive, defensive, and explorative behavior [30].

We now have investigated the neural substrate for the termination of locomotion in a basal vertebrate, the lamprey. This animal species provides numerous advantages to examine such mechanisms. The lamprey nervous system, in many ways, is considered the blueprint for the vertebrate phylum and has been used

extensively to uncover the neural mechanisms underlying locomotion (for recent review, see [31]). Here, we demonstrate that the lamprey MLR not only initiates locomotion, but also stops it, much like a brake pedal. In semi-intact preparations, MLR stimulation induces locomotion in the intact body that often outlasts the stimulation duration. In these cases, a second MLR stimulation delivered at a lower intensity than that used to start locomotion, stops the ongoing locomotor bout. It was also found that a low-intensity stimulation of the MLR was as effective in stopping sensory-evoked and spontaneous locomotion. The low-intensity MLR stimulation elicited a termination burst in the RS stop cells and likely achieved this through monosynaptic connections. These findings reveal state-dependent responses to MLR stimulation and contribute to the knowledge relative to the neural mechanisms underlying the termination of locomotion.

RESULTS

MLR Stimulation Stops Ongoing Locomotion

Three types of discharge patterns are found in RS cells in response to MLR stimulation: start cell, maintain cell and stop cell patterns (Figure 1A; [15]). In this study, we focused on the RS cells that display a stop cell pattern (stop cells) and we first characterized the changes that occur in the termination burst of those cells as we increased the intensity of the MLR stimulation. Stop cells were recorded intracellularly in semi-intact preparations that allowed us to correlate the cellular discharge to the frequency of the swimming movements (Figure 1C). As shown in Figure 1B, low stimulation intensity (2 μA) of the MLR neither elicited discharges nor swimming activity. Increasing the stimulation strength to 4 μA induced discharges in the recorded stop cell, but still no swimming movements. In this case, the characteristic termination burst was absent. A termination burst was only seen when the intensity of MLR stimulation was sufficient to generate swimming movements (Figure 1B; 6 μA, 8 μA, 10 μA). Moreover, for individual neurons, the higher the stimulation intensity was, the larger was the number of spikes in the termination bursts ($R = 0.896$; $p < 0.01$; $n = 8$ samples in one animal; Figure 1D). The same was true for pooled data from several neurons ($R = 0.806$; $p < 0.001$; $n = 52$ samples in 6 animals; Figure 1E). A positive correlation between the number of spikes in the termination burst and the swimming frequency of the whole locomotor bout was also present ($R = 0.757$; $p < 0.001$; $n = 52$ samples in 6 animals).

The close relationship between the intensity of the termination burst and the strength of MLR stimulation suggests that the MLR could be responsible for generating a termination burst and thus stop locomotion. In the semi-intact preparation, swimming activity can be made to outlast the end of the MLR stimulation by using an intensity slightly larger than the threshold for swimming (e.g. Figure 2A1). It is then possible to apply a second MLR stimulation during that period of swimming activity outlasting the stimulation. We applied a second stimulation to the MLR, at lower intensity (intensity of second stimulation was 50 % of control, 2 μA in the case of Figure 2A2) and found that it stopped the swimming episode earlier compared to

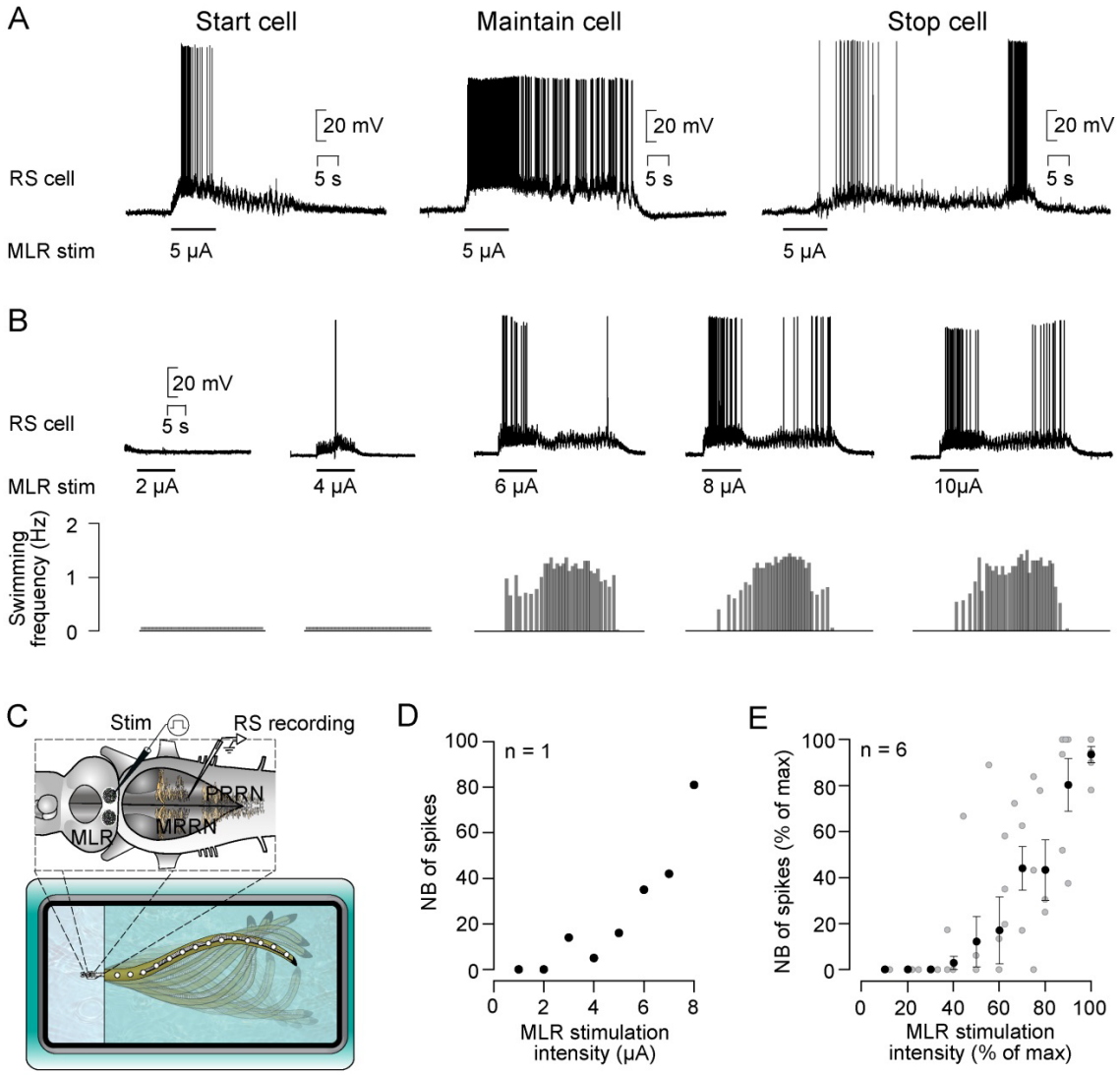

Figure 1. Response of Reticulospinal Stop Cells to MLR Stimulation of Increasing Intensity

(A) Activity pattern of three populations of reticulospinal (RS) cells in response to MLR stimulation: start (left), maintain (middle) and stop cells (right).

(B) Concurrent intracellular recording of a stop cell (top) and swimming activity (bottom) in a semi-intact preparation in response to different MLR stimulation intensities (2 to 10 µA).

(C) Schematic representation of the semi-intact preparation. The brainstem is illustrated with intracellular (RS cells) and stimulation electrodes (MLR). Swimming movements of the intact body are monitored with a video camera.

(D) Relationship between the number of spikes in the termination burst and the intensity of the MLR stimulation (n = 8 trials recorded in one cell).

(E) Similar representation as in D, but for 6 stop cells recorded in 6 preparations. The black dots represent data pooled in 10 % bins of stimulation intensity (52 individual trials; grey dots). The number of spikes and the stimulation intensities were normalized and represented as % of maximal values.

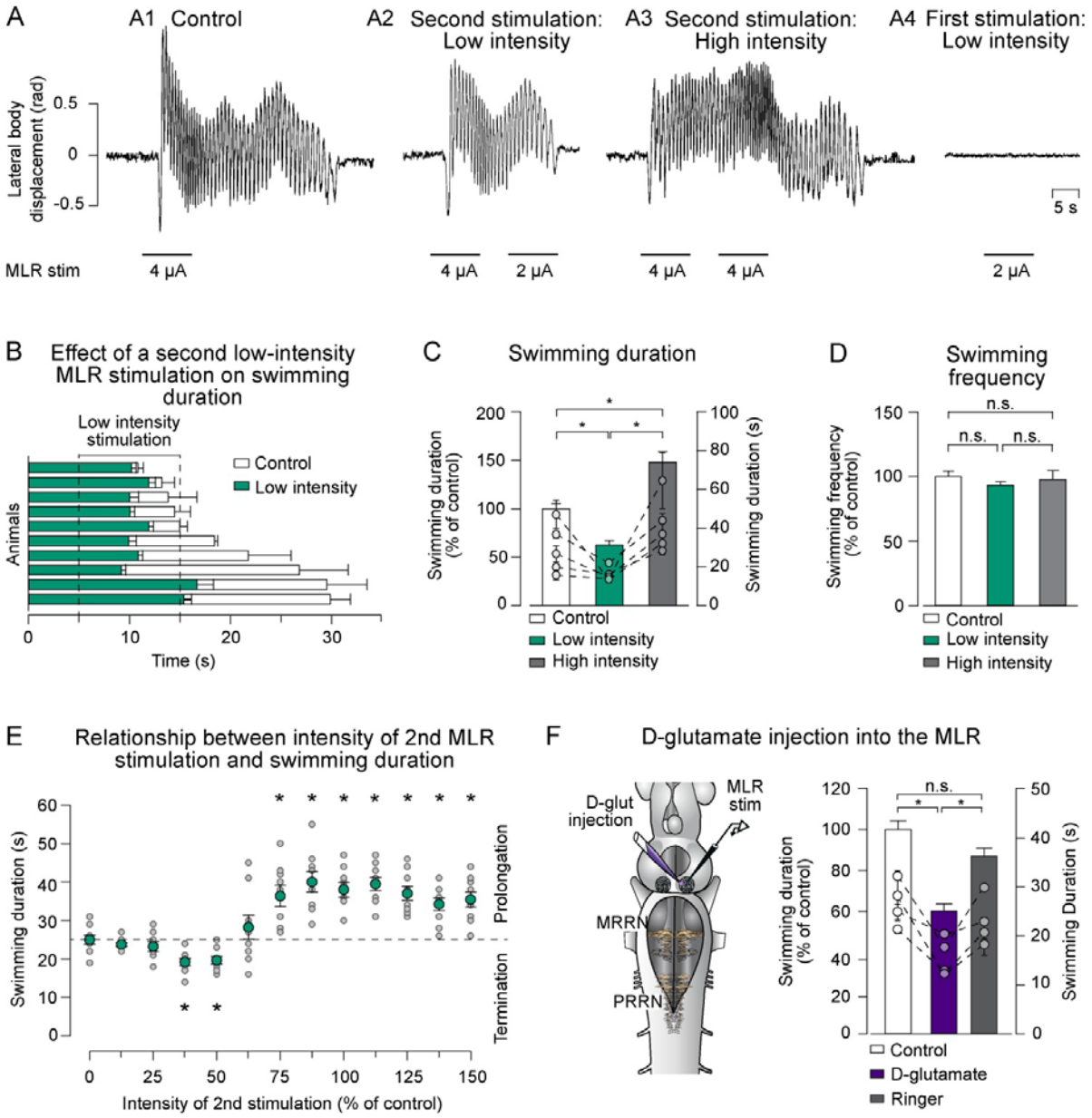

Figure 2. Effect of a Second MLR Stimulation on the Swimming Duration

(A) The lateral displacement of the body (rad) is plotted for swimming bouts elicited by electrical stimulation of the MLR (control condition; 4 µA, A1), when a second MLR stimulation of low intensity (2 µA, A2) or high intensity (4 µA, A3) was delivered 5 s after the end of the first MLR stimulation. MLR stimulation of low intensity did not trigger locomotion at rest (2 µA, A4).

(B) Bar graphs illustrating the swimming duration (mean ± SEM) under control condition (white bars) and when the MLR was stimulated a second time at low intensity while the animal was swimming (green bars). Each line represents one animal (n = 5 stimulation trials for each condition). Time 0 represents the end of the first MLR stimulation.

(C) Histogram illustrating the average swimming duration under control condition (white bar) and when the MLR was stimulated a second time with a low-intensity (green bar) or with a high-intensity stimulation (grey bar). Bars represent mean ± SEM of data that was normalized to control (n = 25 trials in 5 animals). Dots represent mean ± SEM of raw data for each animal (n = 5 stimulations for each animal).

(Continuation of Figure 2)

(D) Comparison of the average swimming frequency in three conditions: control (white bar); when a second MLR stimulation of low intensity is delivered (green bar); when a second MLR stimulation of high intensity is delivered (grey bar). Same animals as illustrated in C.

(E) Swimming duration as a function of the intensity of the second MLR stimulation. For each trial, swimming was elicited by electrical MLR stimulation (100 %). Intensities of the second MLR stimulation were altered from 0 to 150 % in 12.5 % steps. Grey dots represent swimming duration for each individual trial, green dots represent average duration (mean ± SEM) of all animals (n = 3 animals). The doted horizontal line indicates the average swimming duration under control condition, when no second stimulation was delivered to the MLR.

(F) Left: Schematic representation of the experimental setup when the second MLR stimulation was delivered by injection of small D-glutamate quantities or Ringer's solution into the MLR. Right: Bar graph illustrating the average swimming duration in control condition (white bar) when D-glutamate (violet bar) or Ringer's solution (grey bar) was applied into the MLR during ongoing swimming. Data were normalized to the mean of control. Bars represent the mean ± SEM of pooled data (n = 20 trials in 4 animals for each condition). Dots illustrate mean ± SEM for each animal. (* indicates $p < 0.05$; n.s. indicates not statistically significant). See also Figure S1.

control. It is noteworthy that such a low-intensity stimulation (2 μA) did not elicit locomotion at rest (Figure 2A4). Interestingly, the locomotor bout was prolonged when the second MLR stimulation was of the same intensity as the first one, i.e. sufficient to trigger locomotion at rest (4 μA; Figure 2A3).

The duration of the locomotor activity outlasting the end of a MLR stimulation, without a second stimulation (control condition), was on average 19.37 ± 1.24 s (n = 10 animals; Figure 2B, white boxes) before it stopped spontaneously. From one preparation to another, it ranged from 8.9 to 43.3 s. However, when there was a second low-intensity stimulation, the duration of the locomotor activity after the second stimulation was decreased to 6.7 ± 0.37 s (Figure 2B, green boxes). In five of these animals, we compared the effects of a second MLR stimulation of low intensity vs. high intensity (Figure 2C, n = 25 trials). Here, the average swimming duration was significantly reduced to 62.63 ± 4.37 % of control when the MLR was stimulated at a low intensity ($p < 0.05$; Figure 2C, green bar). When the second MLR stimulation was delivered at a high intensity, the average duration significantly increased to 148.0 ± 11.04 % of control ($p < 0.05$; Figure 2C, grey bar). Interestingly, the swimming frequency of the entire locomotor bout was not significantly altered by the second stimulation (Figure 2D).

In another set of experiments, we aimed at defining more precisely the intensity of the second stimulation that was needed to terminate or prolong the swimming bouts (Figure 2E). Therefore, the intensity of the second stimulation was varied from 0 % to 150 % of control (with 12.5 % steps). First, we established the stimulation intensity that was needed to elicit locomotion (1T) and then we set the control intensity to 2T (100 %). Overall, the average duration of the locomotor bouts was 25 ± 1.18 s when the MLR was stimulated only once at 100 % intensity. The intensity of the second stimulation needed to significantly shorten swimming activity was 37.5 % (19.22 ± 0.92 s) and 50 % (19.66 ± 0.96 s) of control ($p < 0.05$; n = 9 trials in 3 animals for each

stimulation intensity). On the other hand, locomotor duration was significantly increased when the MLR was stimulated a second time with intensities 75 % (36.33 ± 2.64 s) of control or higher ($p < 0.05$).

We then replaced electrical MLR stimulation with pharmacological activation to avoid activating fibers of passage (Figure S1). First, the MLR was electrically stimulated to elicit locomotion and then, D-Glutamate was locally injected (0.36 - 0.55 pmol) in the MLR as a second stimulation. As with low intensity electrical stimulation, the locomotor episodes were significantly shortened to 58.43 ± 2.86 % of control ($p < 0.05$; Figure 2F, violet bar; 20 trials in 4 animals). Replacing D-Glutamate with Ringer's solution did not shorten the locomotor episodes (87.0 ± 3.88 % of control, $p > 0.05$; Figure 2F, grey bar).

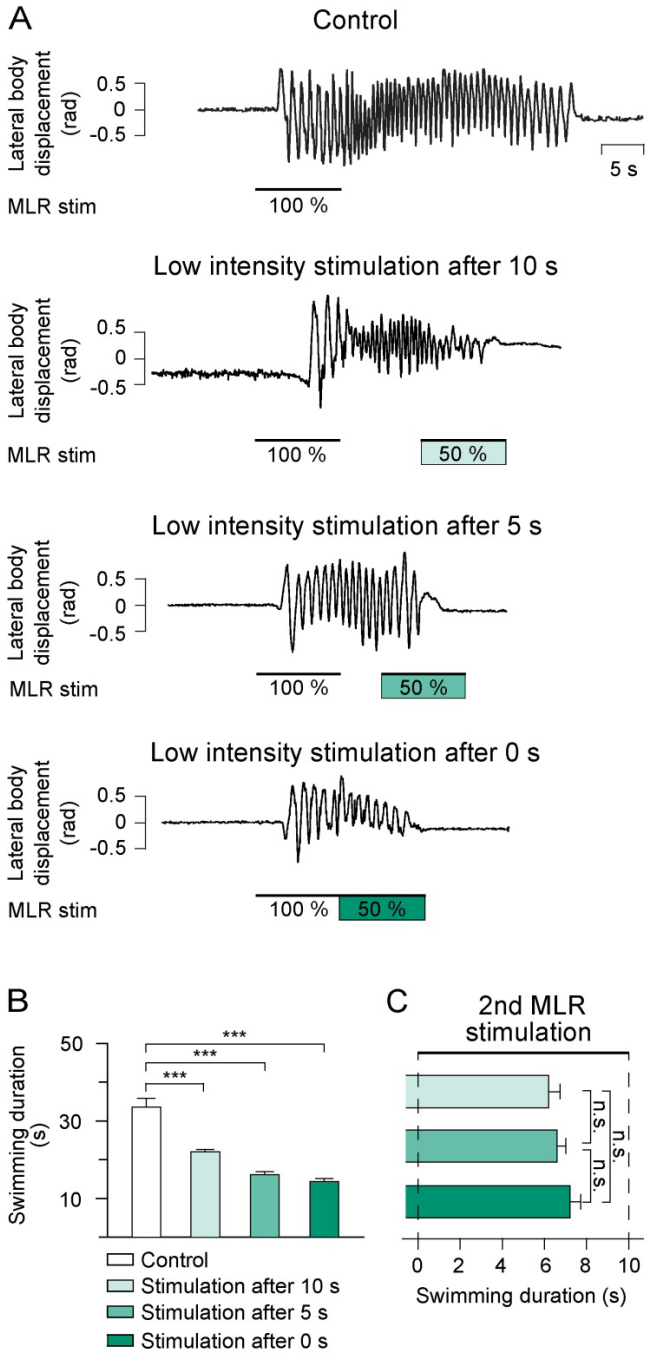

Figure 3. Effect of Applying a Second MLR Stimulation at Different Times after a First MLR Stimulation

(A) In a semi intact preparation, swimming was elicited with high intensity MLR stimulation (100 %, Control). A second MLR stimulation at a low intensity (50 % of control) was delivered 10, 5, or 0 s after the first MLR stimulation had ended.

(B) Histogram illustrating the average swimming duration in control condition (white bar; n = 75 trials), and when a second MLR stimulation of low intensity was delivered 10, 5, and 0 s after the end of the first MLR stimulation. Bars represent mean ± SEM (n = 25 trials for each condition).

(C) Bar Graph illustrating the time it takes to stop swimming after the onset of a second low intensity MLR stimulation delivered 10, 5, or 0 s after the first MLR stimulation. (*** indicates $p < 0.001$; n.s. indicates not statistically different).

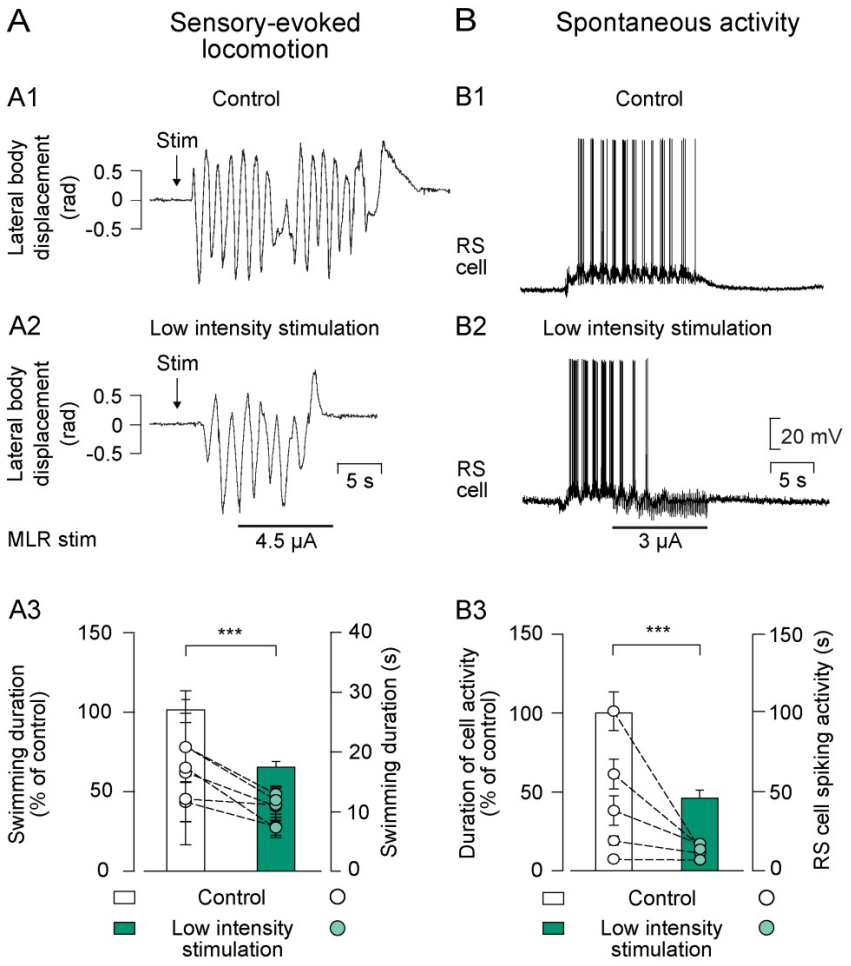

Figure 4. Effect of a Low-Intensity MLR Stimulation on Ongoing Sensory-Evoked or Spontaneous Swimming

(A1) Kinematic analysis of the lateral body displacement (rad) during sensory-evoked swimming that was elicited by pinching the dorsal fin with forceps (Stim). (A2) Representation of sensory-evoked swimming, when a low-intensity stimulation was delivered to the MLR 5 s after the onset of swimming. (A3) Histogram illustrates pooled data of average swimming duration (n = 30 trials in 6 animals) in control condition (white bar) and when MLR was stimulated electrically of low intensity during sensory-evoked swimming (green bar).

(B1) The intracellular recording of a maintain cell that fires action potentials throughout the locomotor bout (monitored visually) was used to analyze spontaneous locomotor activity. (B2) Cellular activity of the same maintain cell is represented when MLR stimulation of low intensity was delivered during spontaneous swimming. (B3) Histogram illustrating pooled data of duration of cellular activity in 5 animals (n = 25 events) in control condition (white bar), and when the MLR was stimulated 5 s after swimming movements have started (green bar). In both histograms, bars represent mean ± SEM of swimming episodes or cellular activity normalized to average value of control. Dots represent average duration of swimming episodes or cellular discharge for each animal (mean ± SEM). In all experiments, MLR intensities were used which would not induce locomotor activity in the resting preparation. (*** indicates $p < 0.001$).

To test whether there was a refractory period during which a second low intensity MLR stimulation could not stop locomotion, the time interval between the end of the first stimulation and the beginning of the second stimulation was reduced from 10, to 5, and 0 s (Figure 3A, B). In all three test conditions, the second low-intensity stimulation shortened the locomotor bout compared to control condition. Locomotion ended 6.27 ± 0.48 s, 6.55 ± 0.46 s, and 7.15 ± 0.52 s after the onset of the second stimulation for intervals of 10, 5, 0 s, respectively (Figure 3C; n = 25 trials in 5 animals).

In semi-intact preparations, swimming also occurred after sensory stimulation or spontaneously [32, 33]. This mimics more closely locomotor activity that occurs in the natural environment. Just like MLR-induced swimming, both sensory-evoked and spontaneous locomotor episodes could be stopped by low intensity MLR stimulation (Figure 4A, B). After pinching the dorsal fin (Stim; Figure 4A1), long lasting swimming movements were elicited in all cases (n = 30 trials in 6 animals). Low intensity MLR stimulation applied during the sensory-evoked swimming activity significantly shortened the locomotor bout (64.31 ± 3.57 % of control; $p < 0.001$; Figure 4A2, A3). Due to their rarity, spontaneous swimming bouts were not recorded kinematically, but by intracellular recordings of RS cells that maintain their discharge (maintain cells, see Figure 1A) throughout locomotor bouts (n = 25 trials in 5 animals; Figure 4B1). As observed for sensory-evoked swimming, spontaneous locomotor episodes were significantly shortened by a MLR stimulation of low intensity (46.02 ± 5.03 % of control; $p < 0.001$; Figure 4B2, B3).

The Termination Burst in Stop Cells is Time-Linked to the Second MLR Stimulation

Stop cells display a termination burst associated with the end of swimming regardless of the way it is initiated (MLR stimulation, cutaneous stimulation, spontaneous) [15]. In the case of MLR-induced swimming, we examined whether this burst was linked to the onset of the second MLR stimulation of low intensity (Figure 5A1). The MLR was stimulated first at the control intensity followed by a low-intensity stimulation, 5 s after the end of the first stimulation. When compared to control, the termination burst appeared earlier in time in cases where a second MLR stimulation was applied (Figure 5A1, bottom). The response discharge pattern from several stop cells was transformed into a raster display and the trials were temporally aligned on the onset of the second stimulation (n = 15 trials in 3 animals; Figure 5A2, top). The raster plot shows that the onset of the termination burst is time-linked with the onset of the second MLR stimulation. This is also apparent in the peristimulus histogram, in which an increase in spiking activity after the onset of the second MLR stimulation is observed (Figure 5A2, bottom). As a comparison, the response pattern of maintain cells was also recorded under the same conditions (Figure 5B1). In contrast to stop cells, maintain cells did not display a termination burst, whether a second MLR stimulation was applied or not (Figure 5B1, top and bottom), and their spiking activity was maintained until the cell repolarized at the end of the swimming bout. When a second MLR stimulation was applied, the duration of their spiking activity was reduced (from 22.51 ±

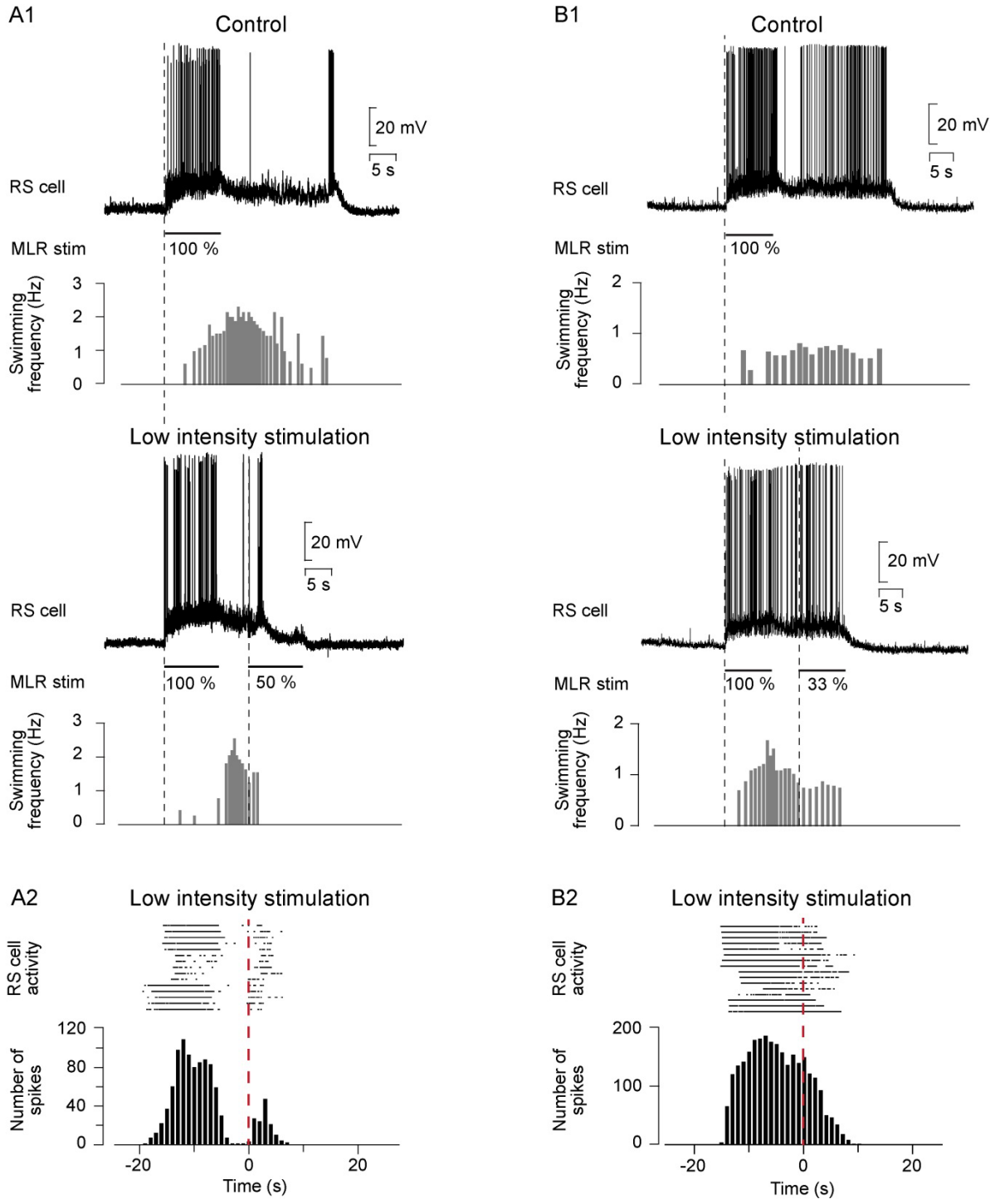

Figure 5. Relationship between Termination Burst and Low-Intensity MLR Stimulation

(A1) In a semi-intact preparation, stop cells were recorded in control condition (top) and when a second MLR stimulation of low intensity (50 % of control) was delivered 5 s after the first MLR stimulation had ended (bottom). (A2) The raster plot (top) and the peristimulus histogram (bottom; bin size = 1 s) illustrate the cellular activity of stop cells (n = 15 trials in 3 animals) that is aligned to the onset of the second MLR stimulation (dashed red line).

(Continuation of Figure 5)

(B1) Same representation for the cellular activity of maintain cells that display activity throughout the swimming episode. Maintain cells were recorded during MLR-induced swimming (control condition, top) and when the MLR was stimulated a second time with low intensity (33 % of control; bottom). (B2) Raster plot and peristimulus histogram represent spiking activity of maintain cells (n = 16 trials in 4 animals) aligned to the onset of MLR stimulation of low intensity (dashed line).

2.53 s to 16.29 ± 0.85 s) as would be expected for shorter locomotor bouts (see Figure 2), but the raster display and the peristimulus histogram did not reveal a change in the activity pattern (n = 16 trials in 4 animals; Figure 5B2).

Connectivity between the MLR and Stop Cells

We then examined the projections between the MLR and stop cells. Stop cells were intracellularly recorded and we examined their response to electric shocks applied to the MLR (Figure 6). The intensity was determined at 50 % of the intensity used to trigger a locomotor bout. Under these conditions, double shocks delivered with a time interval of 50, 25, 16.7, 12.5 ms (20, 40, 60, 80 Hz respectively) elicited short latency EPSPs (2.8 up to 3.2 s; n = 4; Figure 6A). As the time interval between shocks was shortened, the EPSPs remained unchanged. Next, double shocks with a time interval of 40 ms (25 Hz) were delivered to the MLR in normal Ringer's and in Ringer's with high concentration of divalent cations (Figure 6B). This did not change the synaptic responses of recorded stop cells (n = 2), suggesting that at least part of the connection between the MLR and stop cells is monosynaptic.

Anatomical experiments (n = 8) were performed to determine if particular populations of MLR cells projected to stop cell-rich, or to maintain cell-rich areas (see [15]). In these experiments, two fluorescent retrograde tracers were injected on the same side, a few hours apart, the first injection being more extensive and more caudal than the second. The rationale behind this was that MLR neurons that do not reach the caudal injection level will only be labelled by the rostral injection, while the MLR neurons that terminate more caudally will be labeled by the two injections (double-labeled) or only by the more extensive, more caudal one. The caudal injection was made larger to make sure that all the axons that travelled through the rostral injection site and continued down to the caudal injection were labelled. Using this technique, we first wanted to know if a population of MLR neurons projected selectively to an area of the reticular formation rich in stop cells, the caudal MRRN. To label these MLR cells specifically, the first caudal injection was made in the reticular formation (rostral portion of the posterior rhombencephalic reticular nucleus or rPRRN) and the second injection slightly more rostral (in the caudal portion of the medial rhombencephalic reticular nucleus or cMRRN; an area rich in stop cells; Figure 7A). After such injections, cell bodies were retrogradely labeled in

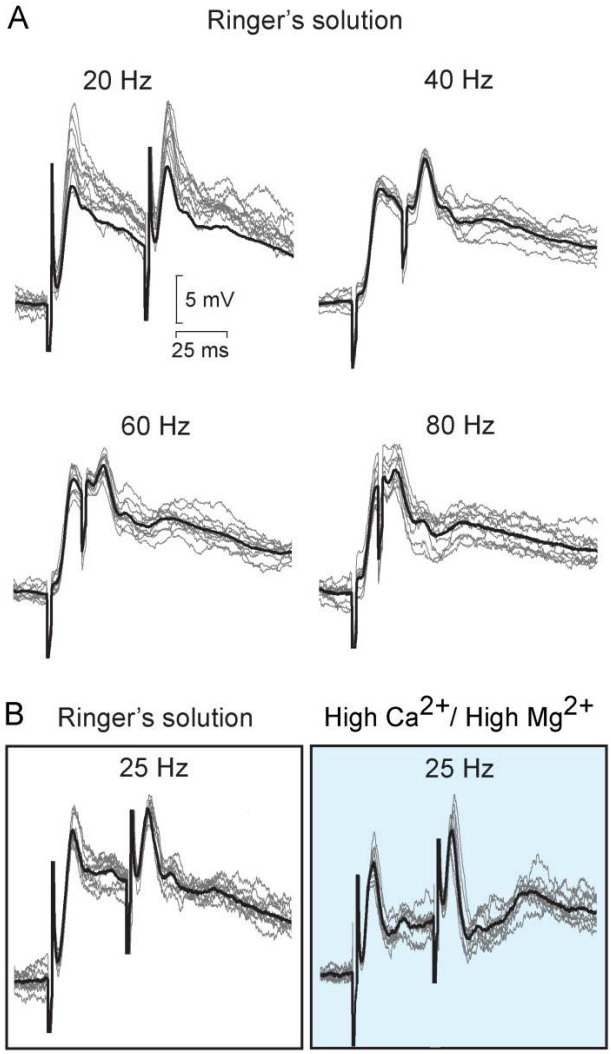

Figure 6. Synaptic Inputs from the MLR to Stop Cells

(A) Response of a stop cell to a pair of electrical shocks delivered to the MLR. Double shocks were delivered to the MLR at different frequencies (20 Hz, 40 Hz, 60 Hz, and 80 Hz). The black traces represent average cellular responses from 1 of 4 recorded stop cells (n = 10 sweeps; grey traces).

(B) Double electrical shocks were delivered to the MLR with a time interval of 40 ms (25 Hz) while a stop cell was recorded intracellularly. To abolish polysynaptic transmission, a high-divalent cation Ringer's solution was applied in the recording chamber (right, blue box). Black traces represent average cellular responses from 1 of 2 recorded stop cells (n = 10 sweeps; grey traces).

the MLR on both sides, but most importantly, many neurons with projections that terminated in the stop cell area were found (red dots in Figure 7B). Their distribution, however, was not segregated from the other labeled MLR cells. With the same rationale, we wanted to know if some MLR cells projected selectively to an area of the reticular formation rich in maintain cells, the rostral MRRN (rMRRN). In this case, a first caudal injection was made in the cMRRN and a second injection, a few hours later, in the rMRRN (area rich in maintain cells; Figure S2A). Again, cell bodies were retrogradely labeled on both sides of the MLR and many neurons with projections that terminated specifically in the maintain cell area were found (red dots in Figure S2B). No distinct cluster of MLR cells projecting to the region of the maintain cells was observed, the labeled MLR populations being mostly intermingled.

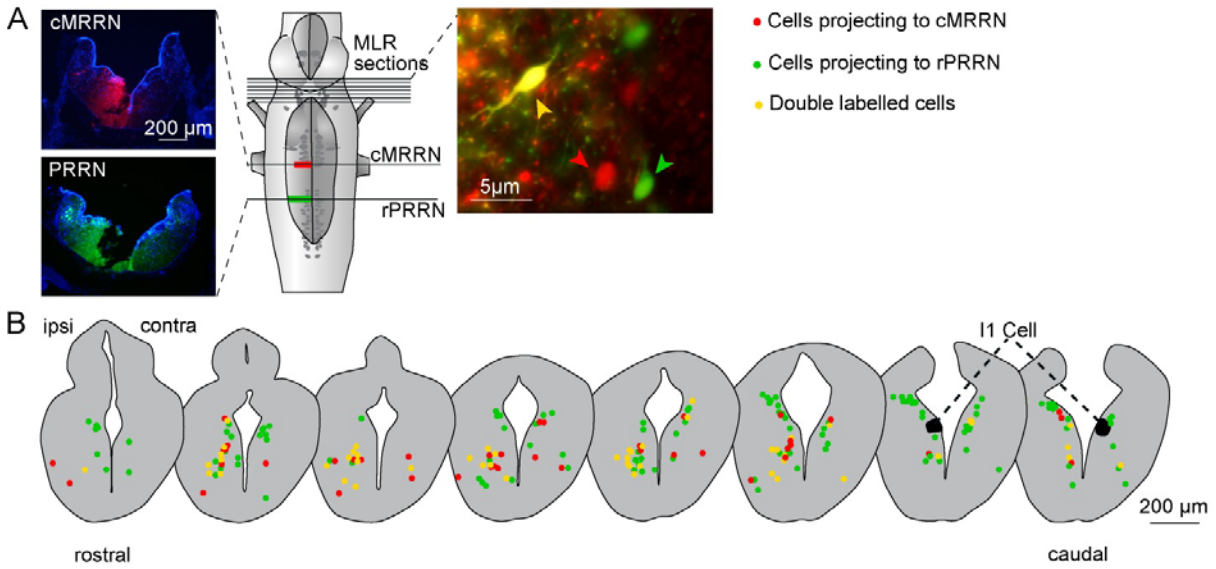

Figure 7. Distribution of MLR Neurons Projecting to a Region of the Reticular Formation where Stop Cells are Predominantly Located

(A) Tracer injections were made at two rostro-caudal levels of the reticular formation, one in the caudal MRRN (cMRRN), the other slightly more caudal, in the rostral PRRN (rPRRN). The extent of each injection is illustrated on photomicrographs of cross sections (to the left). As seen on a high magnification photomicrograph (red and green filter sets images were merged) of a cross section at the isthmic level (to the right), neurons were retrogradely labeled in the MLR, some with one of the tracers (red and green arrowheads), others with both tracers (yellow arrowhead). The MLR neurons that sent projections terminating in the cMRRN, where stop cells predominantly lie, were only labeled with the red tracer, whereas all neurons that sent projections passed the cMRRN were double labeled or labeled only in green.

(B) Schematic cross sections through the rostro-caudal extent of the MLR showing neurons labelled on both sides. Red dots represent single labeled MLR neurons that project to the cMRRN but do not reach the rPRRN. Green and yellow dots represent MLR neurons projecting at least as far as the rPRRN, passed the stop cell-rich region of the cMRRN. The giant RS cell I1 that is used as a landmark to identify the caudal extent of the MLR, is represented in black. See also Figure S2.

DISCUSSION

In the present study, we uncovered a neural substrate that controls the termination of locomotion and we further demonstrate that the responses to MLR stimulation can change depending on the behavioral state of the animal. It was previously known that the MLR activates RS cells to initiate locomotion [7, 17-20, 25] (for review, see [5]): A descending start signal from the MLR activates all RS cell populations in the MRRN and initiates locomotion. The locomotion episode is maintained through the activation of a subgroup of RS cells,

the maintain cells. We now report that MLR stimulation can also produce an opposite behavioral effect consisting in the termination of locomotion, much like a brake pedal. This effect is mediated by the activation of another subgroup of RS cells, the stop cells, which display a typical termination burst that coincides with the end of the locomotion episodes. Our experiments also suggest the presence of a monosynaptic connection between the MLR and stop cells. These results fill an important gap in knowledge relative to the neural mechanisms underlying the termination of locomotion.

Synaptic Inputs to Stop Cells

The concept of brainstem cells involved in the termination of locomotion has been proposed for different vertebrate species [12, 15, 16, 34, 35]. However, little is known about the mechanisms activating these stop cells. In all of the above studies, stimulation of these RS cells (electric, pharmacologic, or optogenetic) led to termination of ongoing locomotion. In the *Xenopus* tadpole, it was shown that the lower brainstem cells are linked to sensorimotor network and are activated by stimulation of the head region [34]. The brainstem cells described in mammals are thought to be controlled by central neural mechanisms, but details of the connections are still unknown [16]. In cats it is considered that a disynaptic pathway from the pedunculopontine nucleus (PPN) (considered part of the MLR in mammals) to medullary RS neurons elicits motor inhibition, but details about this pathway are missing (for review, see [36]). It is well known that projections from the MLR provide a major input to RS cells [7, 9, 17-20, 37, 38] (for review, [5]). In the lamprey, these projections have been characterized extensively. Inputs from the MLR to RS cells were shown to differ in strength of connectivity depending on the localization of the RS cells in the brainstem [7]. Rostral RS cells located in the MRRN receive stronger MLR inputs than caudal RS cells located in the PRRN. The connections were shown to be both mono- and disynaptic [11, 38] and glutamatergic as well as cholinergic projection neurons were identified to be involved in locomotor initiation and speed control [7, 19]. The present results demonstrate that at least a part of the projections from the MLR to stop cells are monosynaptic. Moreover, our anatomical data indicate that numerous cells in the MLR seem to project specifically to an area of the reticular formation rich in stop cells. We have not yet identified neurotransmitters involved in this pathway, but in a previous study, we have shown that stimulating or blocking glutamatergic receptors in the area rich in stop cells, triggered or delayed the termination of locomotion, respectively [15]. These results strongly suggest that glutamatergic transmission is involved, while cholinergic neurotransmission has yet to be tested.

How the MLR Controls the Termination of Locomotion

Classically, the MLR has been described as initiating locomotion [2, 25] (for review, see [5]). Our findings demonstrating that activation of the MLR also terminates locomotion are therefore surprising. However, the MLR is a complex and large region in more recently evolved vertebrates, where it consists of multiple nuclei that seem to contribute in different ways to the locomotor repertoire. Sinnamon (1993) proposed that different MLR sub-regions control different behaviors, such as appetitive, explorative, and defensive behavior [30]. In addition, experiments in cats revealed that electrical stimulation of non-cholinergic neurons in the cuneiform nucleus (CnF) and pendunclopontine nucleus (PPN) triggers movement, and that stimulation of cholinergic PPN neurons stops ongoing spontaneous walking and induces muscle atonia [35, 39] (for review, see [36]). With the development of optogenetic techniques, it has recently been possible to use a more controlled approach to examine the multiple behaviors induced by the MLR [27-29]. Roseberry and colleagues (2016) demonstrated that glutamatergic MLR neurons drive locomotion and cholinergic neurons modulate its speed [27]. Local GABAergic neurons were shown to inhibit glutamatergic MLR neurons and thus stop locomotion when activated. The contribution of glutamatergic neurons in the PPN and CnF to locomotor output has also been examined [28]. It was shown that glutamatergic neurons in both nuclei contribute to slow movements but only glutamatergic CnF neurons control high speed locomotion. The PPN was therefore associated with slow, exploratory movements and the CnF with fast escape behavior. Similar findings were made by Josset and colleagues (2018), who found that glutamatergic CnF neurons initiate and accelerate locomotion as seen in flight [29]. Exploratory behavior was also associated with the PPN, where glutamatergic neurons produced slow walking movements and cholinergic neurons modulated locomotor speed.

As opposed to what is seen in more recently-evolved vertebrates like mammals, our anatomical data on lampreys strongly suggest that MLR sub-populations are highly intermingled in a physically-small region. This makes it difficult to stimulate them specifically by changing the location of the microelectrode. However, it is possible that changing the stimulation intensity instead could activate different sub-populations of neurons. For example, MLR neurons projecting to the stop cells could have specific intrinsic properties (*e.g.* membrane resistance or threshold) and be more excitable than other MLR cells. To test this, more electrophysiological experiments will have to be conducted on the MLR level in the future.

We have yet to identify the mechanisms activating the MLR neurons that control the termination of locomotion in lampreys. In the study of Roseberry and colleagues (2016) in mice, GABAergic neurons from the basal ganglia as well as local GABAergic MLR neurons were shown to inhibit glutamatergic MLR neurons and thus produce termination of locomotion [27]. In the lamprey, a population of local GABAergic neurons was identified in the MLR [40, 41], but it is still unclear whether these neurons are local or projection neurons, since at least some of them have been suggested to be part of the output structure of the basal ganglia [42, 43]. But similarly to the findings in mice, local application of GABAergic agonist into the MLR inhibited ongoing locomotion in semi-intact preparations from lampreys [44]. However, what we found here in the

MLR of lampreys seems to involve a different mechanism for stopping locomotion. In our experiments, locomotion would not be stopped by removing an excitatory output from the MLR but, to the contrary, by activating an excitatory output signal to a population of stop cells in the reticular formation. Importantly, both mechanisms could very well exist in parallel in the MLR. But in our case it means that, an excitatory input to MLR neurons is more likely to be involved and could be provided by forebrain structures. A possible candidate is the posterior tuberculum, a forebrain structure homologous to the mammalian substantia nigra pars compacta. It was recently shown to send glutamatergic and dopaminergic projections to the MLR, and to modulate and control locomotion in a graded fashion, much like the MLR itself [45, 46]. Some forebrain inputs could thus activate specifically MLR neurons that control the termination of locomotion. More experiments will have to be performed in the future to investigate this question.

Behavioural Aspects for Stopping Locomotion

Termination of locomotion occurs in several different contexts (for review, see [47, 48]). In their natural environment, animals have to brake and stop movements frequently in order to survive. Roseberry and Kreitzer (2017) differentiate between freezing behavior in response to fear, startle in response to intense and sudden sensory inputs, and behavioral arrest following goal-directed behavior [47]. Freezing and startle behavior are both associated with a characteristic increase of muscle tone (for review, see [49-51]). In lamprey, freezing behavior per se has not been described, but sudden vibration applied to water, or direct stimulation of the vestibulary otic capsules, triggered startle response characterized by bilateral muscle contractions and stiffening of the body [52]. In the present study, whether the semi-intact preparations stopped locomotion spontaneously or after a second MLR stimulation of low intensity, they did not show any apparent stiffening of the body, but rather exhibited a gradual decrease of their swimming activity until reaching a complete stop. The similarity between spontaneous and MLR-induced stopping suggests that the same mechanisms are involved.

In conclusion, we uncovered that MLR stimulation may have a dual effect depending on the behavioral state of the animal. When the MLR is stimulated at rest, it elicits locomotion, but when stimulated during locomotion it produces very different effects. It halts swimming if it is stimulated at low intensity and prolongs swimming if stimulated at a higher intensity. Understanding the neural substrate underlying the termination of locomotion could have a significant clinical interest. Patients with gait disorders such as in Parkinson's disease (PD) display several motor deficits, including difficulties to stop ongoing movements, especially in unplanned situations [53-55]. A study from Bishop and colleagues (2003) indicates that the 'brake impulse' that is observed in healthy individuals in response to a sudden stop signal is impaired in PD patients [54]. The authors further show that subjects with PD rely on decreasing body propulsion instead of activating a 'brake impulse', which results in a prolonged stop reaction time [54, 55]. It has been proposed

that a deficit in inhibiting ongoing movements results from degeneration of dopamine neurons, for example in the basal ganglia [53]. This seems to be supported by our recent studies showing that the lamprey, salamander, rat, and possibly humans, have a descending dopamine projection from the substantia nigra pars compacta to some populations of MLR neurons [45, 56]. Impairment of this descending dopamine projection to the MLR could directly affect the projection from the MLR to RS stop cells, leading in turn to difficulties in terminating gait swiftly. More studies are needed to resolve this question and to develop new therapeutic approaches for patients with gait disorders.

ACKNOWLEDGEMENTS

We thank Danielle Veilleux for her technical assistance, Frédéric Bernard for his help with the graphics, and Dr. Dimitri Ryczko for the valuable discussions. This work was supported by the Canadian Institutes of Health Research (15129); the Natural Sciences and Engineering Research Council of Canada Grant 217435 (to R.D.); the Great Lakes Fishery Commission Grants 54011 and 54021 (to R.D.). S.G. received scholarships from the University of Cologne and the German Academic Exchange Service.

AUTHOR CONTRIBUTION

S.G., F.A., A.B., and R.D. designed research; S.G., F.A., O.D., E.A., and A.H. performed research; S.G., F.A., O.D., E.A., A.H., A.B., and R.D. analyzed data; S.G., A.B., and R.D. wrote the paper.

DECLARATION OF INTEREST

The authors declare no competing interests.

REFERENCES

1. Grillner, S., Wallén, P., Saitoh, K., Kozlov, A., and Robertson, B. (2008). Neural bases of goal-directed locomotion in vertebrates--an overview. Brain Res. Rev. 57(1):2-12.
2. Shik, M.L., Severin, F.V., and Orlovskii, G.N. (1966). Control of walking and running by means of electric stimulation of the midbrain (in Russian). Biofizika 11(4):659-666.
3. Jordan, L.M. (1998). Initiation of locomotion in mammals. Ann. N Y Acad. Sci. 860:83-93.
4. Dubuc, R., Brocard, F., Antri, M., Fénelon, K., Gariépy, J.F., Smetana, R., Ménard, A., Le Ray, D., Viana Di Prisco, G., Pearlstein, E., Sirota, M.G., Derjean, D., St-Pierre, M., Zielinski, B., Auclair, F., and Veilleux, D. (2008). Initiation of locomotion in lampreys. Brain Res. Rev. 57(1):172-182.
5. Ryczko, D., and Dubuc, R. (2013). The multifunctional mesencephalic locomotor region. Curr. Pharm. Des. 19(24):4448-4470.
6. Drew, T., Dubuc, R., and Rossignol, S. (1986). Discharge patterns of reticulospinal and other reticular neurons in chronic, unrestrained cats walking on a treadmill. J. Neurophysiol. 55(2):375-401.
7. Brocard, F., and Dubuc, R. (2003). Differential contribution of reticulospinal cells to the control of locomotion induced by the mesencephalic locomotor region. J. Neurophysiol. 90(3):1714-1727.
8. Deliagina, T.G., Zelenin, P.V., Fagerstedt, P., Grillner, S., and Orlovsky, G.N. (2000). Activity of reticulospinal neurons during locomotion in the freely behaving lamprey. J. Neurophysiol. 83(2):853-863.
9. Bretzner, F., and Brownstone, R.M. (2013). Lhx3-Chx10 reticulospinal neurons in locomotor circuits. J. Neurosci. 33(37):14681-14692.
10. Kimura, Y., Satou, C., Fujioka, S., Shoji, W., Umeda, K., Ishizuka, T., Yawo, H., and Higashijima, S. (2013). Hindbrain V2a neurons in the excitation of spinal locomotor circuits during zebrafish swimming. Curr. Biol. 23(10):843-849.
11. Smetana, R., Juvin, L., Dubuc, R., and Alford, S. (2010). A parallel cholinergic brainstem pathway for enhancing locomotor drive. Nat. Neurosci. 13(6):731-738.
12. Capelli, P., Pivetta, C., Soledad Esposito, M., and Arber, S. (2017). Locomotor speed control circuits in the caudal brainstem. Nature 551(7680):373-377.
13. Zelenin, P.V. (2011). Reticulospinal neurons controlling forward and backward swimming in the lamprey. J. Neurophysiol. 105(3):1361-1371.
14. Thiele, T.R., Donovan, J.C., and Baier, H. (2014). Descending control of swim posture by a midbrain nucleus in zebrafish. Neuron 83(3):679-691.
15. Juvin, L., Grätsch, S., Trillaud-Doppia, E., Gariépy, J.F., Büschges, A., and Dubuc, R. (2016). A specific population of reticulospinal neurons controls the termination of locomotion. Cell Rep. 15(11):2377-2386.

16. Bouvier, J., Caggiano, V., Leiras, R., Caldeira, V., Bellardita, C., Balueva, K., Fuchs, A., and Kiehn, O. (2015). Descending command neurons in the brainstem that halt locomotion. Cell 163(5):1191-1203.
17. Orlovskii, G.N. (1970). Relations between reticulo-spinal neurons and locomotor regions of the brain stem (in Russian). Biofizika 15(1):171-178.
18. Steeves, J.D., and Jordan, L.M. (1984). Autoradiographic demonstration of the projections from the mesencephalic locomotor region. Brain Res. 307(1-2):263-276.
19. Le Ray, D., Brocard, F., Bourcier-Lucas, C., Auclair, F., Lafaille, P., and Dubuc, R. (2003). Nicotinic activation of reticulospinal cells involved in the control of swimming in lampreys. Eur. J. Neurosci. 17(1):137-148.
20. Ryczko, D., Auclair, F., Cabelguen, J.M., and Dubuc, R. (2016). The mesencephalic locomotor region sends a bilateral glutamatergic drive to hindbrain reticulospinal neurons in a tetrapod. J. Comp. Neurol. 524(7):1361-1383.
21. Skinner, R.D., and Garcia-Rill, E. (1984). The mesencephalic locomotor region (MLR) in the rat. Brain Res. 323(2):385-389.
22. Lee, A.M., Hoy, J.L., Bonci, A., Wilbrecht, L., Stryker, M.P., and Niell, C.M. (2014). Identification of a brainstem circuit regulating visual cortical state in parallel with locomotion. Neuron 83:455-466.
23. Cabelguen, J.M., Bourcier-Lucas, C., and Dubuc, R. (2003). Bimodal locomotion elicited by electrical stimulation of the midbrain in the salamander Notophthalmus viridescens. J. Neurosci. 23(6):2434-2439.
24. Sholomenko, G.N., Funk, G.D., and Steeves, J.D. (1991). Avian locomotion activated by brainstem infusion of neurotransmitter agonists and antagonists. I. Acetylcholine excitatory amino acids and substance P. Exp. Brain Res. 85(3):659-673.
25. Sirota, M.G., Di Prisco, G.V., and Dubuc, R. (2000). Stimulation of the mesencephalic locomotor region elicits controlled swimming in semi-intact lampreys. Eur. J. Neurosci. 12(11):4081-4092.
26. Garcia-Rill, E., Skinner, R.D., and Fitzgerald, J.A. (1985). Chemical activation of the mesencephalic locomotor region. Brain Res. 330(1):43-54.
27. Roseberry, T.K., Lee, A.M., Lalive, A.L., Wilbrecht, L., Bonci, A., Kreitzer, A.C. (2016). Cell-type-specific control of brainstem locomotor circuits by basal ganglia. Cell 164(3):526-537.
28. Caggiano, V., Leiras, R., Goñi-Erro, H., Masini, D., Bellardita, C., Bouvier, J., Caldeira, V., Fisone, G., and Kiehn, O. (2018). Midbrain circuits that set locomotor speed and gait selection. Nature 553(7689):455-460.
29. Josset, N., Roussel, M., Lemieux, M., Lafrance-Zoubga, D., Rastqar, A., and Bretzner, F. (2018). Distinct contributions of mesencephalic locomotor region nuclei to locomotor control in the freely behaving mouse. Curr. Biol. 28(6):884-901.

30. Sinnamon, H.M. (1993). Preoptic and hypothalamic neurons and the initiation of locomotion in the anesthetized rat. Prog. Neurobiol. 41(3):323-344.
31. Grillner, S., and Robertson, B. (2017). Selection of action - A vertebrate perspective. In Neurobiology of Motor Control - Fundamental Concepts and New Directions, S.L. Hooper and A. Büschges, eds. (New Jersey, United States of America: Wiley-Blackwell), pp. 181-191.
32. Di Prisco, G.V., Pearlstein, E., Robitaille, R., and Dubuc, R. (1997). Role of sensory-evoked NMDA plateau potentials in the initiation of locomotion. Science 278(5340):1122-1125.
33. Di Prisco, G.V., Pearlstein, E., Le Ray, D., Robitaille, R., and Dubuc, R. (2000). A cellular mechanism for the transformation of a sensory input into a motor command. J. Neurosci. 20(21):8169-8176.
34. Perrins, R., Walford, A., and Roberts, A. (2002). Sensory activation and role of inhibitory reticulospinal neurons that stop swimming in hatchling frog tadpoles. J. Neurosci. 22(10):4229-4240.
35. Takakusaki, K., Kohyama, J., and Matsuyama, K. (2003). Medullary reticulospinal tract mediating a generalized motor inhibition in cats: III. Functional organization of spinal interneurons in the lower lumbar segments. Neurosci. 121(3):731-746.
36. Takakusaki, K. (2008). Forebrain control of locomotor behaviors. Brain Res. Rev. 57(1):192-198.
37. Garcia-Rill, E., and Skinner, R.D. (1987). The mesencephalic locomotor region. II. Projections to reticulospinal neurons. Brain Res. 411(1):13-20.
38. Brocard, F., Ryczko, D., Fénelon, K., Hatem, R., Gonzales, D., Auclair, F., and Dubuc, R. (2010). The transformation of a unilateral locomotor command into a symmetrical bilateral activation in the brainstem. J. Neurosci. 30(2):523-533.
39. Takakusaki, K., Habaguchi, T., Saitoh, K., and Kohyama, J. (2004). Changes in the excitability of hindlimb motoneurons during muscular atonia induced by stimulating the pedunculopontine tegmental nucleus in cats. Neurosci. 124(2):467-480.
40. Meléndez-Ferro, M., Pérez-Costas, E., Villar-Cheda, B., Rodríguez-Muñoz, R., Anadón, R., and Rodicio, M.C. (2003). Ontogeny of gamma-aminobutyric acid-immunoreactive neurons in the rhombencephalon and spinal cord of the sea lamprey. J. Comp. Neurol. 464(1):17-35.
41. Robertson, B., Auclair, F., Ménard, A., Grillner, S., and Dubuc, R. (2007). GABA distribution in lamprey is phylogenetically conserved. J. Comp. Neurol. 503(1):47-63.
42. Stephenson-Jones, M., Samuelsson, E., Ericsson, J., Robertson, B., and Grillner, S. (2011). Evolutionary conservation of the basal ganglia as a common vertebrate mechanism for action selection. Curr. Biol. 21(13):1081-1091.
43. Stephenson-Jones, M., Ericsson, J., Robertson, B., and Grillner, S. (2012). Evolution of the basal ganglia: dual-output pathways conserved throughout vertebrate phylogeny. J. Comp. Neurol. 520(13):2957-2973.

44. Ménard, A., Auclair, F., Bourcier-Lucas, C., Grillner, S., and Dubuc, R. (2007). Descending GABAergic projections to the mesencephalic locomotor region in the lamprey Petromyzon marinus. J. Comp. Neurol. 501(2):260-273.
45. Ryczko, D., Grätsch, S., Auclair, F., Dubé, C., Bergeron, S., Alpert, M.H., Cone, J.J., Roitman, M.F., Alford, S., and Dubuc, R. (2013). Forebrain dopamine neurons project down to a brainstem region controlling locomotion. Proc. Natl. Acad. Sci. USA. 110(34):E3235-42.
46. Ryczko, D., Grätsch, S., Schläger, L., Keuyalian, A., Boukhatem, Z., Garcia, C., Auclair, F., Büschges, A., and Dubuc, R. (2017). Nigral glutamatergic neurons control the speed of locomotion. J. Neurosci. 37(40):9759-9770.
47. Roseberry, T., and Kreitzer, A. (2017). Neural circuitry for behavioural arrest. Philos. Trans. R. Soc. Lond. B. Biol. Sci. 372(1718).
48. Kim, L.H., Sharma, S., Sharples, S.A., Mayr, K.A., Kwok, C.H.T., and Whelan, P.J. (2017). Integration of descending command systems for the generation of context-specific locomotor behaviors. Front. Neurosci. 11:581.
49. Roelofs, K. (2017). Freeze for action: neurobiological mechanisms in animal and human freezing. Phil. Trans. R. Soc. Lond. B. Biol. Sci. 372(1718).
50. Koch, M. (1999). The neurobiology of startle. Prog. Neurobiol. 59(2):107-128.
51. Yeomans, J.S., Li, L., Scott, B.W., and Frankland, P.W. (2002). Tactile, acoustic and vestibular systems sum to elicit the startle reflex. Neurosci. Biobehav. Rev. 26(1):1-11.
52. Currie, S., and Carlsen, R.C. (1985). A rapid startle response in larval lampreys. Brain Res. 358(1-2):367-371.
53. Gauggel, S., Rieger, M., and Feghoff, T.A. (2004). Inhibition of ongoing responses in patients with Parkinson's disease. J. Neurol. Neurosurg. Psychiatry 75(4):539-544.
54. Bishop, M.D., Brunt, D., Kukulka, C., Tillman, M.D., and Pathare, N. (2003). Braking impulse and muscle activation during unplanned gait termination in human subjects with parkinsonism. Neurosci. Lett. 348(2):89-92.
55. Bishop, M., Brunt, D., and Marjama-Lyons, J. (2006). Do people with Parkinson's disease change strategy during unplanned gait termination? Neurosci. Lett. 397(3):240-244.
56. Ryczko, D., Cone, J.J., Alpert, M.H., Goetz, L., Auclair, F., Dubé, C., Parent, M., Roitman, M.F., Alford, S., Dubuc, R. (2016). A descending dopamine pathway conserved from basal vertebrates to mammals. Proc Natl Acad Sci U S A. 113(17):E2440-9.
57. Ranck, J.B. Jr. (1975). Which elements are excited in electrical stimulation of mammalian central nervous system: a review. Brain Res. 98(3):417-440.
58. Rovainen, C.M. (1967). Physiological and anatomical studies on large neurons of central nervous system of the sea lamprey (Petromyzon marinus). I. Müller and Mauthner cells. J. Neurophysiol. 30(5):1000-1023.

59. Paggett, K.C., Jackson, A.W., and McClellan, A.D. (2004). Organization of higher-order brain areas that initiate locomotor activity in larval lamprey. Neurosci. 125(1):25-33.
60. Jackson, A.W., Pino, F.A., Wiebe, E.D., and McClellan, A.D. (2007). Movements and muscle activity initiated by brain locomotor areas in semi-intact preparations from larval lamprey. J. Neurophysiol. 97(5):3229-3241.

STAR METHODS

Contact for Agent and Resource Sharing

Further information and requests for resources and reagents should be directed to and will be fulfilled by the Lead Contact, Réjean Dubuc (rejean.dubuc@gmail.com).

Experimental Model and Subject Details

All procedures conformed to the guidelines of the Canadian Council on Animal Care and were approved by the animal care and use committees of the Université de Montréal (QC, Canada) and Université du Québec à Montréal (QC, Canada). Care was taken to minimize the number of animals used and their suffering. All experiments were performed in larval sea lampreys, *Petromyzon marinus* that were collected in a river near Notre-Dame-de-Stanbridge (Rivière aux Brochets, QC, Canada). The animals were kept in aerated water at 5° C and received every other week approximately 2 mg of yeast per animal. In the present study, the sex of the individual larval animals was not taken into account.

Method Details

Semi-Intact and Isolated Brain Preparations

Semi-intact preparations (n = 44) were used to simultaneously record RS cell activity and locomotor movements. For this purpose, the brain and rostral spinal cord segments were dissected free and the caudal part of the body was kept intact. Animals were deeply anaesthetized with tricaine methanesulphonate (MS 222, 100 mg / L; Sigma Chemical) and transferred into a cold and oxygenated Ringer's solution of the following composition (in mM): NaCl 130.0, KCl 2.1, $CaCl_2$ 2.6, $MgCl_2$ 1.8, HEPES 4.0, dextrose 4.0 and $NaHCO_3$ 1.0, adjusted to a pH of 7.4. A transverse incision was made on the ventral side at the level of the last pair of gills. Skin and muscle tissue was then removed from the rostral part of the body and around the head. The brain and the rostral spinal cord segments were then exposed dorsally by removing the surrounding tissue, skin, muscles and cranial cartilage. The choroid plexus over the mesencephalic and fourth ventricles was removed to gain access to RS neurons and the MLR. Decerebration was achieved by a complete transverse section of the neuraxis just rostral to the mesencephalon. A dorsal midsagittal transection was performed at the isthmus to provide an easier access to the MLR. The animals were transferred into a recording chamber continuously perfused with cold, oxygenized Ringer's solution. One part of the chamber was shallow and designed to pin down the rostral part of the preparation onto the Sylgard (Dow Corning) lining at the bottom, in order to record the activity of the brainstem neurons. The other part of the chamber was deeper and allowed the intact body (caudal part of the animal) to swim freely (Figure 1B). Animals were allowed to recover for at least 1 hour before recording.

For anatomical experiments, isolated brain preparations of larval lampreys were used (n = 8). The dissection procedure was the same as described above but a complete transverse cut was made at the level of the last gills to remove the body.

Electrophysiological Recordings and Stimulation

Intracellular recordings of RS cells were made using sharp microelectrodes (80 - 120 MΩ), filled with 4M potassium acetate. The signals were amplified and sampled at a rate of 10 kHz (Axoclamp 2A; Axon Instruments) and acquired through a Digidata 1200 series interface coupled to Clampex 8.1 software (Axon Instruments). Intracellular signals were analyzed using Clampfit 10.4 (Axon Instruments) or Spike2 5.19 software (Camebridge Electronic Design Limited). The MLR was electrically stimulated on one side to elicit swimming movements of the intact body. Trains of 2 ms pulses (frequency of 5 Hz for 10 s) were delivered through custom made glass-coated tungsten microelectrodes (4 - 5 MΩ with 10 µm tip exposure) using a Grass S88 stimulator (Astro Med). Stimulation intensities ranged from 0.5 - 15 µA, theoretically corresponding to a maximum current spread of 130 - 281 µm around the stimulation electrode [57]. Stimulation trains were delivered to the MLR with at least a 3 min waiting period in between. The location of the stimulation site was based on previous anatomical and physiological studies in the lamprey MLR, whereby the giant RS cell I1 [58] serves as a MLR landmark [7, 19, 25, 45].

In a series of experiments, the synaptic connectivity was tested using a high-divalent cation Ringer's solution (10.8 mM Ca^{2+}/ 7.2 mM Mg^{2+}; [7, 19]). In these experiments, the recording chamber was split between the head and body using petroleum jelly (Vaseline) and the Ringer's solution in the head chamber was replaced by a high-divalent cation solution. After 30 min of exposure to the high-divalent cation solution, the MLR was stimulated with two electrical shocks (2 ms) applied at a high frequency (20, 40, 60, 80, and 25 Hz).

Drugs

In a series of experiments, the MLR was pharmacologically stimulated with microinjections of D-glutamate (5 mM in Ringer's solution, Sigma-Aldrich). Microinjections were performed as described in previous studies (*e.g.* [15, 45, 59, 60]): a glass micropipette (diameter of opening 10 - 20 µm) was inserted in the MLR and the D-glutamate solution was pressure-ejected (3 - 4 psi, 20 ms pulses, 2 - 3 pulses) using a Picospritzer (General Valve Corporation). The solution was colored with the inactive dye Fast Green for visual guidance of the ejected droplets. Control injections consisted of Ringer's solution alone.

Kinematic Analysis

A video camera (HDR-XR200; Sony) was placed 1 m above the recording chamber to record swimming movements of the intact body (sampling rate: 30 frame / s). Video recordings were analyzed using a custom made script in MatlabR2009A (Math Works, Inc.; [38, 45]). Swimming movements were analyzed by adding equally spaced markers offline along the midline of the body. The lateral displacement of the body curvature was then monitored for each frame. For this, the angle between the longitudinal axis of the non-moving body parts (line along the body midline) and a straight line drawn between two successive markers located in the middle of the body was measured for the entire locomotor bout. The values were expressed in radian (rad).

Anatomical Tracing

Anatomical experiments were performed to investigate the distribution of MLR neurons projecting to the caudal MRRN and the rostral MRRN. Double injections, delayed in time and at different rostro-caudal levels, were carried out in the reticular formation to determine the termination region of specific populations of MLR neurons. In these experiments, two injections were made with a 4 h interval, one more caudal than the other, in isolated brainstem preparations. The first injection, the caudal one, consisted of a unilateral transverse section of the medial tegmentum using a microsurgical knife (Sharpoint). The lesion was quickly filled with crystals of Fluorescein dextran amines (3000 MW; Molecular Probes) left there to dissolve for 10 min. This allowed the tracer uptake by the cut axons. After thorough rinsing of the injected area, the preparation was placed in cold oxygenated Ringer's solution to guarantee tracer transport past the location of the more rostral, future second injection. After 4 h, a second ipsilateral transverse section of the medial tegmentum was made and quickly filled with crystals of Texas Red dextran amines (3000; Molecular Probes) left there to dissolve for 10 min. The second, more rostral injection, was always more restricted medio-laterally than the first, more caudal one. Care was taken so that tracer from the second injection did not spread to the first injection area. After thoroughly rinsing the second injection site, the preparation was again transferred to cold oxygenated Ringer's solution overnight. The next morning, it was transferred into a fixative solution (4 % paraformaldehyde in 0.1 M phosphate buffer with 0.9 % NaCl, pH 7.4 (PBS)) for 24 h, followed by an immersion in a sucrose solution (20 % in phosphate buffer) for at least 24 h. The brain was frozen and cross sectioned (25 µm) on a cryostat. The sections were placed on ColorFrost Plus microscope slides (Fisher Scientific) and rinsed with PBS and coverslipped using Vectashield mounting medium (with DAPI; Vector Laboratories). Labeled cell bodies in the MLR were observed under an E600 epifluorescent microscope equipped with a digital camera (DXM 1200; Nikon). The sections were photographed and levels were adjusted in Photoshop CS5 (Adobe) so that all fluorophores were clearly visible.

Quantification and Statistical Analysis

Data in the text are represented as the mean ± SEM. Statistical analysis was performed with Sigma Plot 11.0 (Systat). Comparisons between two groups were made in which normality and equal variance assumptions were not met. In these two cases, a Man Whitney rank-sum test was applied to compare the two groups. For more than two groups, One-way ANOVA for repeated measures was used as parametric and Friedman repeated measures analysis of variance on ranks as non-parametric analyses. These analyses were followed by a Student-Newman-Keuls post-hoc test as a pairwise multiple comparison procedure.

To calculate correlations between variables, the Pearson product-moment correlation test was used. For all statistical analyses carried out in this study, differences were considered statistically significant when $p < 0.05$. Illustrations were made using Illustrator CS5 (Adobe).

SUPPLEMENTAL INFORMATION

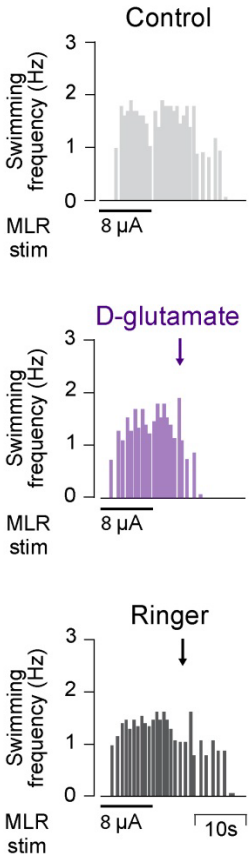

Figure S1. Effect of a Local Application of D-Glutamate in the MLR during Ongoing Swimming

The graphs illustrate the frequency of swimming during bouts of swimming elicited by electrical stimulation of the MLR (10 s train, 8 µA). Top: control bout; Middle: D-glutamate (0.55 pmol) was injected 5 s after the first electrical stimulation period. The arrow indicates when the drug was injected. Bottom: Ringer's was injected 5 s after the electrical stimulation period.

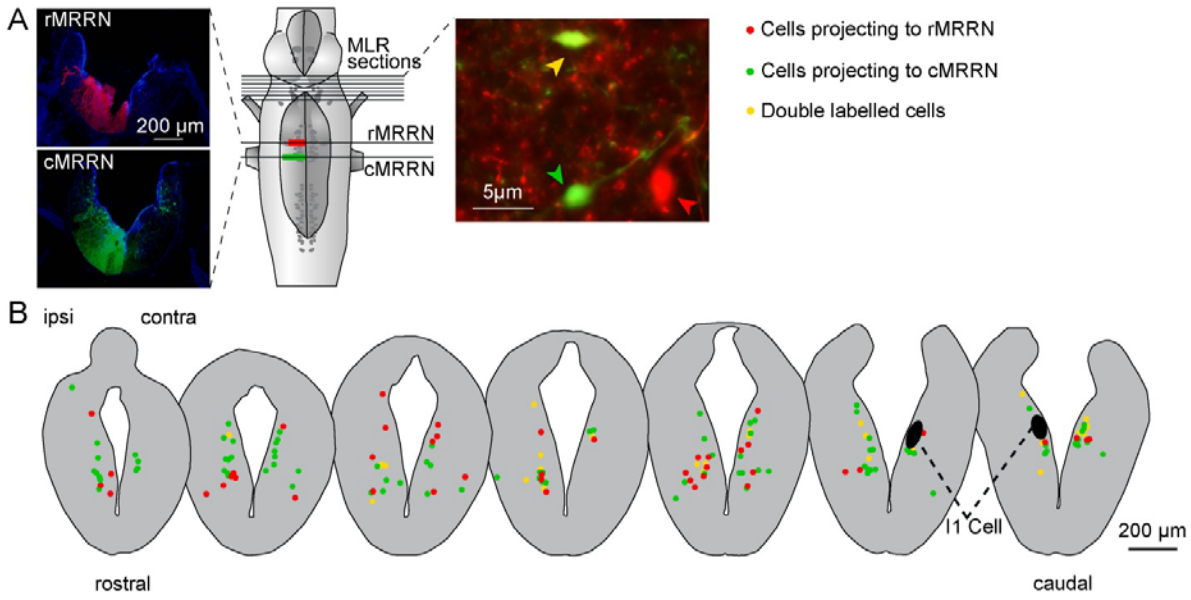

Figure S2. Distribution of MLR Neurons Projecting to a Region of the Reticular Formation where Maintain Cells are Predominantly Located

(A) Tracer injections were made at two rostro-caudal levels of the reticular formation, one in the rostral MRRN (rMRRN), the other slightly more caudal, in the caudal MRRN (cMRRN). The extent of each injection is illustrated on photomicrographs of cross sections (to the left). As seen on a high magnification photomicrograph (red and green filter sets images were merged) of a cross section at the isthmic level (to the right), neurons were retrogradely labeled in the MLR, some with one of the tracers (red and green arrowheads), others with both tracers (yellow arrowhead). The MLR neurons that sent projections terminating in the rMRRN, where maintain cells are predominantly located, were only labeled with the red tracer, whereas all neurons that sent projections further caudally to the rMRRN were double labeled or labeled only in green.

(B) Schematic cross sections through the rostro-caudal extent of the MLR showing neurons labelled on both sides. Red dots represent single labeled MLR neurons that project to the rMRRN but do not reach the cMRRN. Green and yellow dots represent MLR neurons projecting at least as far as the cMRRN, passed the maintain cell-rich region of the rMRRN. The giant RS cell I1 that is used as a landmark to identify the caudal extent of the MLR, is represented in black.

7. Discussion

7.1. Inputs to the MLR: Modulation of locomotion and control of locomotor speed

Dopaminergic modulation of locomotion

Classically, dopaminergic neurons of the mammalian SNc are described to send ascending projections to the striatum, the input region of the basal ganglia (for review, see Ryczko et al., 2017). A similar ascending dopaminergic pathway to the striatum was anatomically identified in the lamprey (Pombal et al., 1997; Ryczko et al., 2013; Peréz-Frenández et al., 2014). Here, dopaminergic neurons of the PT were shown to directly innervate the striatum, suggesting that the PT is homologous to the mammalian SNc. In addition to this ascending projection, we discovered a descending dopaminergic projection originating from the PT (Ryczko et al., 2013). We found that dopaminergic neurons directly innervate the MLR to amplify descending excitatory inputs via a D1 receptor-dependent mechanism. Since many lamprey forebrain structures have been found to be anatomically and neurochemically similar to those of mammals (Stephenson-Jones et al., 2011; 2012; for review, see Grillner and Robertson, 2016), the question emerged whether this descending dopaminergic pathway from the PT to the MLR is also present in higher vertebrates, including mammals. Indications for this were found in anatomical experiments performed in monkeys, in which dopaminergic terminals had been identified in the PPN (Rolland et al., 2009). To examine this in greater detail, Ryczko and colleagues (2016) performed a comparative study in salamanders and rats, and additionally performed experiments in human brain tissue. In salamanders and rats, they provided anatomical and physiological evidence that the dopaminergic cells project from the PT/ SNc to the MLR. Dopaminergic fibers were also anatomically identified in the human PPN. An interesting aspect of the two studies of Ryczko and colleagues (2013; 2016) was that some dopaminergic neurons in the PT/ SNc were found to project to both the MLR and the striatum, but their number differed from one species to another. Only few of these neurons were found in lampreys, and none in salamander. In rats on the other hand, several of these neurons were identified in the SNc and it was speculated that an increase in ascending dopaminergic fibers is based on the increase of basal ganglia size during evolution (for review, see Ryczko and Dubuc, 2017; Grillner and Robertson, 2016).

It has not yet been resolved if the ascending and descending dopaminergic pathways have different functional roles. Considering their targets, it is possible that the descending dopaminergic pathway to the MLR controls the excitability of brainstem motor circuits and directly amplifies the locomotor command that originates from forebrain structures. The ascending pathway could be involved in the selection of motor programs since it is innervating the input region of the basal ganglia, a brain structure known to be involved in action selection

(for review, see Grillner and Robertson, 2016). More experiments will have to be performed in the future in order to answer this question.

Glutamatergic control of locomotor speed

In addition to the descending dopaminergic pathway, a glutamatergic projection from the PT to the MLR has been identified in the lamprey (Ryczko et al., 2017). In Anatomical and physiological experiments it was found that dopaminergic and glutamatergic projections to the MLR have different functions (Ryczko et al., 2017). As previously described, dopaminergic MLR inputs modulate and amplify activity in the MLR. This input, however, is not necessary to initiate locomotion since swimming can still be elicited by electrical PT stimulation after a local blockage of D1 receptors in the MLR. Glutamatergic inputs to the MLR, on the other hand, are necessary to initiate locomotion and they control MLR activity in a graded fashion (Ryczko et al., 2017). The neural mechanisms underlying this function of the MLR are not yet elucidated. In a recent study, Roseberry and colleagues (2016) demonstrated that MLR sub-populations have different functional roles in mice. Glutamatergic MLR neurons are necessary and sufficient to initiate locomotion and their optogenetic activation drives locomotion. Optogenetic activation of cholinergic MLR neurons on the other hand does not trigger locomotion at rest but modulates the speed of the ongoing locomotor bout. In the lamprey, glutamatergic and cholinergic neurons have been identified in the MLR (Le Ray et al., 2003; Brocard et al., 2010), but so far it is unknown if they control the locomotor output differently. It has been reported that local ejections of acetylcholine over the RS cells in the MRRN accelerates the fictive locomotor rhythm induced by NMDA, (Le Ray et al., 2003), similar to what has been observed in mice (Roseberry et al., 2016). Taking these findings into account, it is possible that glutamatergic neurons from the PT project to cholinergic neurons in the MLR to control the locomotor output in a graded fashion (Ryczko et al., 2017). However, since it has not been examined whether PT neurons project to specific cell populations in the MLR, this hypothesis remains speculative. In order to test it, anatomical as well as physiological experiments should be performed in the future.

It also has not been resolved in which context the glutamatergic pathway from the PT to the MLR is recruited. It could be part of the olfactory-locomotor circuit, since fibers from the medial olfactory bulb project directly to the PT and electrical stimulation of this region elicits responses in the MLR that evoke locomotion (Derjean et al., 2010; Ryczko et al., 2017). In this case, olfactory inputs could generate different activity levels in the PT, which in turn could finely tune the locomotor command from the MLR. Such mechanism could play a crucial role for animals to move towards an attractive olfactory stimulus or avoid dangerous ones.

7.2. Outputs of the MLR: Termination of locomotion

Command cells for stopping locomotion and their targets

We demonstrated the presence of RS stop cells that control the end of a locomotor bout in lampreys (Juvin et al., 2016). Anatomical experiments revealed that their axons project to the spinal cord, but neither their spinal targets have been identified nor the neurotransmitter they use. Command cells for stopping locomotor movements have been identified in both invertebrates (crayfish: Kagaya and Takahata, 2010; 2011; cockroach: Kai and Okada, 2013; leech: O'Gara and Friesen, 1995; Taylor et al., 2003) and vertebrates (*Xenopus* tadpole: Perrins et al., 2002; mouse: Bouvier et al., 2015; Capelli et al., 2017; cat: Takakusaki et al., 2001). In vertebrates, different neural mechanisms have been described to be involved in the termination of locomotion. In the *Xenopus* tadpole, ongoing swimming bouts stop if the animal swims into an object (Boothby and Roberts, 1992). Mechanical stimulation of the head's cement gland activates the trigeminal afferents that in turn excite GABAergic neurons in the hindbrain (Perrins et al., 2002). These GABAergic cells send mostly contralateral projections to the spinal cord to inhibit spinal locomotor CPGs (Perrins et al., 2002). More recently, glutamatergic V2a 'stop neurons' were identified in the brainstem of mice (Bouvier et al., 2015). Optogenetic activation of these V2a 'stop neurons' halts ongoing locomotor movements, and a blockade of the synaptic output increases ambulating phases dramatically. These neurons project to inhibitory and excitatory neurons in the lamina VII and X of the lumbar spinal cord, and it was proposed that they make direct and indirect synaptic contacts to inhibitory spinal circuits (Bouvier et al., 2015). Capelli and colleagues (2017) also identified RS neurons in the mouse brainstem that stop locomotion when activated optogenetically. These neurons are glycinergic and send direct descending projections to the spinal cord, where they mostly target motor neurons residing in the ventral laminae (Capelli et al., 2017). Taken together, excitatory (glutamatergic) as well as inhibitory (glycinergic, GABAergic) command neurons have been reported to control the termination of locomotion. In the lamprey, glutamatergic as well as glycinergic RS cells have been identified (Buchanan et al., 1987a; Ohta and Grillner, 1989; Wannier et al, 1995). Both RS groups were shown to project directly to the spinal cord and target spinal interneurons and motor neurons. However, the identified glutamatergic RS cells were either Müller or Mauthner cells located in the rostral MRRN (Buchanan et al., 1987a) or in the PRRN (Ohta and Grillner, 1989), and do not coincide with the location of the stop cells in the caudal MRRN. As Wannier and colleagues performed the experiments only on the axons of RS cells, the localization of the cell bodies of glycinergic RS cells is unknown and cannot be correlated to our findings (Juvin et al., 2016).

Another interesting aspect is that stop cells exhibit two bursts of activity: one burst at the beginning of the locomotor bout and one at the end ('termination burst'). It seems puzzling that stop cells encode two antagonistic signals and so far, the underlying neural mechanism is not yet understood. Interestingly, in motor pathways of vertebrates (*e.g.* cat: Rossignol et al., 1981; Pearson and Collins, 1993) and invertebrates (*e.g.*

locust: Zill, 1985; stick insect: Bässler, 1986) it has been described that motor neurons respond differently to the same synaptic input if the behavioral context of the animal changes (for review, see Rossignol et al, 2006). For example, experiments in spinalized cats demonstrated that motor neurons of the medial gastrocnemius respond differently to a synaptic input originating from group I afferent fibers of the plantaris muscle. The motor neuron responses depend on the state of activity of the animal. During locomotion, electrical stimulation of group I afferents results in the activation of the motor neurons of the medial gastrocnemius, whereas the same stimulation reduces activity in the same group of motor neurons when the animal is at rest (Pearson and Collins, 1993). A similar state-dependent response to synaptic inputs from stop cells could be present in spinal neurons of lampreys. As described for V2a 'stop neurons' in mice, stop cells could be glutamatergic and could provide excitatory input to inhibitory as well as excitatory interneurons in the spinal cord (Bouvier et al., 2015). When the animal is at rest, the spinal neurons that are targeted by stop cells (excitatory and inhibitory interneurons) could have different excitability, such that excitatory interneurons would be highly excitable, whereas inhibitory interneurons would have low excitability. In this context, the first burst of stop cells would allow the excitatory interneurons to reach firing threshold, whereas the inhibitory interneurons would remain subthreshold. The net output of the first burst generated by stop cells would thus be excitatory rather than inhibitory and lead to the activation of motor neurons, thus generating locomotor activity. During swimming, the behavioral state changes and the excitability of spinal inhibitory interneurons could change as well. Excitatory inputs from the spinal locomotor networks could activate specific intrinsic properties that would considerably increase the excitability of the inhibitory interneurons during the active state (*e.g.* Ca^{2+}-dependent non-selective cation cannels; I_{CAN}). That way, the 'termination burst' of stop cells that occurs during locomotor activity could produce a strong discharge of inhibitory interneurons that would be involved in stopping locomotion. This hypothesis could explain opposite functions of the two bursts displayed by stop cells, but it needs to be tested experimentally.

Synaptic inputs to stop cells

It has been shown that synaptic inputs rather than membrane properties of stop cells are responsible for the generation of their characteristic activation pattern, including the 'termination burst'. Inputs to stop cells were examined in detail and the MLR was shown to provide synaptic inputs that generate the 'termination burst' in stop cells (Grätsch et al., under review). Anatomical projections from the MLR to the stop cell-rich region in the caudal MRRN were identified, and electrophysiological experiments demonstrated that at least part of the connections between the MLR and stop cells are monosynaptic. We have not yet examined which neurotransmitter is involved in this projection, but glutamate or acetylcholine would be possible transmitters in this case. The mid-hindbrain neurons in the *Xenopus* tadpole were shown to be activated by glutamatergic inputs from the trigeminal nerve in response to sensory inputs from the cement gland (Perrins et al., 2002). In other species, brainstem neurons that stop locomotion were thought to receive inputs from other regions of the CNS (Takakusaki et al., 2004; Bouvier et al., 2015, Capelli et al., 2017), but not much is known about these

synaptic inputs. In cats, activation of cholinergic neurons of the PPN induces muscle atonia and stops spontaneous locomotion (Takakusaki et al., 2003). It was suggested that these cholinergic neurons project via the *nucleus reticularis pontis oralis* to the RS neurons in the medullary *nucleus reticularis gigantocellularis*, and thus control locomotor suppression (for review, see Takakusaki et al., 2008). In the lamprey, glutamatergic and cholinergic projections from the lamprey MLR to RS cells have been described (Le Ray et al., 2003; Brocard et al., 2010). Activation of stop cells with local glutamate ejections was shown to stop ongoing locomotion (Juvin et al., 2016), which strongly suggests that glutamatergic inputs from the MLR could trigger the 'termination burst' in stop cells, and thus, stop ongoing locomotion. However, cholinergic inputs to stop cells have not yet been tested. It cannot be excluded that cholinergic MLR neurons project to stop cells and provide an excitatory input, which in turn triggers the 'termination burst' which leads to termination of locomotion. This possibility needs to be tested in the future.

MLR activity stops locomotion

In lampreys, electrical MLR stimulation can trigger locomotor activity that often exceeds the duration of the electrical stimulation. When the animal is swimming after the MLR stimulation has ended, a second MLR stimulation stops locomotion if it is of lower intensity than the initial MLR stimulation (Grätsch et al., under review). The MLR is a complex and anatomically diffuse brain region comprising neurons that express different neurotransmitters (glutamate, acetylcholine, GABA). In mammals, it comprises at least two nuclei, the PPN and the CuN. In basal vertebrates, like salamanders and lampreys, the MLR includes at least in part the nuclei that contain cholinergic neurons, the PPN and the LDT (for review, see Martinez-Gonzalez et al., 2011; Ryczko et al., 2013). There is still a controversy relative to the motor output that is produced by the MLR. Sinnamon (1993) proposed that different parts of the MLR control specific locomotor behaviors, e.g. appetitive, explorative, or escape behavior. Recent optogenetic studies support such an organization of the MLR (Roseberry et al., 2016; Caggiano et al., 2018; Josset et al., 2018). It was shown that glutamatergic and cholinergic neurons of the PPN control slow explorative movements, whereas activation of glutamatergic CuN neurons induces fast escape behavior (Caggiano et al., 2018; Josset et al., 2018). Considering this, it could also be possible that a sub-population of MLR cells is responsible to control the termination of locomotion and that this population projects predominantly to stop cells in the caudal MRRN. In our experiments, we used the I1 RS cell (Rovainen, 1967), located at the junction between the mesencephalon and rhombencephalon as a landmark for positioning the stimulation electrode in the MLR. If the prior assumption is valid, the sub-population of MLR cells that controls termination of locomotion could be located close to I1 and could be activated with low stimulation intensities. Electrical MLR stimulation of higher intensities on the other hand would spread further in the brain tissue (Ranck, 1975) and activate MLR neurons that are located further away from the electrode and possibly control the initiation of locomotion and the intensity of the locomotor output. Using anatomical approaches, we could not provide evidence for this hypothesis. In fact, MLR neurons that project to the stop cell-rich caudal MRRN are intermingled with MLR neurons projecting

to maintain cells. Another possibility would be that MLR neurons, that project to the stop cell region, have different membrane properties (*e.g.* lower threshold) and are therefore specifically activated with lower stimulation intensity. Another hypothesis could be proposed, in which excitability of MLR cells changes depending on the behavioral state of the animal. In this sense, MLR neurons that control the initiation of locomotion or the intensity of the locomotor output could be excitable at rest and be recruited by the first MLR stimulation. This excitability could decrease during ongoing swimming episodes, possibly due to adaptation. The excitability of MLR neurons that control the termination of locomotion on the other hand, could increase gradually during ongoing swimming movements (*e.g.* due to I_{CAN}). Like this, a second MLR stimulation of low intensity would specifically recruit MLR neurons controlling termination of locomotion but not those that control the initiation or the intensity of the locomotor output. As this hypothesis is highly speculative, it will have to be tested experimentally.

Classically, locomotor suppression in mammals is described to occur through GABAergic projections from the SNr and GPi to the MLR (for review, see Grillner and Robertson, 2017; Roseberry and Kreitzer, 2017). Roseberry and colleagues (2016) demonstrated that descending GABAergic neurons from the basal ganglia as well as local neurons in the MLR inhibit glutamatergic MLR neurons that drive locomotion. GABAergic projections from the basal ganglia output regions were also identified in the lamprey and local activation of GABAergic receptors in the MLR suppressed ongoing locomotion (Robertson et al., 2006; Ménard et al., 2007). However, this mechanism for locomotor suppression is not involved in the pathway that is described here, since electrical and pharmacological activation of the MLR stops ongoing locomotion. It is very likely that both strategies for locomotor termination exist in parallel and occur in different contexts, but this is not yet understood.

7.3. Significance for clinical research

Fundamental research on the neural control of movements could have a significant impact on the clinical research field. Motor deficits (*e.g.* freezing of gait, falls, difficulty to terminate gait) are often observed in patients with neurodegenerative diseases, such as in Parkinson's disease (PD) (for review, see Bloem et al., 2004). These deficits have often been associated to the degeneration of the ascending dopaminergic pathway from the SNc to the striatum (Albin et al., 1989; Ehringer and Hornykiewicz, 1998). In the study of Ryczko and colleagues (2013), a descending dopaminergic pathway that is projecting from the PT (homologue of the mammalian SNc) to the MLR has been identified and shown to modulate activity in the MLR. This pathway was later shown to be conserved in salamanders, rats, and possibly humans (Ryczko et al., 2016). Considering this, it is possible that motor deficits in PD patients could not only arise from the degeneration of ascending dopaminergic neurons projecting to the striatum, but they could also be explained by the loss of neurons at the

origin of a descending dopaminergic pathway to the MLR. Results obtained by Rolland and colleagues (2009) in monkeys support this hypothesis. In that study, monkeys were intoxicated with 1-methyl-4-phenyl-1,2,3,6-tetrahydropyridine (MPTP), a substance that is classically used to mimic the symptoms of PD by depleting the population of dopaminergic neurons in the SNc. It was shown that the number of dopaminergic terminals in the PPN was dramatically reduced as a consequence of MPTP intoxication (Rolland et al., 2009). Interestingly, lampreys that were intoxicated with MPTP showed severe motor deficits, including impairment in initiation and maintenance of locomotion (Thompson et al., 2008). Taken together, degeneration of dopaminergic neurons in the SNc results in motor deficits and it is likely that this is not only a result of cell loss in the ascending dopaminergic pathway but also due to neural loss in the descending dopaminergic pathway that projects to the MLR.

Furthermore, PD patients often display an impaired ability to stop ongoing movement, particularly in unplanned situations (Gauggel et al., 2004; Bishop et al., 2003; 2006). It was shown that they change their strategy in order to stop in response to a sudden stop signal (Bishop et al., 2003): the 'brake impulse' that is present in healthy individuals can be absent in PD patients in these situations. PD patients decrease the propulsion of the body in order to stop walking, which often results in a prolongation in stopping time (Bishop et al., 2003; Gauggel et al., 2004). It is presumed that the deficit in the termination of movement in PD patients results from the degeneration of dopaminergic neurons, most likely within the basal ganglia (Gauggel et al., 2004). The descending dopaminergic pathway could also affected in these patients (Ryczko et al., 2013; 2016), directly affecting MLR activity and in turn inputs to the stop cells. This could have an impact on the ability to stop locomotion swiftly in unplanned situations. More research is needed to resolve this question and develop new therapeutic approaches for patients with PD or other gait disorders.

7.4. Concluding remarks and future perspectives

Taken together, the studies presented in this thesis have contributed to the understanding of the descending control of locomotion in the lamprey. Yet, some questions remain unanswered and more experimental work will have to be performed in the future.

For example, it is not known whether or how specific sub-populations of MLR neurons (e.g. glutamatergic or cholinergic cells) are innervated by glutamatergic PT neurons in order to control the locomotor output in a graded fashion. In mice, it was shown that glutamatergic MLR neurons drive locomotion and cholinergic MLR neurons control locomotor speed (Roseberry et al., 2016). To test if a similar mechanism is present in the lamprey, the locomotor output in response to increasing stimulation intensities of the PT could be recorded and cholinergic inputs to RS cells could be blocked simultaneously. Local applications of a nicotinic antagonist over the MRRN (*e.g.* D-tubocurarine) could be used in a semi-intact preparation and locomotor

activity could then be observed in response to incrementally increasing PT stimulation. It should then be analyzed whether locomotor speed is still increasing linearly with increasing PT stimulation intensities. Next, intracellular recordings of MLR neurons (glutamatergic and cholinergic) could be performed to examine if MLR neurons respond differently to electrical stimulation of the PT. To identify MLR neurons that project to RS cells in the brainstem, retrograde tracers could be injected into the MRRN. Labelled cell bodies located in the MLR could then be patch-clamped to record synaptic responses to PT simulations. In this experiment, glutamatergic (CNQX/ AP5) and dopaminergic (SCH23390) receptor antagonist could be injected locally into the MLR to discriminate if glutamatergic and dopaminergic PT cells target glutamatergic or cholinergic MLR cells differentially. Filling the recorded MLR neuron with biocytin at the end of the experiment would allow immunohistochemical, *a posteriori* identification of the neurotransmitter expressed by the recorded MLR cell.

Spinal targets and the neurotransmitters expressed by stop cells have not yet been identified. To examine this, stop cells could be recorded intracellularly and labelled using biocytin in the recording pipette, as described previously (Juvin et al., 2016). Immunohistochemistry experiments could then be performed to test the labelled neuron against glutamate, glycine, or GABA (in respect to the findings of Bouvier et al., 2015; Capelli et al., 2017; Perrins et al., 2002). After the identification of neurotransmitters expressed in stop cells, targets in the spinal cord can be investigated. First, postsynaptic potentials of spinal neurons (*e.g.* excitatory or inhibitory interneurons, motor neurons) could be recorded in response to electrical or pharmacological stimulation of the caudal MRRN, a stop cell-rich region. As a next step, intracellular recordings of spinal cord neurons should be combined with a local blockade of receptors. Depending on the neurotransmitter expressed by stop cells, CNQX/AP5 (antagonists of AMPA / kainate and NMDA receptors), strychnine (antagonist of glycine receptors), or gabazine (antagonist of $GABA_A$ receptors) could be injected locally over the recorded spinal neurons. In order to test connectivity, double recordings of a stop cell and a potential target neuron in the spinal cord should be performed. High frequency current pulses that are injected into the stop cell would provide insight as to whether the connection is mono- or polysynaptic. Additionally, the cation concentration in the Ringer's solution could be increased to disrupt polysynaptic projections. Again, intracellular labelling of the spinal neuron with biocytin could help to identify them on the basis of their location or morphology. Once spinal target neurons are identified, it could be tested whether they have intrinsic properties needed for a gating mechanism.

It is not yet known how the MLR specifically activates stop cells in order to control the end of a locomotor bout. As a first step, the neurochemical nature (glutamatergic or cholinergic) of the MLR inputs to stop cells should be determined (Le Ray et al., 2003; Brocard et al., 2010). In semi-intact preparations, local application of D-glutamate over the stop cell-rich brainstem region (caudal MRRN) was shown to stop an ongoing locomotor bout, whereas a blockade of glutamate receptors in this region impaired the swift termination of locomotion (Juvin et al., 2016). However, the role of cholinergic inputs to stop cells has not yet been tested. To do so, similar experiments could be performed (Juvin et al., 2016), but this time with local application of cholinergic agonists (nicotinic receptors: nicotine; muscarinic receptors: muscarine) or antagonists (nicotinic

receptors: D-tubocurarine, α-bungarotoxin; muscarinic receptors: atropine) over the caudal MRRN. As a next step, the cellular activity, membrane properties, and morphology of the MLR neurons that project to stop cells could be examined and compared to that of MLR cells that project to other cell populations in the MRRN. For this, Ca^{2+} imaging experiments could be performed in which MLR neurons are labelled retrogradely from the caudal MRRN with Calcium Green dextran amines, a calcium indicator. The Ca^{2+} response of these MLR neurons could then be recorded in response to PT stimulation, which reliably elicits MLR cell activity and locomotion (Derjean et al., 2010; Ryczko et al., 2013; 2017). If a characteristic pattern can be observed in these MLR neurons, Ca^{2+} response to PT stimulation should be compared to other MLR neurons that are retrogradely labelled from the rostral MRRN (maintain cell-rich region; Juvin et al., 2016). The Ca^{2+} experiments can be combined with intracellular recordings in order to investigate intrinsic properties of the MLR neurons projecting to the stop cell region. Additionally, intracellular labelling of the recorded neurons would allow the analysis of their morphology, *e.g.* size of the cell bodies or axon diameter and projection.

In conclusion, this thesis has contributed to a better understanding about the neural networks that control locomotion in a basal vertebrate, the lamprey. It provided insight into the functional role the descending dopaminergic and glutamatergic inputs to the MLR, which modulate locomotion and control it in a graded fashion respectively. Additionally, a neural substrate that underlies the termination of locomotion has been identified and shown to arise from a descending output from the MLR to RS stop cells in the hindbrain.

8. Bibliography

Albin, R.L., Young, A.B., and Penney, J.B. (1989). The functional anatomy of basal ganglia disorders. Trends Neurosci. 12(10):366-375.

Antri, M., Fénelon, K., and Dubuc, R. (2009). The contribution of synaptic inputs to sustained depolarizations in reticulospinal neurons. J. Neurosci. 29(4):1140-1151.

Bässler, U. (1986). Afferent control of walking movements in the stick insect *Cuniculina impigra* II. Reflex reversal and the release of the swing phase in the restrained foreleg. J. Comp. Physiol. A 158(3):351-362.

Beckstead, R.M., Domesick, V.B., and Nauta, W.J. (1979). Efferent connections of the substantia nigra and ventral tegmental area in the rat. Brain Res 175(2):191-217.

Bishop, M., Brunt, D., and Marjama-Lyons, J. (2006). Do people with Parkinson's disease change strategy during unplanned gait termination? Neurosci. Lett. 397(3):240-244.

Bishop, M.D., Brunt, D., Kukulka, C., Tillman, M.D., and Pathare, N. (2003). Braking impulse and muscle activation during unplanned gait termination in human subjects with parkinsonism. Neurosci. Lett. 348(2):89-92.

Bloem, B.R., Hausdorff, J.M., Visser, J.E., and Giladi, N. (2004). Falls and freezing of gait in Parkinson's disease: a review of two interconnected, episodic phenomena. Mov. Disord. 19(8):871-884.

Boothby, K.M., and Roberts, A. (1992). The stopping response of *Xenopus laevis* embryos: pharmacology and intracellular physiology of rhythmic spinal neurones and hindbrain neurones. J. Exp. Biol. 169:65-86.

Bouvier, J., Caggiano, V., Leiras, R., Caldeira, V., Bellardita, C., Balueva, K., Fuchs, A., and Kiehn, O. (2015). Descending command neurons in the brainstem that halt locomotion. Cell 163(5):1191-1203.

Bretzner, F., and Brownstone, R.M. (2013). Lhx3-Chx10 reticulospinal neurons in locomotor circuits. J. Neurosci. 33(37):14681-14692.

Brocard, F., and Dubuc, R. (2003). Differential contribution of reticulospinal cells to the control of locomotion induced by the mesencephalic locomotor region. J. Neurophysiol. 90(3):1714-1727.

Brocard, F., Ryczko, D., Fénelon, K., Hatem, R., Gonzales, D., Auclair, F., and Dubuc, R. (2010). The transformation of a unilateral locomotor command into a symmetrical bilateral activation in the brainstem. J. Neurosci. 30(2):523-533.

Buchanan, J.T. (1982). Identification of interneurons with contralateral, caudal axons in the lamprey spinal cord: synaptic interactions and morphology. J. Neurophysiol. 47(5):961-975.

Buchanan, J.T. (2001). Contributions of identifiable neurons and neuron classes to lamprey vertebrate neurobiology. Prog. Neurobiol. 63(4):441-466.

Buchanan, J.T. (2011). Spinal locomotor inputs to individually identified reticulospinal neurons in the lamprey. J. Neurophysiol. 106(5):2346-2357.

Buchanan, J.T., and Grillner, S. (1987). Newly identified 'glutamate interneurons' and their role in locomotion in the lamprey spinal cord. Science 236(4799):312-314.

Buchanan, J.T., Brodin, L., Dale, N., and Grillner, S. (1987). Reticulospinal neurones activate excitatory amino acid receptors. Brain Res. 408(1-2):321-325.

Büschges, A., Scholz, H., and El Manira, A. (2011). New moves in motor control. Curr. Biol. 21(13):R513-524.

Bussières, N. (1994). Les systèmes descendants chez la lamproie. Étude anatomique et fonctionnelle. Doctoral thesis. Université de Montréal.

Cabelguen, J.M., Bourcier-Lucas, C., and Dubuc, R. (2003). Bimodal locomotion elicited by electrical stimulation of the midbrain in the salamander *Notophthalmus viridescens*. J. Neurosci. 23(6):2434-2439.

Caggiano, V., Leiras, R., Goñi-Erro, H., Masini, D., Bellardita, C., Bouvier, J., Caldeira, V., Fisone, G., and Kiehn, O. (2018). Midbrain circuits that set locomotor speed and gait selection. Nature 553(7689):455-460.

Capelli, P., Pivetta, C., Soledad Esposito, M., and Arber, S. (2017). Locomotor speed control circuits in the caudal brainstem. Nature 551(7680):373-377.

Cohen, A.H., and Harris-Warrick, R.M. (1984). Strychnine eliminates alternating motor output during fictive locomotion in the lamprey. Brain Res. 293(1):164-167.

Cohen, A.H., and Wallén, P. (1980). The neuronal correlate of locomotion in fish. "Fictive swimming" induced in an in vitro preparation of the lamprey spinal cord. Exp. Brain Res. 41(1):11-8.

Cruce, W. L. R., & Newman, D. B. (1984). Evolution of motor systems: The reticulospinal pathways. American Zoologist, 24, 733-753.

Daghfous, G., Green, W.W., Alford, S.T., Zielinski, B.S., and Dubuc, R. (2016). Sensory activation of command cells for locomotion and modulatory mechanisms: lessons from lampreys. Front. Neural. Circuits. 10:18 doi: 10.3389/fncir.2016.00018.

Dale, N. (1986). Excitatory synaptic drive for swimming mediated by amino acid receptors in the lamprey. J. Neurosci. 6(9):2662-2675.

Deliagina, T.G., and Orlovsky, G.N. (2002). Comparative neurobiology of postural control. Curr. Opin. Neurobiol. 12(6):652-657.

Deliagina, T.G., Orlovsky, G.N., Grillner, S., and Wallén, P. (1992). Vestibular control of swimming in lamprey. III. Activity of vestibular afferents: convergence of vestibular inputs on reticulospinal neurons. Exp Brain Res. 90(3):499-507.

Deliagina, T.G., Orlovsky, G.N., Grillner, S., and Wallén, P. (1992). Vestibular control of swimming in lamprey. III. Activity of vestibular afferents: convergence of vestibular inputs on reticulospinal neurons. Exp. Brain Res. 90(3):499-507.

Deliagina, T.G., Orlovsky, G.N., Grillner, S., and Wallén, P. (1992). Vestibular control of swimming in lamprey. II. Characteristics of spatial sensitivity of reticulospinal neurons. Exp. Brain Res. 90(3):489-498.

Derjean, D., Moussaddy, A., Atallah, E., St-Pierre, M., Auclair, F., Chang, S., Ren, X., Zielinski, B., and Dubuc, R. (2010). A novel neural substrate for the transformation of olfactory inputs into motor output. PLoS Biol. 8(12):e1000567.

Dubuc, R., Bongianni, F., Ohta, Y., and Grillner, S. (1993). Anatomical and physiological study of brainstem nuclei relaying dorsal column inputs in lampreys. J. Comp. Neurol. 327(2):260-270.

Dubuc, R., Bongianni, F., Ohta, Y., and Grillner, S. (1993). Dorsal root and dorsal column mediated synaptic inputs to reticulospinal neurons in lampreys: involvement of glutamatergic, glycinergic, and GABAergic transmission. J. Comp. Neurol. 327(2):251-259.

Dubuc, R., Brocard, F., Antri, M., Fénelon, K., Gariépy, J.F., Smetana, R., Ménard, A., Le Ray, D., Viana Di Prisco, G., Pearlstein, E., Sirota, M.G., Derjean, D., St-Pierre, M., Zielinski, B., Auclair, F., and Veilleux, D. (2008). Initiation of locomotion in lampreys. Brain Res. Rev. 57(1):172-182.

Ehringer, H., and Hornykiewicz, O. (1998). Distribution of noradrenaline and dopamine (3-hydroxytyramine) in the human brain and their behavior in diseases of the extrapyramidal system. Parkinsonism Relat. Disord. 4(2):53-57.

Einum, J.F., and Buchanan, J.T. (2005). Membrane potential oscillations in reticulospinal and spinobulbar neurons during locomotor activity. J. Neurophysiol. 94(1):273-281.

El Manira, A., Pombal, M.A., and Grillner, S. (1997). Diencephalic projection to reticulospinal neurons involved in the initiation of locomotion in adult lampreys *Lampetra fluviatilis*. J. Comp. Neurol. 389(4):603-616.

Ericsson, J., Stephenson-Jones, M., Kardamakis, A., Robertson, B., Silberberg, G., and Grillner, S. (2013). Evolutionarily conserved differences in pallial and thalamic short-term synaptic plasticity in striatum. J. Physiol. 591(4):859-874.

Fagerstedt, P., Orlovsky, G.N., Deliagina, T.G., Grillner, S., and Ullén, F. (2001). Lateral turns in the Lamprey. II. Activity of reticulospinal neurons during the generation of fictive turns. J. Neurophysiol. 86(5):2257-2265.

Fetcho, J.R., and Svoboda, K.R. (1993). Fictive swimming elicited by electrical stimulation of the midbrain in goldfish. J. Neurophysiol. 70(2):765-80.

Garcia-Rill, E., and Skinner, R.D. (1987). The mesencephalic locomotor region. II. Projections to reticulospinal neurons. Brain Res. 411(1):13-20.

Garcia-Rill, E., and Skinner, R.D. (1987). The mesencephalic locomotor region. I. Activation of a medullary projection site. Brain Res. 411(1):1-12.

Garcia-Rill, E., Skinner, R.D., and Fitzgerald, J.A. (1985). Chemical activation of the mesencephalic locomotor region. Brain Res. 330(1):43-54.

Gariépy, J.F., Missaghi, K., Chevallier, S., Chartré, S., Robert, M., Auclair, F., Lund, J.P., and Dubuc, R. (2012). Specific neural substrate linking respiration to locomotion. Proc. Natl. Acad. Sci. U. S. A. 109(2):E84-92.

Gauggel, S., Rieger, M., and Feghoff, T.A. (2004). Inhibition of ongoing responses in patients with Parkinson's disease. J. Neurol. Neurosurg. Psychiatry 75(4):539-544.

Grillner, S. (2003). The motor infrastructure: from ion channels to neuronal networks. Nat. Rev. Neurosci. 4(7):573-586.

Grillner, S., and Robertson, B. (2017). Selection of action - A vertebrate perspective. In Neurobiology of Motor Control - Fundamental Concepts and New Directions, S.L. Hooper and A. Büschges, eds. (New Jersey, United States of America: Wiley-Blackwell), pp. 181-191.

Grillner, S., and Robertson, B. (2016). The basal ganglia over 500 million years. Curr. Biol. 26(20):R1088-R1100.

Grillner, S., and Zangger, P. (1975). How detailed is the central pattern generation for locomotion? Brain Res. 88(2):367-371.

Grillner, S., and Zangger, P. (1979). On the central generation of locomotion in the low spinal cat. Exp. Brain Res. 34(2):241-261

Islam, S.S., Zelenin, P.V., Orlovsky, G.N., Grillner, S., and Deliagina, T.G. (2006). Pattern of motor coordination underlying backward swimming in the lamprey. J. Neurophysiol. 96(1):451-460.

Jordan, L.M. (1998). Initiation of locomotion in mammals. Ann. N Y Acad. Sci. 860:83-93.

Josset, N., Roussel, M., Lemieux, M., Lafrance-Zoubga, D., Rastqar, A., and Bretzner, F. (2018). Distinct contributions of mesencephalic locomotor region nuclei to locomotor control in the freely behaving mouse. Curr. Biol. 28(6):884-901.

Juvin, L., Grätsch, S., Trillaud-Doppia, E., Gariépy, J.F., Büschges, A., and Dubuc, R. 2016. A specific population of reticulospinal neurons controls the termination of locomotion. Cell Rep. 15(11):2377-2386.

Kagaya, K., and Takahata, M. (2011). Sequential synaptic excitation and inhibition shape readiness discharge for voluntary behavior. Science 332(6027):365-368.

Kagaya, K., and Takahata, M. (2010). Readiness discharge for spontaneous initiation of walking in crayfish. J. Neurosci. 30(4):1348-1362.

Kahn, J.A., and Roberts, A. (1982). Experiments on the central pattern generator for swimming in amphibian embryos. Philos. Trans. R. Soc. Lond. B Biol. Sci. 296(1081):229-243.

Kai, K., and Okada, J. (2013). Characterization of locomotor-related spike activity in protocerebrum of freely walking cricket. Zoolog. Sci. 30(7):591-601.

Kimura, Y., Satou, C., Fujioka, S., Shoji, W., Umeda, K., Ishizuka, T., Yawo, H., and Higashijima, S. (2013). Hindbrain V2a neurons in the excitation of spinal locomotor circuits during zebrafish swimming. Curr. Biol. 23(10):843-849.

Klemm, W.R. (2001). Behavioral arrest: in search of the neural control system. Prog. Neurobiol. 65(5):453-471.

Kozlov, A.K., Ullén, F., Fagerstedt, P., Aurell, E., Lansner, A., and Grillner, S. (2002). Mechanisms for lateral turns in lamprey in response to descending unilateral commands: a modeling study. Biol. Cybern. 86(1):1-14.

Kravitz, A.V., Freeze, B.S., Parker, P.R., Kay, K., Thwin, M.T., Deisseroth, K., and Kreitzer, A.C. (2010). Regulation of parkinsonian motor behaviours by optogenetic control of basal ganglia circuitry. Nature 466(7306):622-626.

Kreitzer, A.C., and Malenka, R.C. (2008). Striatal plasticity and basal ganglia circuit function. Neuron 60(4):543-554.

Kudo, N., and Yamada, T. (1987). N-methyl-D,L-aspartate-induced locomotor activity in a spinal cord-hindlimb muscles preparation of the newborn rat studied in vitro. Neurosci. Lett. 75(1):43-48.

Kumar, S., and Hedges, S.B. (1998). A molecular timescale for vertebrate evolution. Nature 392(6679):917-920.

Le Ray, D., Brocard, F., Bourcier-Lucas, C., Auclair, F., Lafaille, P., and Dubuc, R. (2003). Nicotinic activation of reticulospinal cells involved in the control of swimming in lampreys. Eur. J. Neurosci. 17(1):137-148.

Le Ray, D., Juvin, L., Boutin, T., Auclair, F., and Dubuc, R. (2010). A neuronal substrate for a state-dependent modulation of sensory inputs in the brainstem. Eur. J. Neurosci. 32(1):53-59.

Le Ray, D., Juvin, L., Ryczko, D., and Dubuc, R. (2011). Chapter 4--supraspinal control of locomotion: the mesencephalic locomotor region. Prog. Brain. Res. 188:51-70.

Lee, A.M., Hoy, J.L., Bonci, A., Wilbrecht, L., Stryker, M.P., and Niell, C.M. (2014). Identification of a brainstem circuit regulating visual cortical state in parallel with locomotion. Neuron 83:455-466.

Martinez-Gonzalez, C., Bolam, J.P., and Mena-Segovia, J. (2011). Topographical organization of the pedunculopontine nucleus. Front. Neuroanat. 5:22.

Matsushima, T., and Grillner, S. (1992). Neural mechanisms of intersegmental coordination in lamprey: local excitability changes modify the phase coupling along the spinal cord. J. Neurophysiol. 67(2):373-388.

McClellan, A.D., and Grillner, S. (1984). Activation of 'fictive swimming' by electrical microstimulation of brainstem locomotor regions in an in vitro preparation of the lamprey central nervous system. Brain Res. 300(2):357-361.

McDearmid, J.R., and Drapeau, P. (2006). Rhythmic motor activity evoked by NMDA in the spinal zebrafish larva. J. Neurophysiol. 95(1):401-417.

Ménard, A., Auclair, F., Bourcier-Lucas, C., Grillner, S., and Dubuc, R. (2007). Descending GABAergic projections to the mesencephalic locomotor region in the lamprey *Petromyzon marinus*. J. Comp. Neurol. 501(2):260-273.

Missaghi, K., Le Gal, J.P., Gray, P.A., and Dubuc, R. (2016). The neural control of respiration in lampreys. Respir. Physiol. Neurobiol. 234:14-25.

Mullins, O.J., Hackett, J.T., Buchanan, J.T., and Friesen, W.O. (2011). Neuronal control of swimming behavior: comparison of vertebrate and invertebrate model systems. Prog. Neurobiol. 93(2):244-269.

Nieuwenhuys, R., Donkelaar, H.J., ten Donkelaar, H.J., and Nicholson, C. (1998). The central nervous system of vertebrates. Springer-Verlag Berlin Heidelberg.

Ocaña, F.M., Suryanarayana, S.M., Saitoh, K., Kardamakis, A.A., Capantini, L., Robertson, B., and Grillner, S. (2015). The lamprey pallium provides a blueprint of the mammalian motor projections from cortex. Curr. Biol. 25(4):413-423.

O'Gara, B.A., and Friesen, W.O. (1995). Termination of leech swimming activity by a previously identified swim trigger neuron. J. Comp. Physiol A. 177(5):627-636.

Ohta, Y., and Grillner, S. (1989). Monosynaptic excitatory amino acid transmission from the posterior rhombencephalic reticular nucleus to spinal neurons involved in the control of locomotion in lamprey. J. Neurophysiol. 62(5):1079-1089.

Orlovskiĭ GN. (1970).Work of reticulo-spinal neurons during locomotion [in Russian]. Biofizika. 15(4):728-737.

Pearson, K.G., and Collins, D.F. (1993). Reversal of the influence of group Ib afferents from plantaris on activity in medial gastrocnemius muscle during locomotor activity. J. Neurophysiol. 70(3):1009-1017.

Pérez-Fernández, J., Stephenson-Jones, M., Suryanarayana, S.M., Robertson, B., and Grillner, S. (2014). Evolutionarily conserved organization of the dopaminergic system in lamprey: SNc/VTA afferent and efferent connectivity and D2 receptor expression. J. Comp. Neurol. 522(17):3775-3794.

Perrins, R., Walford, A., and Roberts, A. (2002). Sensory activation and role of inhibitory reticulospinal neurons that stop swimming in hatchling frog tadpoles. J. Neurosci. 22(10):4229-4240.

Peterson, B.W., Pitts, N.G., and Fukushima, K. (1979). Reticulospinal connections with limb and axial motoneurons. Exp. Brain. Res. 36(1):1-20.

Pombal, M.A., El Manira, A., and Grillner, S. (1997). Afferents of the lamprey striatum with special reference to the dopaminergic system: a combined tracing and immunohistochemical study. J. Comp. Neurol. 386(1):71-91.

Ranck, J.B. Jr. (1975). Which elements are excited in electrical stimulation of mammalian central nervous system: a review. Brain Res. 98(3):417-440.

Robertson, B., Kardamakis, A., Capantini, L., Pérez-Fernández, J., Suryanarayana, S.M., Wallén, P., Stephenson-Jones, M., and Grillner, S. (2014). The lamprey blueprint of the mammalian nervous system. Prog. Brain Res. 212:337-349.

Rolland, A.S., Tandé, D., Herrero, M.T., Luquin, M.R., Vazquez-Claverie, M., Karachi, C., Hirsch, E.C., and François, C. (2009). Evidence for a dopaminergic innervation of the pedunculopontine nucleus in monkeys, and its drastic reduction after MPTP intoxication. J. Neurochem. 110(4):1321–1329.

Roseberry, T., and Kreitzer, A. (2017). Neural circuitry for behavioural arrest. Philos. Trans. R. Soc. Lond. B Biol. Sci. 372(1718).

Roseberry, T.K., Lee, A.M., Lalive, A.L., Wilbrecht, L., Bonci, A., and Kreitzer, A.C. (2016). Cell-type-specific control of brainstem locomotor circuits by basal ganglia. Cell 164(3):526-537.

Rossignol, S., Dubuc, R., and Gossard, J.P. (2006). Dynamic sensorimotor interactions in locomotion. Physiol. Rev. 86(1):89-154.

Rossignol, S., Julien, C., Gauthier, L., and Lund, J.P. (1981). State-dependent responses during locomotion. In: *Muscle Receptors and Movement*. Taylor, A., and Prochazka, A. (Eds.). London: Macmillan, p. 389-402.

Rovainen, C.M. (1967). Physiological and anatomical studies on large neurons of central nervous system of the sea lamprey (Petromyzon marinus). I. Müller and Mauthner cells. J. Neurophysiol. 30(5):1000-1023.

Rovainen, C.M. (1974). Synaptic interactions of reticulospinal neurons and nerve cells in the spinal cord of the sea lamprey. J. Comp. Neurol. 154(2):207-223.

Rovainen, C.M., (1978). Müller cells, ‘Mauthner’ cells, and other identified reticulospinal neurons in the lamprey. In: Neurobiology of the Mauthner Cell. Faber, D.S., Korn, H. (Eds.). Raven Press, New York, pp. 245–269.

Rovainen, C.M., Johnson, P.A., Roach, E.A., and Mankovsky, J.A. (1973). Projections of individual axons in lamprey spinal cord determined by tracings through serial sections. J. Comp. Neurol. 149, 193–202.

Ryczko, D., and Dubuc, R. (2013). The multifunctional mesencephalic locomotor region. Curr. Pharm. Des. 19(24):4448-4470.

Ryczko, D., and Dubuc, R. (2017). Dopamine and the brainstem locomotor networks: from lamprey to human. Front. Neurosci. 11:295.

Ryczko, D., Auclair, F., Cabelguen, J.M., and Dubuc, R. (2016). The mesencephalic locomotor region sends a bilateral glutamatergic drive to hindbrain reticulospinal neurons in a tetrapod. J. Comp. Neurol. 524(7):1361-1383.

Ryczko, D., Cone, J.J., Alpert, M.H., Goetz, L., Auclair, F., Dubé, C., Parent, M., Roitman, M.F., Alford, S., and Dubuc, R. (2016). A descending dopamine pathway conserved from basal vertebrates to mammals. Proc. Natl. Acad. Sci. U. S. A. 113(17):E2440-2449.

Ryczko, D., Dubuc, R., and Cabelguen, J.M. (2010). Rhythmogenesis in axial locomotor networks: an interspecies comparison. Prog. Brain. Res. 187:189-211.

Ryczko, D., Grätsch, S., Auclair, F., Dubé, C., Bergeron, S., Alpert, M.H., Cone, J.J., Roitman, M.F., Alford, S., and Dubuc, R. (2013). Forebrain dopamine neurons project down to a brainstem region controlling locomotion. Proc. Natl. Acad. Sci. U. S. A. 110(34):E3235-3242.

Ryczko, D., Grätsch, S., Schläger, L., Keuyalian, A., Boukhatem, Z., Garcia, C., Auclair, F., Büschges, A., and Dubuc, R. (2017). Nigral Glutamatergic Neurons Control the Speed of Locomotion. J. Neurosci. 37(40):9759-9770.

Saitoh, K., Hattori, S., Song, W.J., Isa, T., and Takakusaki, K. (2003). Nigral GABAergic inhibition upon cholinergic neurons in the rat pedunculopontine tegmental nucleus. Eur. J. Neurosci. 8(4):879-886.

Shaw, A.C., Jackson, A.W., Holmes, T., Thurman, S., Davis, G.R., and McClellan, A.D. (2010). Descending brain neurons in larval lamprey: spinal projection patterns and initiation of locomotion. Exp. Neurol. 224(2):527-541.

Shik, M.L., Severin, F.V., and Orlovskii, G.N. (1966). Control of walking and running by means of electric stimulation of the midbrain [in Russian]. Biofizika 11(4):659-666.

Sholomenko, G.N., Funk, G.D., and Steeves, J.D. (1991). Avian locomotion activated by brainstem infusion of neurotransmitter agonists and antagonists. I. Acetylcholine excitatory amino acids and substance P. Exp. Brain Res. 85(3):659-673.

Sinnamon, H.M. (1993). Preoptic and hypothalamic neurons and the initiation of locomotion in the anesthetized rat. Prog. Neurobiol. 41(3):323-344.

Sirota, M.G., Di Prisco, G.V., and Dubuc, R. (2000). Stimulation of the mesencephalic locomotor region elicits controlled swimming in semi-intact lampreys. Eur. J. Neurosci. 12(11):4081-4092.

Skinner, R.D., and Garcia-Rill, E. (1984). The mesencephalic locomotor region (MLR) in the rat. Brain Res. 323(2):385-389.

Smetana, R., Juvin, L., Dubuc, R., and Alford, S. (2010). A parallel cholinergic brainstem pathway for enhancing locomotor drive. Nat. Neurosci. 13(6):731-738.

Steeves, J.D., and Jordan, L.M. (1984). Autoradiographic demonstration of the projections from the mesencephalic locomotor region. Brain Res. 307(1-2):263-276.

Stephenson-Jones, M., Ericsson, J., Robertson, B., and Grillner, S. (2012). Evolution of the basal ganglia: dual-output pathways conserved throughout vertebrate phylogeny. J. Comp. Neurol. 520(13):2957-2973.

Stephenson-Jones, M., Samuelsson, E., Ericsson, J., Robertson, B., and Grillner, S. (2011). Evolutionary conservation of the basal ganglia as a common vertebrate mechanism for action selection. Curr. Biol. 21(13):1081-1091.

Swain, G.P., Snedeker, J.A., Ayers, J., and Selzer, M.E. (1993). Cytoarchitecture of spinal-projecting neurons in the brain of the larval sea lamprey. J. Comp. Neurol. 336(2):194-210.

Takakusaki, K. (2008). Forebrain control of locomotor behaviors. Brain Res. Rev. 57(1):192-198.

Takakusaki, K., Habaguchi, T., Saitoh, K., and Kohyama, J. (2004). Changes in the excitability of hindlimb motoneurons during muscular atonia induced by stimulating the pedunculopontine tegmental nucleus in cats. Neuroscience 124(2):467-80.

Takakusaki, K., Kohyama, J., and Matsuyama, K. (2003). Medullary reticulospinal tract mediating a generalized motor inhibition in cats: III. Functional organization of spinal interneurons in the lower lumbar segments. Neuroscience 121(3):731-46.

Takakusaki, K., Kohyama, J., Matsuyama, K., and Mori, S. (2001). Medullary reticulospinal tract mediating the generalized motor inhibition in cats: parallel inhibitory mechanisms acting on motoneurons and on interneuronal transmission in reflex pathways. Neuroscience 103(2):511-527.

Taylor, A.L., Cottrell, G.W., Kleinfeld, D., Kristan, and W.B. Jr. (2003). Imaging reveals synaptic targets of a swim-terminating neuron in the leech CNS. J. Neurosci. 23(36):11402-11410.

Thiele, T.R., Donovan, J.C., and Baier, H. (2014). Descending control of swim posture by a midbrain nucleus in zebrafish. Neuron 83(3):679-691.

Thompson, R.H., Ménard, A., Pombal, M., and Grillner, S. (2008). Forebrain dopamine depletion impairs motor behavior in lamprey. Eur. J. Neurosci. 27(6):1452-1460.

Villar-Cerviño, V., Barreiro-Iglesias, A., Mazan, S., Rodicio, M.C., and Anadón, R. (2011). Glutamatergic neuronal populations in the forebrain of the sea lamprey, Petromyzon marinus: an in situ hybridization and immunocytochemical study. J. Comp. Neurol. 519(9):1712-1735.

Wallén, P., and Williams, T.L. (1984). Fictive locomotion in the lamprey spinal cord in vitro compared with swimming in the intact and spinal animal. J. Physiol. 347:225-239.

Wannier, T., Orlovsky, G., and Grillner, S. (1995). Reticulospinal neurones provide monosynaptic glycinergic inhibition of spinal neurones in lamprey. Neuroreport. 6(12):1597-1600.

Zelenin, P.V. (2011). Reticulospinal neurons controlling forward and backward swimming in the lamprey. J. Neurophysiol. 105(3):1361-1371.

Zelenin, P.V., Orlovsky, G.N., and Deliagina, T.G. (2007). Sensory-motor transformation by individual command neurons. J. Neurosci. 27(5):1024-1032

Zill, S.N. (1985). Plasticity and proprioception in insects. II. Modes of reflex action of the locust metathoracic femoral chordotonal organ. J. Exp. Biol. 116:463-480.

Zompa, I.C., and Dubuc, R. (1996). A mesencephalic relay for visual inputs to reticulospinal neurones in lampreys. Brain Res. 718(1-2):221-227.

Acknowledgements

During my Ph.D. time, I met many inspiring and supporting people that made this time an exciting and unforgettable experience, full with new discoveries and joy. Here, I would like to take the opportunity to thank a couple of these very important people.

Special thanks go to my fantastic supervisors, Prof. Dr. Ansgar Büschges and Prof. Dr. Réjean Dubuc.

Ansgar, thank you so much for your support, for sharing your ambition and scientific curiosity, and of course your endless optimism. You are right, in the end everything works out.

Réjean, thank you very much for everything you did for me, for your endless support, the opportunity to work on exciting projects, and for sharing your scientific passion. This has been an amazing experience!

Furthermore, I would like to thank my jury and thesis committee members, Prof. Dr. Silvia Daun and Prof. Dr. Matthias Hammerschmidt. Thank you for the lively discussions and advices that helped to plan and improve my experiments.

Scientific and emotional support was always provided by my marvellous colleagues in Montréal and Cologne.

François, Danielle, Dimitri, Laurent, Gheylen, Jean-Patrick, Kianoush, Philipp-Antoine, Emilie, Catherine, Fréderic, and Christian: Merci beaucoup pour tout! Vous êtes les meilleurs collègues au monde.

Big thanks also go to the members of the laboratories Kolta, Robitaille, Lacaille, Rossignol, Arya and the ADÉNUM. Merci pour les évènements plaisants et les bons moments.

Tommi, Carmen, Eli, Anna, Joscha, Till, Chalalompos, Felix I, Felix II, Laura, Alex, Gesa, Sander, Micha, Jochen, Volker, Matthias, Jan, Philipp, Eva, Jens, Anne und Tino: Tausend Dank für die unvergesslichen Konferenzaufenthalte, stimulierenden Diskussionen, Verrücktheiten und Freundschaften. Ihr ward in meinem Herzen immer bei mir!

Many thanks go to my dear friends who were always cheering from near and far. Jules, Lara, Kerstin, Isidora, Sarah, Barbro, Camille and Lucie, Violeta and Benjamin, Andréanne and Laurent, Nadine and Vincent, Eliane and Guillaume, Julie and Fred, Maxi and Lena, Alexandra, Anni, Mo, Oke, Eliza, Alexandra, Lisa. Danke schön! Merci beaucoup! Tack så mycket!

Family support is so very important especially if you are far away from home. Therefore I am thanking my whole family who I deeply missed but who made me feel close by writing, calling, and sending tons of Yogi Tea and Haribo to Montréal.

A special shout-out goes to my small family Günter, Irmela, Annika, Jasper, Philipp, and of course Kalle. Danke für eure Unterstützung und eure Liebe. Ihr seid meine Liebsten, ihr seid die Besten!

Also, I would like to thank my québécois family Shahram, Carmelle, Shaida, and Jules. Thanks for being awesome, kind, and jovial. I love you guys!

And of course I would like to thank Kianoush, who is always there for me. Thanks for your motivation, for taking care of my worries, and believing in me. Thank you for all this joy and laughter!

Finally, I would like to thank Sanft & Sorgfältig/ Fest & Flauschig, the only real podcast in Germany for making the weekend experiments and long hours of kinematic analysis more than enjoyable. Tausend Dank für die Unterhaltung. Wegen euch war ich die, die alleine in der Ecke sitzt und laut lacht.

Financial support for this work came from my two supervisors but also from the University of Cologne and the Deutscher Akademischer Austauschdienst (DAAD), who I would like to thank as well for making this project and collaboration possible.

Teilpublikationen

Artikel
(mit peer-review Verfahren)

Ryczko D, **Grätsch S**, Schläger L, Keuyalian A, Boukhatem Z, Garcia C, Auclair F, Büschges A, Dubuc R. „*Nigral glutamatergic neurons control the speed of locomotion.*“ J. Neuroscience 37(40):9759-9770.

Juvin L *, **Grätsch S** *, Trillaud- Doppia E, Gariépy JF, Büschges A, Dubuc R. 2016. „*A Specific Population of Reticulospinal Neurons Controls the Termination of Locomotion.*“ Cell Rep. 15(11):2377-86.
* Ko-Erstautoren

Ryczko D, **Grätsch S**, Auclair F, Dubé C, Bergeron S, Alpert M, Cone J, Roitman M, Alford S, Dubuc R. 2013. „*Forebrain dopamine neurons project down to a brainstem region controlling locomotion*“. Proc. Natl. Acad. Sci. USA 110(4):E3235-42.

Artikel
(im Begutachtungs-verfahren)

Grätsch S, Auclair F, Demers O, Auguste E, Hanna A, Büschges A, Dubuc R. „*A brainstem neural substrate for stopping locomotion.*“ Im Begutachtungsverfahren bei Current Biology (CURRENT-BIOLOGY-D-18-00650)

Posterbeiträge
2017

Grätsch S, Demers O, Auguste E, Auclair F, Veilleux D, Büschges A, Dubuc R. 2017. „*A neural substrate involved in stopping locomotion.*“ 47. Jahrestagung der Society for Neuroscience, Washington, USA
Grätsch S, Demers O, Auguste E, Auclair F, Veilleux D, Büschges A, Dubuc R. 2017. „*A neural substrate involved in stopping locomotion.*“ 10. SfN Satellitensymposium über Motorische Systeme, Bethesda, USA
Grätsch S, Auclair F, Veilleux D, Büschges A, Dubuc R. 2017. „*On mechanisms for stopping locomotion.*“ 2. Jahrestagung „NeuroSymposium“, Montréal, Canada

Grätsch S, Auclair F, Veilleux D, Büschges A, Dubuc R. 2017. „*A neural mechanism underlying swimming termination in lamprey.*“ 12. Jahrestagung der Neurowissenschaftlichen Gesellschaft, Göttingen, Deutschland

2016

Grätsch S, Auclair F, Veilleux D, Büschges A, Dubuc R. 2016. „*A stop signal for swimming originates from the mesencephalic locomotor region.* “ 46. Jahrestagung der Society for Neuroscience, San Diego, USA

Grätsch S, Auclair F, Veilleux D, Büschges A, Dubuc R. 2016. „*A stop signal for swimming originates from the mesencephalic locomotor region.* “ 9. SfN Satellitensymposium über Motorische Systeme, La Jolla, USA

Grätsch S, Auclair F, Veilleux D, Büschges A, Dubuc R. 2016. „*The mesencephalic locomotor region controls stopping of locomotion in the lamprey.*“ 6. Jahrestagung der Groupe de Recherche en Activité Physique Adaptée (GRAPA), Montréal, Kanada

Grätsch S, Auclair F, Veilleux D, Büschges A, Dubuc R. 2016. „*Termination of locomotion in the lamprey is controlled by a descending neural mechanism.*“ 2. Jahrestagung der Neurowissenschaftsstudenten der Université de Montréal (ADÉNUM), Montréal, Kanada

2015 **Grätsch S**, Juvin L, Auclair F, Veilleux D, Büschges A, Dubuc R. 2015. „*Identification of a descending neural mechanism that controls termination of locomotion in the lamprey.*“ 45. Jahrestagung der Society for Neuroscience, Chicago, USA

Grätsch S, Juvin L, Auclair F, Veilleux D, Büschges A, Dubuc R. 2015. „*Identification of a descending neural mechanism that controls termination of locomotion in the lamprey*. “ 9. SfN Satellitensymposium über Motorische Systeme, Chicago, USA

Grätsch S, Juvin L, Auclair F, Veilleux D, Büschges A, Dubuc R. 2015. „*A descending pathway that controls termination of locomotion in the lamprey.*“ 5. Jahrestagung der Groupe de Recherche en Activité Physique Adaptée (GRAPA), Montréal, Kanada

2014 **Grätsch S**, Auclair F, Büschges A, Dubuc R. 2014. „*Differential contribution of reticulospinal neurons to locomotor control in the lamprey*.“ 4. Jahrestagung der Groupe de Recherche en Activité Physique Adaptée (GRAPA), Montréal, Kanada

Ryczko D, **Grätsch S**, Auclair F, Dubé C, Bergeron S, Alpert M, Cone J, Roitman M, Alford S, Dubuc R. 2013. „*Forebrain dopamine neurons send descending projections to a brainstem region controlling locomotion. Possible implication for Parkinson's disease.*“ 3. Jahrestagung der Groupe de Recherche en Activité Physique Adaptée (GRAPA), Montréal, Kanada

2012 Ryczko D, **Grätsch S**, Dubé C, Auclair F, Dubuc R. 2012. „*Evidence that lamprey dopaminergic neurons from the posterior tuberculum are homologous to those in the substantia nigra and/or ventral tegmental area, and control locomotion.*“ 42. Jahrestagung der Society for Neuroscience, New Orleans, USA

Ryczko D, **Grätsch S**, Lamontagne V, Dubuc R. 2012. „*Innervation dopaminergique de la region locomotrice mesencephalique: 2. Role dans le maintien de l'activite locomotrice.*“ 2. Jahrestagung der Groupe de Recherche en Activité Physique Adaptée (GRAPA), Montréal, Kanada

Mündliche Vorträge

2018 „Brainstem command cells controlling the locomotor output“. 2018. 4. Jahrestagung der Neurowissenschaftsstudenten der Université de Montréal (ADÉNUM), Montréal, Kanada

2017 *„A stop signal for swimming originates from the Mesencephalic Locomotor Region“*. 2017. Studentenseminar der Groupe de recherche sur le système nerveux central (GRSNC) der Université de Montréal, Montréal, Canada

„On the mechanisms for stopping locomotion.“ 2017. Pitch talk bei der 2. Jahrestagung „NeuroSymposium“, BaNQ Grande Bibliothèque, Montréal, Canada

„Stopping locomotion: Identification of a neural mechanism that controls termination of swimming in the lamprey“. 2017. Max Planck Institute of Neurobiology, Martinsried, Germany

Erklärung

Ich versichere, dass ich die von mir vorgelegte Dissertation selbständig angefertigt, die benutzten Quellen und Hilfsmittel vollständig angegeben und die Stellen der Arbeit – einschließlich Tabellen, Karten und
Abbildungen –, die anderen Werken im Wortlaut oder dem Sinn nach entnommen sind, in jedem Einzelfall als Entlehnung kenntlich gemacht habe; dass diese Dissertation noch keiner anderen Fakultät oder Universität zur Prüfung vorgelegen hat; dass sie – abgesehen von unten angegebenen Teilpublikationen – noch nicht veröffentlicht worden ist sowie, dass ich eine solche Veröffentlichung vor Abschluss des Promotionsverfahrens nicht vornehmen werde.

Die Bestimmungen der Promotionsordnung sind mir bekannt. Die von mir vorgelegte Dissertation ist von Prof. Dr. Ansgar Büschges betreut worden.

_____

Swantje Grätsch